ELS XXI

21st Electromagnetic and Light Scattering Conference

Milazzo, Italy, 23-27 June 2025

This booklet is based on the AMCOS conference booklet by Maxime Lucas and Pau Clusella. The LaTeX template is freely available at https://github.com/maximelucas/AMCOS_booklet along with examples, additional codes, and information about its use and distribution policy.

You can download the latest version of the booklet from the conference website at https://portale2.unime.it/els2025/. Please address any comments (e.g. reporting errors) and suggestions on this booklet to maria.donato@cnr.it.

Contents

About

ELS XXI

ELS XXI will be held in June 23-27, 2025, in Milazzo, a town in Sicily, long referred to as “the pearl of the Tyrrhenian sea”.

The Electromagnetic and Light Scattering (ELS) XXI meeting will focus on theoretical, computational, and experimental advances in electromagnetic and light scattering by particles with arbitrary sizes, shapes, and optical properties. Contributions will cover a broad range of topics from cosmic dust, atmospheric aerosols, remote sensing observations, particle detection and characterization, to optical trapping and nano-optics.

The specific topics that will be covered include (but are not limited to) the following:

- New theoretical developments, numerical simulations, and laboratory measurements of light scattering by nonspherical and morphologically complex particles and particle groups
- Detection and characterization of atmospheric particulates using laboratory, in situ, and remote sensing techniques
- Scattering of light by terrestrial aerosols and clouds, oceanic particulates, solar system objects, exoplanets, stellar disks, and various astrophysical objects
- Applications of light scattering methods in biology and biomedicine
- Near-field and coherent effects in light scattering, optical trapping, and manipulation
- Light scattering methods to control material properties and technological applications

During the conference the winners will be announced of the prestigious young-scientists awards granted by Elsevier together with the Journal of Quantitative Spectroscopy and Radiative Transfer (JQSRT): the Richard M. Goody Award (2024 and 2025) for outstanding early-career scientists in the field of atmospheric radiation, remote sensing, and climate science, and the Peter C. Waterman Award (2024 and 2025) for outstanding early-career scientists who work on the theory and applications of electromagnetic scattering. Moreover, the winners will be announced of the prestigious awards for senior scientists granted by Elsevier and JQSRT: the 2025 van de Hulst Light Scattering Award and the 2025 Michael I. Mishchenko Medal.

Credits

The conference is jointly organized by the Dipartimento di Scienze Matematiche e Informatiche, Scienze Fisiche e Scienze della Terra (MIFT) of the University of Messina and by the Istituto per i Processi Chimico-Fisici (IPCF) del Consiglio Nazionale delle Ricerche (CNR).

We gratefully acknowledge the PRIN2022 ”Cosmic Dust II” (grant No. 2022S5A2N7), the PRIN 2022 “EnantioSelex” (grant. No. 2022P9F79R), the PRIN 2022 “EXO-CASH” (grant No. 2022J7ZFRA) and the Project “Space It Up” funded by ASI and MUR – Contract n. 2024-5-E.0.

Our special thanks go to Sabrina Rizzo, Meeting Planner at Lisciotto Congressi, Messina.

Timetable

Start	End	SUNDAY 22	MONDAY 23	TUESDAY 24	WEDNESDAY 25	THURSDAY 26	FRIDAY 27
8:45	9:00		**Opening ceremony**				
9:00	9:15		**Michael I. Mishchenko Medal 2023 - M. Pinar Mengüç**	**Karri Muinonen**	**Wang Chuji**	**Van de Hulst Awardee 2025 Andreas Macke**	**Giovanni Volpe**
9:15	9:45		Ballington	Virkki	Nieminen	**Van de Hulst Awardee 2025 Akhlesh Lakhtakia**	Nieminem
9:45	10:00		Baran	Yurkin	Gouesbet	Freimanis	Chabrol
10:00	10:15		Bi	Bouillon	Infusino	Garcia-Izquierdo	Grynko
10:15	10:30		Ceolato	Gienger	Perrin	Geffrin	
10:30	10.45		**Coffee Break**	**Coffee Break**	Zemanek	**Coffee Break**	**Coffee Break**
10:45	11:00				**Coffee break**		
11:00	11:15		**Matthew Berg**	**Ludmilla Kolokolova**		**Michael I. Mishchenko Medal 2025 - Olga Munoz**	**Vincenzo Amendola**
11:15	11:30				**Giuseppe Strangi**		
11:30	11:45		Xi Chen	Leppälä		**Goody Awardee 2024 Xi Chen**	Vasi
11:45	12:00		Haarig	Lin	Litman	**Goody Awardee 2025 Jianyu Zheng**	Karamehmedović
12:00	12:15		Hesse	Ménard	Isernia	**Waterman Awardee 2024 Guanglang Xu**	Garcia-Valenzuela
12:15	12:30		Gialitaki	Pentikäinen	Garcia-Martin	**Waterman Awardee 2025 Jiachen Ding (presented by Feng Xu)**	Lopushenko
12:30	12:45		Ping Yang	Sun Bingqiang	Veltri	**Group photo**	Napoli
12:45	13:00		**Light Lunch**	**Light Lunch**	Sánchez-Gil	**Light Lunch**	**Light Lunch**
13:00	14:30				**Light Lunch**		
14:30	15:00		**Evgenij Zubko**	Di Noia	**Pablo Albella**	**Poynting Awardee 2025 Yung Yuk**	
				La Mura			
15:00	15:15		Renyi Zhang	Le Ru	González-Colsa	Surkov	
15:15	15:30		Semwal	Penttilä	Roy	Auguié	
15:30	15:45		Qie	Markkannen	Corsaro	Triolo	
15:45	16:00		Tsekeri	Argentin	Roy	Yon	
16:00	16:05		**Coffee Break**			Allen	
16:05	16:15						
16:10	16:30						
16:30	16:45		Xu Feng	Arnaut	**Guided visit to the Castle of Milazzo**		**Excursion to Capo Milazzo**
16:45	17:00		Martikainen	Zerna			
17:00	17:15	**Registration desk opening**	Konoshonkin	Ivanova			
17:15	17:30			Vuori			
17:30	18:00			**POSTER SESSION**			
18:00	19:00						
19:00	20:00	**Welcome Cocktail**					
20:00					**Conference dinner**		

Monday

08:45	09:00	**Opening Ceremony**	
		Session I: Atmospheric particles I **Chair: Gorden Videen**	
9:00	9:30	Michael I. Mishchenko Medal 2023 - M. Pinar Mengüç : *Light, Heat, Particles, Plasmons, and Engineering*	
9:30	9:45	Ballington	Effects of Surface Roughness on Ice Particle Single Scattering
9:45	10:00	Baran	Are observed small, rounded ice particles important in a climate model?
10:00	10:15	Bi	An Accurate and Efficient Radar Observation Operator: ZJU-AERO
10:15	10:30	Ceolato	Backscattering by soot fractal aggregates: a model for lidar applications

		Session II: Atmospheric particles II **Chair: Karri Muinonen**	
11:00	11:30	Matthew Berg	*Aerosol Characterization with Digital In-Line Holography*
11:30	11:45	Xi Chen	Analytical prediction of scattering properties of non-spherical dust particles with machine learning
11:45	12:00	Haarig	OLALA – Optical Lab for Lidar Applications
12:00	12:15	Hesse	Backscattering by Ice Crystals in Artificial Cirrus
12:15	12:30	Gialitaki	Modelling of lidar-related dust properties during ASKOS campaign, using irregular hexahedral and spheroid shape mixtures
12:30	12:45	Yang	A Vector Radiative Transfer Model for Atmospheric and Oceanic Polarimetric Remote sensing

		Session III: Polarimetry and atmospheric aerosols **Chair: Hanna Pentikainen**	
14:30	15:00	Evgenij Zubko	*What polarimetry may say about the microphysics of atmospheric aerosols*
15:00	15:15	Zhang	Light scattering and absorption by black carbon during atmospheric aging
15:15	15:30	Semwal	Laboratory Measurement of the Depolarization Ratio of Size Selected Salt Particles at 180° Scattering Angle
15:30	15:45	Qie	Simulation of the polarized reflectance at TOA over ocean for satellite in-flight polarimetric calibration
15:45	16:00	Tsekeri	Reproduce the backscatter of dust using realistic dust shapes

		Session IV: Atmospheric particles III **Chair: Matthew Berg**	
16:30	16:45	Xu Feng	A Markov Chain Solution to Polarized Infrared Radiative Transfer in an Optically Anisotropic Media
16:45	17:00	Martikainen	Effect of complex refractive index on the scattering matrix of dust aerosols with narrow particle size distributions
17:00	17:15	Konoshonkin	SciIce: Light Scattering Database for Ice Crystals of Cirrus Clouds

Tuesday

		Session V: Numerical simulations I Chair: Evgenij Zubko	
9:00	9:30	Karri Muinonen	*Scattering and absorption of light synoptically modeled for particulate planetary surfaces*
9:30	9:45	Virkki	Microwave scattering by rough polyhedral particles on a surface
9:45	10:00	Yurkin	Recent developments of the ADDA code
10:00	10:15	Bouillon	Implementation of the weighted discretization in the ADDA code
10:15	10:30	Gienger	Glare points of spheroidal microparticles - simulation study

		Session VI: Light scattering in the astrophysical environment I Chair: Olga Munoz	
11:00	11:30	Ludmilla Kolokolova	*Photopolarimetric journey through the diverse world of solar system dust*
11:30	11:45	Leppälä	Photometric and Polarimetric Modeling for the Galilean Satellite Europa
11:45	12:00	Lin	Probing Dust Properties of Protoplanetary Disks through ALMA's High-Resolution Polarization
12:00	12:15	Ménard	3D-Printed Dust analogs for Protoplanetary Disk Studies
12:15	12:30	Pentikäinen	Polarimetry and spectroscopy of regolith simulants at different illumination and observation geometries
12:30	12:45	Bingqiang Sun	Planetary Atmospheric Profile Inversion through Curved Path Occultation

		Session VII: Numerical simulations II Chair: Anne Virkki	
14:30	14:45	Di Noia	Circular polarisation scattering from chiral aerosols
14:45	15:00	La Mura	Nano-particle Transition matrix code: A parallel implementation of the T-matrix formalism
15:00	15:15	Le Ru	Stable Computation of the Electromagnetic T-matrix for High Aspect Ratio Cylinders
15:15	15:30	Penttilä	Simple empirical approximation for integrated reflected intensity of particulate surfaces in geometric optics regime
15:30	15:45	Markkanen	Fast surface integral equation method for scattering by homogeneous particles with rough surfaces
15:45	16:00	Argentin	Accelerating iterative solvers in the discrete dipole approximation using dedicated initial guesses

		Session VIII: Light scattering in the astrophysical environment II Chair: Ludmilla Kolokolova	
16:30	16:45	Arnaut	Imaging Polarimetry of the Tail and Coma of the Comet C/2023 A3 (Tsuchinshan-ATLAS)
16:45	17:00	Zerna	Comparison of scattering properties of meteorite inclusion analogs
17:00	17:15	Ivanova	The scattering properties of distant comet C/2020 V2 (ZTF)
17:15	17:30	Vuori	Modeling the surface properties of asteroid (3200) Phaethon using CY-chondrite meteorites
17:30	19:00	**POSTER SESSION**	

Wednesday

		Session IX: Acoustic and optomechanical interactions Chair: Alessandro Magazzù	
9:00	9:30	Chuji Wang	*Optical trapping and light scattering from single particles*
9:30	9:45	Nieminen	Limits of direct optical measurement of optical forces and torques
9:45	10:00	Gouesbet	On relationships between EM and acoustical scatterings
10:00	10:15	Infusino	Acoustic and optical Raman tweezers as a tool to manipulate and analize cosmic dust analogues
10:15	10:30	Perrin	A Multipolar method to optimize the opto-mechanical interactions in levitodynamics with complex wavefronts
10:30	10:45	Zemanek	Nonequilibrium dynamics of levitated nanoparticles

		Session X:Light scattering and material properties I Chair: Maria Grazia Donato	
11:00	11:30	Giuseppe Strangi	*Boron-doped diamond and the discovery of new properties in an old material*
11:30	11:45	Litman	Extracting cross-sections from partially measured electromagnetic scattered fields of single particles
11:45	12:00	Isernia	Analysis and engineering of scattering from multiple cylinders in the presence of planar PECs
12:00	12:15	Garcia-Martin	Torsional mechanical modes in acousto-plasmonic antennas
12:15	12:30	Veltri	The Geometry Matrix Formalism for Gain Assisted Plasmonic Resonators
12:30	12:45	Sánchez-Gil	Cloaked quasi-bound states in the continuum in out-of-plane symmetry broken Si nanodisk metasurfaces

		Session XI: Biomedical applications Chair: Giuseppe Strangi	
14:30	15:00	Pablo Albella	*Light scattering by plasmonic and dielectric nanostructures: Biomedical applications*
15:00	15:15	González-Colsa	Optical Modelling of Complex Thermoplasmonic Agents in the Context of Advanced Therapies
15:15	15:30	Roy	Light scattering investigations of Black turmeric (Curcuma Caesia) as potent antibacterial agent and its response at different temperatures
15:30	15:45	Corsaro	Raman Spectroscopy analyses to study the physiological features of a 3D HepG2 Model
15:45	16:00	Roy	Synergizing light scattering and Machine learning for morphological quantification of small particles

16:30	19:00	**Guided visit to the Castle of Milazzo**

Thursday

		Session XII: Elsevier/JQSRT award I **Chair: Pinar Menguc**	
9:00	9:30	Van de Hulst Award 2025 - Andreas Macke: *The role of cloud microphysical versus cloud macrophysical variability in solar cloud radiative transfer - review and recommendations for future work*	
9:30	9:45	Van de Hulst Award 2025 - Akhlesh Lakhtakia: *Living off Scattered Light*	
9:45	10:00	Freimanis	Temperatures of dust grains in some circumstellar environments
10:00	10:15	García-Izquierdo	Effect of Surface Roughness and Composition on Scattered Light by Regolith Surfaces
10:15	10:30	Geffrin	Mueller parameters of non-homogeneous scatterers obtained from microwave analogy and additive manufacturing

		Session XIII: Elsevier/JQSRT award II **Chair: Andreas Macke**	
11:00	11:30	Michael I. Mishchenko Medal 2025 - Olga Munoz : *The IAA Cosmic Dust Laboratory, 15 years studying scattering by non-spherical particles*	
11:30	11:45	Goody Award 2024 - Xi Chen: *Aerosol optical centroid height retrieval from hyperspectral measurements in oxygen absorption bands: perspectives from polar orbiting satellite to geostationary satellite constellation*	
11:45	12:00	Goody Award 2025 - Jianyu Zheng: *A combined retrieval of mid-visible and thermal infrared dust optical depth and coarse mode particle size from MODIS observation.*	
12:00	12:15	Waterman Award 2024 - Guanglang Xu: *Unveiling Hidden Characteristics of Scattering Phase Function: From Spherical to Complex Ice Crystals*	
12:15	12:30	Waterman Award 2025 - Jiachen Ding (presented by Feng Xu) : *Light scattering by two-layer spheroids: Separation of variable method in spheroidal coordinates*	
12:30	12:45	Group photo	

		Session XIV: Light scattering in complex media **Chair: Pavel Zemanek**	
14:30	15:00	Poynting Award 2025 - Yung Yuk: *Decoding the Hazy Mysteries of the Cosmos: Aerosol Remote Sensing from Earth to Exoplanets*	
15:00	15:15	Surkov	Light scattering from clusters of helical particles
15:15	15:30	Auguié	Recent advances in UV–vis spectroscopy of turbid solutions
15:30	15:45	Triolo	Wavelength-dependent tuning of thermal and thermo-plasmonic response in aggregates of porphyrins
15:45	16:00	Yon Jerome	Structure factor of fractal aggregates based on pair correlation modeling : comparison with current modeling and impacts
16:00	16:05	Yon Jerome	Introducing LIP LII 2026, July 5-10 Rouen France
16:05	16:15	Allen	European Office of Aerospace Research and Development

Friday

		Session XV: Photonics I Chair: Melissa Infusino	
9:00	9:30	**Giovanni Volpe**	What can deep learning do for electromagnetic light scattering?
9:30	9:45	Nieminen	Simple scheme for design of 3D structured light
9:45	10:00	Chabrol	From the Lorenz-Mie theory in the near-field to the Fresnel Diffraction
10:00	10:15	Grynko	3D Anderson localization of light in disordered dielectric media

		Session XVI: Photonics II Chair: Pablo Albella	
11:00	11:30	**Vincenzo Amendola**	*Using the optical properties of plasmonic nanoalloys for the assessment and design of biodegradable nanomedicines*
11:30	11:45	Vasi	Hybrid Au-Metal Oxide Nanostructures for UV-SERS Sensing Applications
11:45	12:00	Karamehmedović	Phase engineering for steerable photonic nanojets
12:00	12:15	Garcia- Valenzuela	Method and conditions to retrieve the refractive index of particles of arbitrary shapes and size distribution
12:15	12:30	Lopushenko	Modeling scattering of polarization-entangled photons
12:45	13:00	Napoli	Perfect Absorption and Hermitian Subspaces

16:30	20:00	**Excursion to Capo Milazzo**

Posters

PRESENTING AUTHOR	POSTER NUMBER	Title
Bjorn	1	Photometric modeling of the regolith in the Reiner Gamma lunar swirl
Chabrol	2	Asymptotic model for the forward scattering of large refracting spheres: interference of refraction with the diffraction of a disk and a complex ring.
Grynko	3	Transmission of millimeter electromagnetic waves through pigmented automotive coatings
Isernia	4	RELAX : REtrieve complex fieLds from Amplitude via X-words (on some recent recent advances in 2D Phase Retrieval Problems)
Jayasinghe	5	Aerosol Retrievals using GRASP from LES and 1D/3D RT Simulations for HARP like instruments in Twilight Regions
La Luna	6	Scattering Properties and Lidar Characteristics of Asian Dust Particles Based on Realistic Shape Models
Lecadre-Scotto	7	Optical signature modeling of proton-irradiated space white paint
Lombardo	8	Carbon Dots from Laser Ablation of Graphene Oxide in Biocompatible Solutions
Oppermann	9	Modeling the Spectral Slope of the Lidar and Depolarization Ratio of Mineral Dust
Ottaviani	10	Satellite retrievals over snow-covered surfaces: a Global Sensitivity Analysis of polarimetric measurements
Puthukkudy	11	Aerosol Products from PACE Polarimeter HARP2 Observations using GRASP
Regmi	12	Combined Lidar and MAP dust retrieval using Spheroid and Hexahedral aerosol shape models in GRASP
Rezaei	13	Enhanced optical behaviour of micro and nano-plastics coupled with metal nanoparticles
Sanchez-Jimenez	14	Hygroscopic behavior of inorganic salt from inelastic scattering and extinction cross-section measurements
Savenkov	15	Partial Mueller polarimetry for some natural scattering scenes
Schnaiter	16	Light Scattering from Single Atmospheric Ice Particles
Senyi	17	Non-Spherical and Inhomogeneous Effects on Deriving Mineral Dust Refractive Indices from Laboratory Measurements
Shubina	18	Polarimetric properties of cometary dust based on DBCP V3.0
Valenzuela	19	Brown carbon formed by a microreactor of levitated aqueous Fe (III) droplet with fumaric acid
Magazzù	20	Highly Focused Laser Beams for Driving Janus Microengines and detecting sea microplastics
Trusso	21	Electric field induced effect on dipole moment and vibrational properties of the biosynthetic dye Violacein
Abdullah	22	Zr-MOFs as an efficient adsorbent of biomolecules and environmental analytes

Abstracts – Talks

Light, Heat, Particles, Plasmons, and Engineering

M. Pinar Mengüç
Center for Energy, Environment and Economy (CEEE/EÇEM)
Ozyegin University, Cekmekoy, Istanbul 34794, Turkey
pinar.menguc@ozyegin.edu.tr; mpmenguc@gmail.com

The interaction of light, or more generally, electromagnetic waves with matter is fundamental to the existence of the universe. These interactions give rise to a wide range of physical phenomena, depending on the optical properties of particles, gases, and surfaces at specific frequencies, and are governed by Maxwell's equations. At near-infrared frequencies, radiative transfer is a statistical phenomenon that arises from the principles of thermodynamics. The underlying formulation of radiative transfer is based on the Boltzmann transport equation (BTE), which can be simplified to the radiative transfer equation (RTE) when photons are used as energy carriers. The BTE can also be adapted to describe electron, neutron, and phonon transport, depending on the nature of the energy carriers.

In this talk, a summary of the research conducted by the author and their groups will be presented. First, the details of the BTE and RTE, along with their applications to various problems, will be discussed. The relationship between the RTE and the generalized Maxwell equations, based on Michael Mishchenko's formulation, will be highlighted. The necessary modifications for calculating energy exchanges at distances much smaller than the wavelength, i.e., in the near-field regime, will be summarized. Additionally, light-particle interactions that lead to the characterization of particles will be examined. Finally, the talk will discuss near-field plasmonic interactions between particles and surfaces, which can be applied in the development of engineering tools ranging from sensors to energy harvesting and radiative cooling devices. Some of the engineering challenges associated with measurements and the development of these devices will also be addressed.

Effects of Surface Roughness on Ice Particle Single Scattering

Harry Ballington,[1]* Emma Järvinen,[1] and Martin Schnaiter[1]

[1]*Institute for Atmospheric and Environmental Research, University of Wuppertal, Wuppertal, Germany*

An accurate understanding of light scattering by ice particles is important for climate modelling and remote sensing. Despite significant advancements in the availability of theoretical methods for light scattering, the influence of surface roughness on optical properties remains a key uncertainty. Recent studies suggest that ice particles not only exhibit surface roughness, but also have shapes much more complex than previously thought. An improved understanding of how these factors affect the single scattering properties is therefore important for parametrisations in modelling, which play a crucial role in the accuracy of radiative transfer and cloud process simulations.

The orientation-averaged scattering from hexagonal ice plates over 96 uniformly distributed orientations with varying surface roughness properties is computed using ADDA [1] and the PBT method; a recently developed physical-optics hybrid method for particles with surface roughness [2]. The ADDA results find that the scattering is primarily determined by the roughness amplitude and is insensitive to the lateral length scale. The PBT method shows best agreement against ADDA when the roughness length scale is several times the wavelength. The presence of roughness is found to decrease asymmetry parameter by $\sim$ 2%. The PBT method computes the asymmetry parameter and scattering cross sections to within 1% and 3% of the ADDA results, respectively. The applicability of the PBT method for reproducing angular scattering from laboratory generated cirrus is also investigated.

[1] M.A. Yurkin and A.G. Hoekstra, J. Quant. Spectrosc. Radiat. Transf. **112**, 2234 (2011).

[2] H. Ballington and E. Hesse, J. Quant. Spectrosc. Radiat. Transf. **323**, 109054 (2024).

Are observed small, rounded ice particles important in a climate model?

Anthony J. Baran[1,2]*, Evelyn Hesse[2], James Manners[1], Elizabeth Mathen[2], and Harry Ballington[2]

[1]*Met Office – Exeter, UK (*anthony.baran@metoffice.gov.uk)*
[2]*Dept. of Physics, Astronomy, and Mathematics, University of Hertfordshire – Hatfield, UK*

The importance of cirrus or ice crystal clouds in the tropical tropopause layer (TTL) in terms of their impact on the radiative balance of the layer through heating, spatial distribution, opacity, and composition is well known [1]. However, despite cirrus being important to the radiative balance of the TTL, there is little known about their ice crystal composition owing to their very high altitudes and low temperatures, making them difficult to access using research aircraft. This situation changed in 2014 when NASA flew its high-altitude UAV in the Western Pacific during the Airborne Tropical Tropopause Experiment (ATTREX) [2]. As part of the ATTREX campaign in 2015, the University of Hertfordshire flew its Aerosol Ice Interface Transition Spectrometer (AIITS) on board NASA's UAV, which provided 2D light scattering images of single ice particles in the size range 1–100 μm [3].

Analysis of the 2D light scattering images by Mathen [4] and subsequent modelling of the images using a physical–optics beam tracing method developed by Ballington and Hesse [5] found that at the colder temperatures in the TTL, the small ice crystals were dominated by rounded particles with some degree of surface roughening up to sizes of about 45 μm. At sizes between 45 and 100 μm, at the colder temperatures, the particles were smooth thin hexagonal plates.

Here, the beam tracing method has been employed to calculate the total optical properties (extinction and scattering cross sections, single-scattering albedo, and asymmetry parameter) of the surface-roughened rounded ice particles and smooth plates, with sizes ranging between 5 and 45 and 55 to 95 μm, respectively. In the Met Office's single-scattering database of the ensemble model (consisting of hexagonal columns, rosettes, and aggregates of hexagonal columns) developed by Baran and Labonnote [6], the columns and rosettes are replaced by the rounded particles and thin plates found in the TTL at sizes up to 100 μm.

In this presentation, we will explore two-stream radiative transfer simulations and climate model runs to assess the potential significance of rounded ice particles. The climate model runs will investigate any differences between the rounded particles and the ensemble model over a ten–year period, focusing on globally–averaged short–wave radiation fields and zonally–averaged temperatures. These experiments aim to determine whether rounded ice particles are important enough to be considered operationally in climate model radiation and temperature simulations. If so, this will have significant implications for climate modelling in the tropics, particularly in the TTL region, where currently rounded ice particles are precluded in all climate models.

[1] S. Lei, B-J. Sohn, J. Kim, and C. Liu, Atmos. Res. **293**, 106919 (2023).
[2] S. Woods, R. P. Lawson, E. Jensen et al., J. Geophys. Res. **123**, 6053(2018).
[3] C. Stopford, P. Kaye, J. Ulanowski, and E. Hirst, AIITS: Preliminary light scattering data from tropical tropopause cirrus (Composition and Transport in the Tropical Troposphere and Lower Stratosphere, 2015).
[4] E. R. Mathen, E. Hesse, A. Baran, Analysis and modelling of TTL ice crystals based on in-situ measurements of scattering patterns (19th Electromagnetic and light scattering conference, 2021).
[5] H. Ballington and E. Hesse, JQSRT, **323**, 109054 (2024).
[6] A. J. Baran and L. Labonnote, Quart. Jour. Royal. Meteorol. Soc., **133**, 1899 (2007).

An Accurate and Efficient Radar Observation Operator: ZJU-AERO

Lei Bi,[1,*] Hejun Xie,[1] Zheng Wang,[1] and Wei Han[2]

[1]*School of Earth Sciences, Zhejiang University– Hangzhou, China (*bilei@zju.edu.cn)*

[2]*CMA Earth System Modeling and Prediction Centre (CEMC), China Meteorological Administration, Beijing 100081, China*

In this talk, we introduce the Accurate and Efficient Radar Operator (ZJU-AERO) developed by ZheJiang University, a novel forward polarimetric radar simulator capable of modeling observations from both space-borne and ground-based radar systems. ZJU-AERO leverages the invariant-imbedding T-matrix (IITM) method to compute hydrometeor optical properties, enabling precise simulations for non-spherical and inhomogeneous atmospheric particles. The IITM approach ensures computational robustness while accommodating nonspherical and inhomogeneous particle morphologies and orientations [1-3].

Central to ZJU-AERO's innovation is nonspherical and inhomogeneous hydrometeor models as well as its multi-layered optical database architecture, designed to balance flexibility and computational efficiency. This architecture comprises three layers: (1) a base layer storing single-scattering properties for discrete particle sizes, shapes, and orientations; (2) an intermediate layer integrating properties across shape and orientation distributions; and (3) a bulk-scattering layer incorporating size-averaged parameters for operational applications. This hierarchical structure allows users to tailor simulations to specific microphysical assumptions without sacrificing performance.

We detail the core design principles, physical foundations, and hydrometeor specification framework of ZJU-AERO, emphasizing its adaptability to diverse observational scenarios [4-5]. Case studies illustrate its practical utility in generating synthetic radar observations and enhancing data assimilation workflows, underscoring its value for weather prediction and atmospheric research. By bridging advanced scattering physics with operational efficiency, ZJU-AERO offers a versatile tool for advancing polarimetric radar applications.

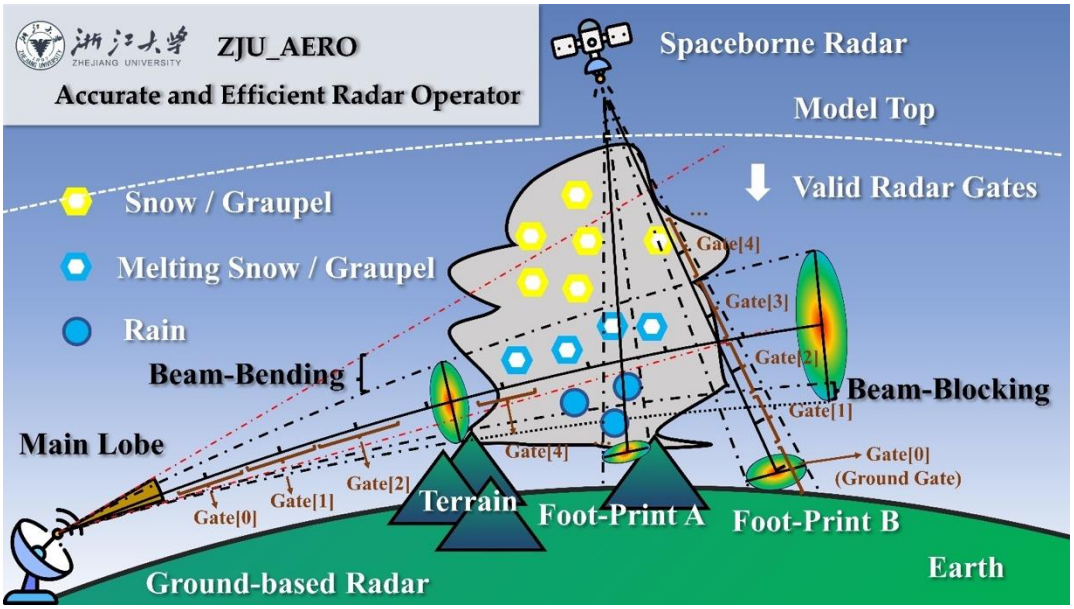

Figure 1: A Conceptual graph of ZJU-AERO [4].

[1] L. Bi, P. Yang, J. Quant. Spectrosc. Radiat. Transfer, **138**, 17–35(2014).

[2] L. Bi, Z. Wang, W. Han, W. Li, X. Zhang, Front. Remote Sens. **3**, 903312 (2022)

[3] Z. Wang, L. Bi, S. Kong, Opt. Express, **31**(18), 29427–29439 (2023).

[4] H. Xie, L. Bi, W. Han, Geosci. Model. Dev. **17**, 5657–5688 (2024)

[5] H. Xie, L. Bi, Z. Wang, W. Han, J. Geophys. Res.-Atmos. **129**, e2024JD040725 (2024).

Backscattering by soot fractal aggregates: a model for lidar applications

Romain Ceolato,[1,*] Jerome Yon,[2] and Matthew J. Berg[3]

[1]*ONERA, The French Aerospace Lab - University of Toulouse – Toulouse, France (*Romain.Ceolato@onera.fr)*
[2]*Normandie Université, INSA Rouen, CNRS, CORIA – Rouen, France*
[3]*Kansas State University, Department of Physics – Manhattan, KS, USA*

Aerosol lidar remote sensing relies on the interpretation of backscattered light to retrieve particle properties of interest. This study presents a novel analytical backscattering model for soot or black carbon aerosols, based on the Rayleigh-Debye-Gans for Fractal Aggregates (RDG-FA) approximation. This model is used to derive simple expressions for common lidar-relevant parameters are derived using this model, including differential backscattering cross section, lidar ratio (LR), mass-backscattering coefficients (MBC), backscattering color ratio (CR), and Ångström exponent (BAE). The behavior of these lidar parameters is investigated as a function of wavelength, size, and aging. Key findings include a general decrease in LR, along with a clear dependence of CR and BAE on aerosol size as black carbon aggregates grow, for both freshly emitted and aged soot. These findings have highlighted the ability to model the variations of these parameters throughout the life cycle of black carbon, capturing the evolution from chain-like freshly emitted particles to more spherical aged particles. Furthermore, this study demonstrates the potential of the RDG-FA backscatter model to calculate key lidar parameters and improve the retrieval of soot aerosol products.

[1] R. Ceolato, A.E. Bedoya-Velásquez, F. Fossard, Black carbon aerosol number and mass concentration measurements by picosecond short-range elastic backscatter lidar. Sci Rep 12, 8443 (2022).

[2] R. Ceolato, M. J. Berg, Aerosol light extinction and backscattering: A review with a lidar perspective. JQSRT, 262 (2021).

Aerosol Characterization with Digital In-Line Holography

Matthew J. Berg,*

[1]*Kansas State University, Department of Physics – Manhattan, KS, USA (*mberg2@ksu.edu)*

Light-scattering techniques are commonly used to characterize micron and submicron particulate matter, such as aerosols, and can do so in a rapid and collection-free way. A typical objective is to infer the size and shape of particles from their light-scattering patterns. While the approach is useful for simple shapes, difficulties arise for large irregularly shaped particles. In short, the reason for the difficulty is the inverse problem, i.e., the fundamental inability to uniquely associate light-intensity observables to particle characteristics in an unambiguous way.

An alternative that is well-suited for relatively large particles is digital in-line holography. Here, a particle is illuminated by an expanded laser beam and the interference pattern produced by unscattered and scattered light is recorded on an image sensor as shown in Fig. 1(a). The pattern is the hologram. An example of a hologram measured for a free-flowing aerosol particle is presented in Fig. 1(b). Because the hologram encodes optical-phase information in the interference pattern, it is possible to render an image of the particle producing the hologram [1]. The process thus avoids many limitations of the inverse problem as the shape and size is evident provided the image is well-resolved. To obtain the image, the hologram is processed by the Fresnel diffraction integral. The integral numerically propagates the optical-wave from the measured interference pattern to an image plane [1]. See Fig. 1(c) for an example of such an image.

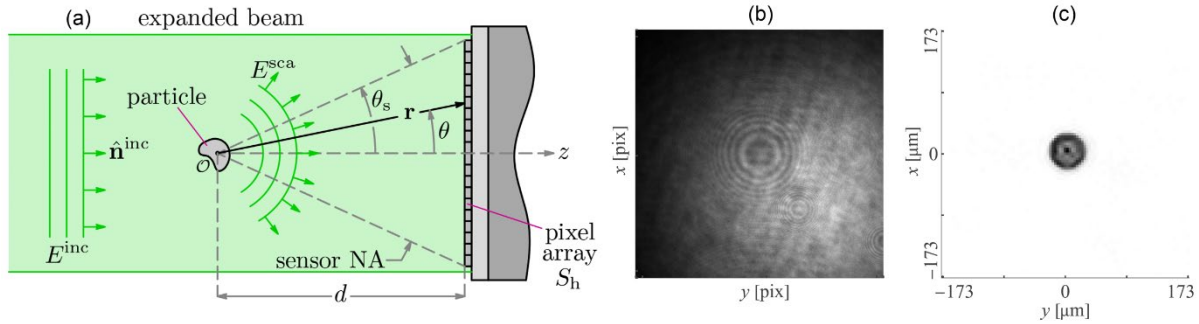

Figure 1: Particle imaging in digital holography. In (a) is the general layout of a simple in-line holography measurement. An example of a measured hologram for a free-flowing 50 μm diameter spherical glass aerosol particle is shown in (b), and in (c) is the particle image resulting from the Fresnel integral [1].

If the holography is carried out with red, green, and blue lasers simultaneously, color images of the particles are possible as well, which can aid particle-material classification efforts [2]. We have applied the method to a variety of aerosols, in both the laboratory and the outdoor environment with a drone-based instrument [3]. We have also improved the image resolution by magnifying the hologram with a bi-telecentric lens. That method permits imaging particles as small as 1 μm [4]. The talk will give an overview of our work in this area and describe how we are advancing the capabilities of digital in-line holography in our ongoing research.

[1] M. J. Berg, J. Aerosol Sci. **165**, 106023 (2022).

[2] R. Giri and M. J. Berg, *Sci. Rep.* **13**, 1594 (2023).

[3] O. Kemppinen, J. C. Laning, R. D. Mersmann, G. Videen, and M. J. Berg, *Sci. Rep.* **10**, 16085 (2020).

[4] M. J. Berg, J. Jacquot, J. M. Harris, and X. Shen, *Opt. Lett.* **49**(10) 2653 (2024).

Analytical prediction of scattering properties of non-spherical dust particles with machine learning

X. Chen[1, 2], J. Wang[1, 2, 3], J. Gomes[1], O. Dubovik[4], Ping Yang[5, 6], Masanori Saito[5]

[1]*Department of Chemical and Biochemical Engineering and Iowa Technology Institute, The University of Iowa, Iowa City, IA 52242, USA.*
[2]*Center for Global and Regional Environmental Research, The University of Iowa, Iowa City, IA 52242, USA.*
[3]*Department of Physics and Astronomy, The University of Iowa, Iowa City, IA 52242, USA.*
[4]*Laboratoire d'Optique Atmosphérique, CNRS–Université de Lille, Lille, 59655, France.*
[5]*Department of Atmospheric Sciences, Texas A&M University, College Station, TX 77843, USA.*
[6]*Department of Oceanography and Department of Physics & Astronomy, Texas A&M University, College Station, TX 77843, USA.*

Dust particles affect both solar and terrestrial radiative transfer, but whether they cool or warm the climate is currently an open question in the literature. Accurate estimation of dust scattering and absorption properties, while critical for climate studies, is hindered by the fact that dust particles have irregular shapes and large size ranges; hence, no single method can be applied for all particle sizes and shapes. Often, a comprehensive look-up-table of these properties is created by combining multiple methods. The application of such databases, however, is cumbersome and inaccurate due to the need for multi-variable interpolation. Furthermore, look-up-table approach lacks mathematical rigor needed to determine the sensitivity (Jacobians) of the single-scattering properties to the dust size, shape, and refractive index that are needed in the remote sensing algorithms. These challenges are tackled here by developing a novel approach within the neural network (NN) framework.

A neural network (NN) model is trained with a database widely used in the aerosol remote sensing community to rapidly predict the single-scattering optical properties of non-spherical dust particles. Analytical solutions for their Jacobians with respect to microphysical properties are derived based on the functional form of the NN. The Jacobian predictions are improved by adding Jacobians from a linearized T-matrix model into the training. Out-of-database testing implies that NN-based predictions perform better than the business-as-usual method that interpolates optical properties from the database. Independent validation further demonstrates the efficacy of the NN-based predictions by reducing computational costs while maintaining accuracy. This work represents the first use of machine learning-based function approximation to computationally expedite the application of the existing non-spherical dust properties database; the resultant NN model can be implemented in atmospheric models and satellite retrieval algorithms with high accuracy, computational efficiency, and the rigor of analytical solutions.

OLALA – Optical Lab for Lidar Applications

Moritz Haarig[1,*], Esha Semwal[1], Thomas Oppermann[1], Markus Hartmann[1], Ronny Engelmann[1], Dietrich Althausen[1], Heike Wex[1], Albert Ansmann[1], Ulla Wandinger[1], and Andreas Macke[1]

[1] *Leibniz Institute for Tropospheric Research – Leipzig, Germany (*haarig@tropos.de)*

Lidar systems are the only tools to provide continuously and height-resolved the optical properties of the atmospheric constituents. The observation geometry requires measurements at exact backscatter, i.e., at 180° scattering angle. Meanwhile, most lidar systems are able to detect the depolarization ratio, which represents the ratio of cross-polarized to co-polarized backscattered light. The depolarization ratio contains valuable information about the particle's non-sphericity. Mineral dust particles exhibit enhanced depolarization ratios due to their irregular shape, whereas the rather spherical haze, wet sea-salt and tropospheric biomass-burning smoke particles show a low depolarization ratio in the backscatter direction. The irregular shape of mineral dust particles makes it easy to separate them from other tropospheric aerosol types, but causes difficulties to retrieve the microphysical properties such as the effective radius or number concentration from optical measurements. Thus, optical models including shape parameterizations are utilized to retrieve the microphysical properties.

However, the shape of the mineral dust particles is highly irregular and varies from particle to particle, which makes it difficult to properly consider the shape characteristics in optical models. Comparisons of optical modelling results with lidar field observations have shown discrepancies in the spectral behavior of the backscattering properties such as the depolarization ratio (e.g., [1]). However, precise information on the particle size distribution and/or refractive index was often missing in these comparisons.

Therefore, laboratory studies are necessary to constrain the optical models at a scattering angle of 180°. The Optical Lab for Lidar Applications (OLALA) proposes to study the depolarization ratio at 180° scattering angle of size-selected irregularly-shaped mineral dust particles at several wavelengths. Currently, we are in the process of setting up the laboratory. We expand upon previous research [2,3], especially the ones of [4,5]. On top of these existing approaches, we carefully do a size selection to achieve almost mono-modal size distributions. First promising results for NaCl particles will be presented at the conference by [6]. The laboratory is linked on one hand to the field observations by our lidar systems organized in PollyNET [7], especially to the triple-wavelength polarization lidar at Cabo Verde in the outflow of Saharan dust. And on the other hand, it is linked to the optical modeling of dust particles, e.g., by Josef Gasteiger [8] and Masanori Saito [9].

The concept of the laboratory, some first results and the input from lidar field observations of the spectral slope of the depolarization ratio will be presented at the conference.

[1] T. Oppermann, M.Haarig, M.Saito, A. Walser, B.Weinzierl, U. Wandinger, and A. Macke, ELS XXI (2025).

[2] T. Sakai, T. Nagai, Y. Zaizen and Y. Mano, Appl. Opt., **49**, 4441–4449 (2010).

[3] E. Järvinen, O. Kemppinen, T. Nousiainen, T. Kociok, O. Möhler, T. Leisner and M. Schnaiter, JQSRT, **178**, 192-208 (2016).

[4] A. Miffre, T. Mehri, M. Francis and P. Rairoux, JQSRT, **169**, 79-90 (2016).

[5] A. Miffre, D. Cholleton, C. Noël, and P. Rairoux, AMT, **16**, 403–417 (2023).

[6] E. Semwal, M. Haarig, M Hartmann, R. Engelmann, D. Althausen, H. Wex, T. Oppermann, and M. Saito, ELS XXI (2025).

[7] H. Baars et al., ACP, **16**, 5111–5137 (2016).

[8] J. Gasteiger, M. Wiegner, S. Groß, V. Freudenthaler, C. Toledano, M. Tesche und K. Kandler, Tellus B, **63**, 725–741 (2011).

[9] M. Saito, P. Yang, J. Ding und X. Liu, JAS, **78**(7), 2089-2111 (2021).

Backscattering by Ice Crystals in Artificial Cirrus

Andrew R.D. Smedley[1], Evelyn Hesse[2,*], Harry Ballington[2], Anthony J. Baran[3,2], and Ann R. Webb[1]
[1]*Department of Earth and Environmental Science, University of Manchester – Manchester, UK*
[2]*Dept. of Physics, Astronomy, and Mathematics, University of Hertfordshire – Hatfield, UK*
[3] *Met Office, Exeter, UK*
*(*e.hesse@herts.ac.uk)*

Cirrus clouds, which cover about 30% of the global land area, contribute to the largest determining factors of radiative forcing in the atmosphere. Of particular importance is scattering in the direct backscattering direction, which is used for retrievals from satellites and ground-based instruments. The colour ratio χ, a ratio of the backscattering coefficients at 1.064 and 0.532 µm, has been used to support phase discrimination in mixed phase clouds [1]. By way of laboratory-produced clouds in the Manchester Ice Cloud Chamber [2], we find direct experimental evidence for the near backscatter enhancement in the scattering phase function for a range of crystal habits representative of naturally occurring cirrus ice crystals. Furthermore, the colour ratio has been investigated for clouds consisting of predominantly ice columns, plates and compacts, respectively. The experimental results are compared with modelling results obtained by our Physical Optics Beam Tracer (PBT) model [3].

Best agreement with measured intensity distributions between 175° and 180° was achieved for rounded, slightly rough hexagonal prisms models. The experimentally obtained mean colour ratios for columns, plates and compacts are 0.485, 0.818 and 0.645, respectively. These findings agree broadly with CALIPSO Cloud Physics Lidar measurements [4] and with simulations by Bi et al. [5], who found colour ratio values less than unity with a peak value near 0.7 for columns and 0.8 for plates for random particle orientation. Colour ratios measured within the study presented here increase with particle size, which is consistent with modelling results in [5] and in this study. Furthermore, our modelling results indicate that surface roughness increases the colour ratio compared to smooth pristine hexagonal prisms, whereas particle rounding and indentations decrease it.

[1] Y.Hu, D. Winker, M. Vaughan, B. Lin, A. Omar et al. J. Atmos. Oceanic Technol., **26**, 2293–2309 (2009).
[2] H.R. Smith, P.J. Connolly, A.J. Baran, E. Hesse, A.R.D. Smedley, and A.R. Webb, JQSRT **157**, 106–118 (2015).
[3] H. Ballington, E Hesse JQSRT, **323**,109054 (2024).
[4] M.A. Vaughan, Z. Liu, M.J. McGill, Y. Hu, M.D. Obland JGR, **115**, D14206 (2010).
[5] L. Bi, P. Yang, G.W. Kattawar, B.A. Baum, Y.X. Hu et al. JGR, **114**, D00H08 (2009).

Modelling of lidar-related dust properties during ASKOS campaign, using irregular hexahedral and spheroid shape mixtures

Anna Gialitaki [1,2], Alexandra Tsekeri[1], Matthew O'Callaghan[3], Dimitra Kouklaki[1,4], Kyriaki Papachristopoulou[5], Moritz Haarig[6], Athena Augusta Floutsi[6], Maria Kezoudi[7], Alkistis Papetta[7], Franco Marenco[7], Konrad Kandler[8], Sudharaj Aryasree[8], Melanie Eknayan[8] and Vassilis Amiridis[1]

[1]*National Observatory of Athens, IAASARS, Greece (*togialitaki@noa.gr)*
[2]*School of Physics and Astronomy, Earth Observation Science Group, University of Leicester, UK*
[3]*Institute of Astronomy, University of Cambridge, UK*
[4]*Department of Geology and Geoenvironment, National and Kapodistrian University of Athens, Greece*
[5]*Physikalisch-Meteorologisches Observatorium Davos/World Radiation Center (PMOD/WRC)*
[6]*Leibniz Institute for Tropospheric Research (TROPOS), Leipzig, Germany*
[7]*Climate and Atmosphere Research Centre, The Cyprus Institute, Nicosia, Cyprus*
[8]*Technical University of Darmstadt, Germany*

Vertically-resolved polarimetric remote sensing provides a comprehensive understanding of atmospheric dust properties and effects on radiation, weather and climate. Profiles of dust optical properties such as the lidar ratio (S_p) and depolarization ratio (d_p) derived from lidar observations are sensitive to the aerosol morphology. However, to extract particle microphysical properties from these observations requires the accurate modelling of dust scattering properties. Dust particles appear to be highly-irregular and while complex shape models have been developed to describe them (e.g. [1]), the scattering calculations are expensive in terms of computational power, limiting their applicability.

Thus in most cases, dust shapes are modelled using simplified descriptions such as spheroids. Spheroid mixtures well reproduce the angular dependence of light scattering from dust aerosols, nevertheless deviations are observed, particularly for backscattering [2]. Recent developments show that irregular hexahedral mixtures can better reproduce the measured dust lidar-relevant properties. In all cases, additional assumptions are needed with respect to the distribution of the different particle shapes considered in the ensemble (i.e. a shape distribution).

Herein, we employ mixtures of irregular hexahedrals [3] and spheroids [4] to simulate the spectral dependence of lidar-derived dust d_p and S_p. Since the considered particle shapes are not realistic, we do not constrain the simulations with measured shape distributions, but rather allow the different particle shapes to vary randomly in the mixtures. The size distributions and complex refractive indices considered for the calculations, are provided by collocated AERONET observations and height-resolved, airborne in-situ data, acquired during the ASKOS-ESA campaign, implemented in Mindelo, Cabo Verde [5]. The simulated d_p and S_p for dust particles are evaluated against polarization lidar data from ASKOS and lidar-derived climatological values.

As an independent consistency check of the simulation results, the derived random spheroids/hexahedral mixtures are utilized in radiative transfer calculations to simulate multi-wavelength sky-radiances from AERONET almucantar sequences. The modelled sky radiances are then compared to the co-located sun-photometer measurements.

First results show that the random hexahedral/spheroid mixtures can accurately reproduce the spectral dependence of triple-wavelength d_p and S_p measurements for a selected dust case study of ASKOS, while the results are also within the uncertainty of the corresponding climatological lidar data.

[1] J. Gasteiger, M. Wiegner, S. Groß, V.Freudenthaler, C. Toledano, M. Tesche, K. Kandler, *Tellus B: Chem. Phys. Meteorology*, *63*(4), 725–741 (2011).

[2] O. Dubovik, A. Sinyuk, T. Lapyonok, B.N. Holben, M. Mishchenko, P. Yang, T.F. Eck, H. Volten, O. Muñoz, B. Veihelmann, W.J. van der Zande, J.-F. Leon, M. Sorokin, and I. Slutsker, *J. Geophys.Res.*, *111*(D11), D11208 (2006).

[3] M. Saito, P. Yang, J. Ding and X. Liu, *J. Atm. Scien.*, *78*(7), 2089–2111 (2021).

[4] J. Gasteiger and M. Wiegner, *Geosci. Model Dev.*, *11*(7), 2739–2762 (2018).

[5] E. Marinou, E., et al., "An Overview of the ASKOS Campaign in Cabo Verde", p. 200 in Environmental Sciences Proceedings 26 (2023).

A Vector Radiative Transfer Model for Atmospheric and Oceanic Polarimetric Remote Sensing

Ping Yang[1,2,3,*], Jiachen Ding[1], and Jian Wei[1]

[1]*Dept. of Atmospheric Sciences, Texas A&M University – College Station, Texas, USA (*pyang@tamu.edu)*

[2]*Dept. of Physics & Astronomy, Texas A&M University – College Station, Texas,USA*

[3]*Dept. of Oceanography, Texas A&M University – College Station Texas, USA*

As a core component of inversion algorithms for polarimetric remote sensing, a vector radiative transfer model (VRTM) is required to simulate the transfer of polarized radiation in the atmosphere-ocean coupled system. In recent years, the research community has witnessed a rapid advancement in spaceborne polarimetric remote sensing technologies and theories, including the deployments of new spaceborne polarimeters and the development of new retrieval algorithms. Therefore, there is a pressing need to maintain and improve the vector radiative transfer computational capabilities.

The TAMU-VRTM features: 1) an accurate atmosphere, ocean, and land surface optics model; 2) an accurate and efficient vector radiative transfer solver based on a two-component method; 3) an analytical approach to compute Jacobian matrix using tangent-linear and adjoint methods.

We recently improved the aerosol, ice cloud, and hydrosol optical properties in the TAMU-VRTM. Specifically, we use state-of-the-art light scattering computational methods [3,4] to compute the optical properties of nonspherical ice crystals, and aerosol and hydrosol particles. Meanwhile, we extended the applicability of TAMU-VRTM to scattering layers with aligned particles, such as airborne dust affected by atmospheric electric field.

This presentation will include a brief introduction to TAMU-VRTM [1,2], its recent improvements, and some examples of applications in polarimetric remote sensing. Specifically, our team developed an Oceanic Phytoplankton Single-Scattering Database (OPSD) [5] to model the optical properties of phytoplankton. The OPSD considers an ensemble of an ensemble of ten irregular core-shell particle shapes, covering a broad range of refractive indices and layer thicknesses that represent various phytoplankton morphologies and compositions. We will present an example of using TAMU-VRTM to examine how polarimetric signals at the ocean surface and the top of the atmosphere (TOA) respond to variations in phytoplankton optical properties characterized by the OPSD. These simulated polarization signatures at the TOA will be compared with NASA's Plankton, Aerosol, Cloud, ocean Ecosystem (PACE) satellite polarimetric observations to estimate variations in phytoplankton optical properties.

[1] J. Ding, P. Yang, M. D. King, S. Platnick, X. Liu, K. G. Meyer, and C. Wang, J. Quant. Spectrosc. Radiat. Transf. **239**, 106667 (2019).

[2] J. Ding and P. Yang, J. Atmos. Sci. **80**(1), 73–89 (2023).

[3] P. Yang, J. Ding, R. Lee Panetta, K.-N. Liou, G. W. Kattawar, and M. Mishchenko, Prog. Electromagn. Res. **164**, 27–61 (2019).

[4] J. Ding and P. Yang, Opt Express **31**(24), 40937 (2023).

[5] Y. Zhang, P. Yang, M. Gao, X. Zhang, J. Quant. Spectrosc. Radiat. Transf. under revision

What polarimetry may say about the microphysics of atmospheric aerosols

Evgenij Zubko[1,*] and Gorden Videen[2]

[1]*Planetary Atmospheres Group, Institute for Basic Science (IBS) – Daejeon, Republic of Korea (*evgenij.s.zubko@gmail.com)*

[2]*Space Science Institute – Boulder, CO, USA*

Introduction: When unpolarized sunlight is scattered by aerosols it acquires a partial linear polarization. This polarization is invoked through the microphysics of aerosols and, hence, it could be used for retrieval their size distribution, chemical composition, and shape of target particles at a distance. In practice, however, measuring polarization in single-scattering aerosol particles is not a trivial problem. Indeed, such data cannot be immediately obtained by means of spaceborne measurements and ground-based observations during daytime because of the light-contaminating contribution of the underlying terrain. In this circumstance, extracting the light-scattering response in the single-scattering particles is accompanied with large uncertainties arising from additional modeling of polarization in the underlying terrain and multiple scattering between aerosols and that terrain. On the other hand, a robust result emerge from ground-based measurements in twilight, when the underlying terrain are shadowed; whereas, the aerosols are illuminated by direct sunlight. A recent polarimetric survey of the atmosphere in twilight over the Ussuriysk Astrophysical Observatory (Russia) has provided an extended dataset on polarization of single-scattering aerosol particles [1]. Aerosol particles nearly always reveal negative polarization near backscattering (i.e., $P < 0$), where the scattering angle $\theta < 150°$. On the contrary, at side scattering, polarization always takes a positive value ($P > 0$), which reaches its maximum at $\theta \sim 90°$.

Although the light-scattering response is dependent on several microphysical characteristics, their impact is not equally strong. Surprisingly, the least important effect arises from the aerosol particle shape [2,3]. While there is indeed a dramatic difference between light scattering from a single perfect sphere and irregularly shaped particles, such a difference is significantly dampened when considering two different types of irregularly shaped particles whose morphology attains a high level of disorder. For instance, the size distribution of forsterite particles inferred from their polarimetric response appears to be hardly affected by the specific choice model of irregular particles [3].

The polarimetric response has a greater dependence on the real part of refractive index Re(m). For example, one can discriminate in practice between water-ice particles and mineral dust particles. Lower value of Re(m) places the minimum value of the negative polarization at larger scattering angle θ (i.e., closer to the backscattering direction) [4]. Furthermore, the particles with lower Re(m) yield a stronger polarization maximum at side scattering that tends to be shifted toward backscattering $\theta > 90°$. Interestingly, when the size distribution of aerosols is abundant in small particles, it also gives raise to the polarization maximum. However, unlike water-ice particles, the small particles produce their polarization maximum at $\theta = 90°$ and dampen the phenomenon of negative polarization near backscattering [2].

The strongest effect on the polarimetric response is produced by the imaginary part of refractive index Im(m). For instance, an increase of material absorption to Im(m) ≥ 0.1 causes almost a complete disappearance of the negative polarization, making it possible to discrimination between water-ice/mineral-dust particles and black-carbon particles. Similar to the real part of refractive index and size distribution, the growing Im(m) increases the amplitude of positive polarization. However, at large values of Im(m), the polarization maximum appears to be shifted toward forward scattering, $\theta < 90°$, resolving this ambiguity. Using these discriminative features, one can interpret the polarimetric measurements of atmospheric aerosols with high confidence.

[1] E. Zubko, M. Zheltobryukhov, E. Chornaya, K.A. Shmirko, V.V. Lisitsa, A.N. Pavlov, A. Kochergin, G. Kornienko, and G. Videen, Front. Remote Sens. **4**, 1321621 (2023).

[2] E. Zubko, Yu. Shkuratov, and G. Videen, J. Quant. Spectrosc. Radiat. Transfer **150**, 42 (2015).

[3] E. Zubko, J. Quant. Spectrosc. Radiat. Transfer **323**, 109053 (2024).

[4] E. Zubko, G. Videen, and Yu. Shkuratov, J. Quant. Spectrosc. Radiat. Transfer **151**, 38 (2015).

Light scattering and absorption by black carbon during atmospheric aging

Renyi Zhang

Department of Atmospheric Sciences, Texas A&M University – College Station, USA

*(*Renyi-zhang@tamu.edu*)*

Abstract: Atmospheric aerosols scatter and absorb solar radiation, directly affecting the Earth's radiative budget. In particular, absorption of solar radiation by black carbon (BC) particles represents a central issue in climate research, since BC is the second most important global warming agent after carbon dioxide. Understanding the aging and associated variations in the optical properties of BC particles is complex, and the available results on absorption enhancement are highly conflicting. Here I present experimental, theoretical, and field measurement studies to reveal that BC light absorption is highly enhanced due to rapid coating by organic and inorganic species under polluted conditions. BC aging exhibits two distinct stages, i.e., initial transformation from a fractal to spherical morphology with little absorption variation and subsequent growth of fully compact particles with a large absorption enhancement. Our results reveal that the BC direct radiative forcing is dependent on the rate and timescale of aging, which were unaccounted for in atmospheric models. Such absorption enhancement leads to atmospheric stabilization and a diminished diurnal variation of the planetary boundary layer, exacerbating pollution development. Using an innovative upscale approach, our result provides a refined estimate of the BC direct radiative forcing, with a value of 0.77 W·m^{-2} (in comparison to 2.2 W m^{-2} for carbon dioxide).

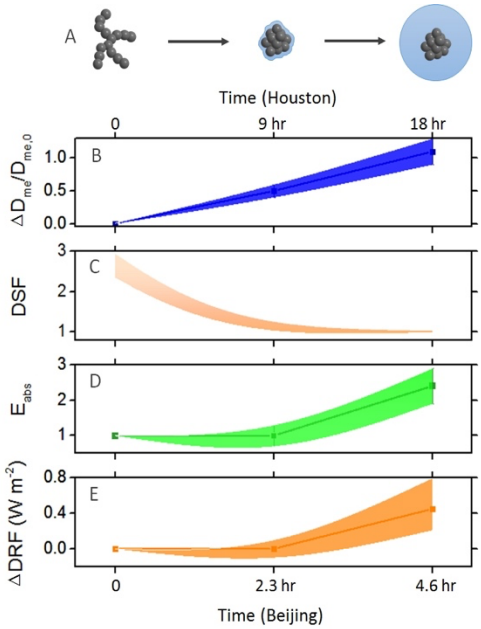

Figure 1: Enhanced light absorption due to BC morphological change.

Laboratory Measurement of the Depolarization Ratio of Size Selected Salt Particles at 180° Scattering Angle

Esha Semwal[1,*], Moritz Haarig[1], Markus Hartmann[1], Ronny Engelmann[1], Dietrich Althausen[1], Heike Wex[1], Thomas Oppermann[1], Masanori Saito[2]

[1]*Leibniz Institute for Tropospheric Research, Leipzig, Germany (*semwal@tropos.de)*
[2]*Department of Atmospheric Science, University of Wyoming, USA*

The study of light backscattering by atmospheric aerosols is essential for understanding their impact on climate, air quality, weather, and atmospheric dynamics. Lidar systems provide height-resolved bulk optical properties of atmospheric aerosols at a scattering angle of 180°. However, these atmospheric measurements do not directly reveal the physical and chemical characteristics of individual aerosol types. To overcome this, theoretical scattering models are used to derive the microphysical properties of aerosols from their optical properties. The greatest challenge in this process arises with irregularly shaped aerosol particles, as their complex shapes are difficult to represent accurately in the optical models. Over the past decades, several optical models [1-2] have been developed, but they remain inadequate in accurately describing the spectral dependence of polarization properties of non-spherical particles.

The Leibniz junior research group OLALA (Optical Lab for Lidar Applications) intends to solve this problem by constructing a new scattering laboratory to measure the depolarization ratio at exactly 180° scattering angle of size-selected non-spherical aerosol particles at the Leibniz Institute for Tropospheric Research. The laboratory studies will allow us to perform controlled, repeatable, and precise investigation of aerosol properties, which will help to refine the accuracy and interpretation of lidar observations and optical models. We intend to conduct measurements using size-selected natural mineral dust samples due to their highly irregular particle shapes. The setup currently uses a single wavelength of 532 nm. However, it will be extended to cover the full triple-wavelength (355, 532 and 1064 nm) capabilities for linear polarization and circular polarization, enabling ellipsometry measurements of irregularly shaped aerosol particles by the end of this year.

Here we present the first laboratory results of OLALA using NaCl particles. NaCl particles are also non-spherical but have a less complex structure. Under low humidity, NaCl crystallizes into cubic shapes which results in an enhanced depolarization ratio [3]. [3] observed a depolarization ratio of 21 % for an ensemble of NaCl particles with a mode diameter of 240 nm. But we study the depolarization ratio of size selected NaCl particles with sizes between 200 and 800 nm. The measured depolarization ratio of three different sizes of NaCl at 532 nm in the laboratory will be compared to modeling results using a cubic version of the irregular hexahedra proposed by [2] with the refractive index of NaCl. It is work in progress and the latest results will be presented at the conference.

[1] J. GASTEIGER et al., “Modelling lidar-relevant optical properties of complex mineral dust aerosols,” Tellus B, vol. 63, no. 4, pp. 725–741, 2011.

[2] M. Saito, P. Yang, J. Ding, and X. Liu, “A Comprehensive Database of the Optical Properties of Irregular Aerosol Particles for Radiative Transfer Simulations,” J Atmos Sci, vol. 78, no. 7, pp. 2089–2111, 2021.

[3] T. Sakai, T. Nagai, Y. Zaizen, and Y. Mano, “Backscattering linear depolarization ratio measurements of mineral, sea-salt, and ammonium sulfate particles simulated in a laboratory chamber,” Appl. Opt., vol. 49, no. 23, pp. 4441–4449, Aug. 2010.

Simulation of the polarized reflectance at TOA over ocean for satellite in-flight polarimetric calibration

Lili Qie,[1,*] Mengyao Zhu,[1] Hua Xu,[1] Yisong Xie, [1] and Zhengqiang Li[1]

[1] *Aerospace Information Research Institute, Chinese Academy of Sciences, – Beijing, China (*qiell@aircas.ac.cn)*

Polarimetric observation is an important atmospheric detection method. Numerous of space-borne polarimetric instruments have been developed or scheduled for launch to monitor global atmospheric changes, such as the DPC, POSP, SpexOne, HARP, 3MI, etc. Accurate in-flight polarimetric measurement of these polarimetric sensors is required for the aerosols and clouds' multi-parameters retrievals. The vicarious calibration methods using Earth reference scenes are essential for these satellite polarimeters that both are equipped with onboard polarimetric calibration system or not, to validate the polarization measurements or verify the onboard polarimetric calibration results.

The principle of vicarious calibration is comparing the polarization simulation with actual satellite measurement over natural targets that can be well characterized with radiative models. The sun glint over ocean has been proven to be a valuable natural polarization calibration target because it is strongly polarized, and its intrinsic polarization characteristics can be accurately simulated with models. For the area outside sun glint over ocean, the molecular Rayleigh scattering is the main process contributing to the TOA signal at the short visible spectral band, which may be a potential natural target for satellite in-flight polarimetric calibration. Assuming clear water and atmosphere, low aerosol content, low wind speed, viewing conditions within the glint spot (sun glint angle (SGA) $\leqslant$ 40°) and far away from the glint (SGA$\geqslant$60°), separately, the radiance and polarized radiance observed over ocean can be theoretical predicted by a coupled atmosphere–ocean system radiative transfer model, which allows polarimetric calibration of the sensors. Meanwhile, the accuracy of polarization simulation is affected by several atmospheric and oceanic surface factors and depends on the specific solar-viewing geometry and wavelength. In this study, the sensitivity of the degree of linear polarization (DOLP) at the TOA to the uncertainties of aerosol optical depth (AOD), aerosol model (AM), absorption gases content (CWV, O3), sea surface instantaneous wind speed (WS), chlorophyll concentration (Chl) under different solar-viewing geometries is analyzed via radiative transfer simulation. For the sun glint condition, the error budget indicates that aerosols and wind speed are the main error factors for polarization calibration, while the uncertainties of Chl and absorbing gases can be disregarded. The total DOLP error increases with the solar zenith angle (SZA) and viewing zenith angle (VZA) (i.e., the increase of atmospheric optical path), and SGA. For the Rayleigh scattering condition, the AOD and AM are the main error factors for polarization calibration, while the uncertainties of wind speed, Chl and absorbing gases can be approximatively neglected. The total DOLP error increases with wavelength rapidly, the DOLP error at 670 nm is twice of that at 490 nm. The DOLP error is mainly dominated by the scattering angle (SCA) and increases with the SZA and VZA very slightly. Then optimized solar-viewing geometry screening strategy for both sun glint and Rayleigh scattering conditions is proposed to ensure that the simulated DOLP error is limited to 0.02.

At last, the selected sun glint and Rayleigh scattering targets over six oceanic calibration sites are used for the in-flight DOLP calibration of DPC/GF-5(02), separately. The results show that, the proposed screening strategies of both sun glint and Rayleigh scattering conditions provide small standard error of calibration samples, which indicate stable calibration results can be obtained for both vicarious polarimetric calibration methods. This research presents theoretic guide for screening the calibration samples of satellite in-flight polarimetric calibration, using the sun glint and Rayleigh scattering over ocean.

[1] B. Toubbe, T. Bailleul, J. L. Deuze et al., IEEE Transactions on Geoscience and Remote Sensing **37**, 513 (1999).

[2] Z. Li, W. Hou, J. Hong et al., Journal of Quantitative Spectroscopy and Radiative Transfer 218, 21 (2018).

Reproduce the backscatter of dust using realistic dust shapes

Alexandra Tsekeri,[1,*] Anna Gialitaki,[1] Matthew O' Callaghan[1,2], Thanasis Georgiou[1], Josef Gasteiger[3], Alexander Konoshonkin[4], Natalia Kustova[4], Maxim Yurkin[5], Eleni Marinou[1], Maria Kezoudi[6], Franco Marenco[6], Alkistis Papetta[6], Sudharaj Aryasree[7], Konrad Kandler[7], Moritz Haaring[8], Athena Floutsi[8], Holger Baars[8], Amin Nehrir[9], James Collins[9], Ewan Crosbie[9], Rory Barton-Grimley[9], Edward P. Nowottnick[10], Bernadett Weinzierl[11], and Vassilis Amiridis[1]

[1] *IAASARS, National Observatory of Athens, Athens, Greece (*atsekeri@noa.gr), [2]Institute of Astronomy, University of Cambridge, Cambridge, UK, [3] Hamtec Consulting GmbH, EUMETSAT, Darmstadt, Germany, [4] V. E. Zuev Institute of Atmospheric Optics SB RAS, Tomsk, Russia, [5] Center for Energy, Environment and Economy, Ozyegin University, Cekmekoy, Istanbul, Turkey, [6] Climate and Atmosphere research Centre (CARE-C), The Cyprus Institute, Nicosia, Cyprus, [7]Institute of Applied Geosciences, Technical University of Darmstadt, Darmstadt, Germany, [8]Leibniz Institute for Tropospheric Research, Leipzig, Germany, [9]NASA Langley Research Center, Hampton, VA, [10]NASA Goddard Space Flight Center, Greenbelt, Maryland, [11]Faculty of Physics, Aerosol Physics and Environmental Physics, University of Vienna, Vienna, Austria*

The accurate modelling of the optical properties of atmospheric mineral dust particles is an open scientific question, particularly for the backscatter, mainly due to the irregular shape and large size of the particles. Scattering calculations considering realistic irregular shapes are computationally costly, and as of yet, are provided in tabulated form, only from the MOPSMAP scattering database [1], for (cross-section-equivalent) size parameters up to 30, for the irregular shapes presented in Gasteiger et al. [2], using the ADDA code [3].

We have extended these calculations to size parameters up to 68, for four dust refractive indices ((1.48-1.6) + i(0-0.002)). We calculated the backscatter properties for dust particles in Cabo Verde, during the ASKOS-ESA and CPEX-CV campaigns in June and September 2022 [4], using airborne in-situ size and aspect ratio distributions, and we compare them with ground-based and airborne lidar measurements at 1064 nm (Fig. 1). The comparisons show good agreement, and improvement compared to the calculations using spheroids. More comparisons from previous and on-going campaigns are also foreseen.

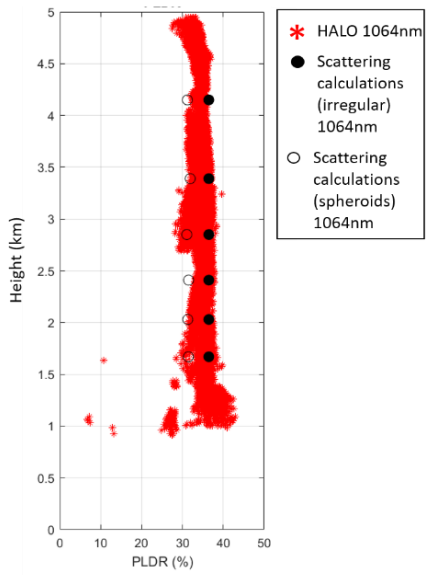

Figure 1: Comparison of particle linear depolarization ratio (PLDR) at 1064 nm, calculated using realistic irregular shapes (black circles) and spheroids (open circles), and measured with the HALO HSRL lidar [8] (red), during ASKOS-ESA and CPEX-CV campaigns.

For size parameters >70 (super-coarse dust particles) the ADDA calculations are challenging even for high-performance computing (HPC) systems, due to the large number of dipoles and very slow convergence of the iterative solver [3]. Thus, in order to formulate a complete (back)scattering database for dust we further investigate:

- The applicability of the much faster Physical Optics (PO) approximation [5] for dust particles with faceted shapes.
- The modelling of the optical properties of the irregular-shaped particles, using mixtures of spheres, spheroids (from MOPSMAP) and hexahedrals (from TAMUdust2020 [6]), as shown in O' Callaghan et al. [7].

[1] J. Gasteiger and M. Wiegner, Geosci. Model Dev., **11**, 2739 (2018). **[2]** J.M. Gasteiger, et al., Tellus B **63**, 725 (2011). **[3]** M.A. Yurkin and A. G., Hoekstra, J. Quant. Spectrosc. Radiat. **112**, 2234 (2011). **[4]** E. Marinou, et al., "An Overview of the ASKOS Campaign in Cabo Verde", p. 200 in *Environmental Sciences Proceedings* 26 (2023). **[5]** A. Konoshonkin, et al., J. Quant. Spectrosc. Radiat. Transf. **195**, 132 (2017). **[6]** M. Saito, et al., Journal of the Atmospheric Sciences, **78**(7), 2089 (2021). **[7]** M. O' Callaghan, "Approaching the optical properties of irregularly shaped particles through numerical methods and simpler ensembles", *ELS XXI* (2025). **[8]** B. J. Carroll, et al., Atmos. Meas. Tech., **15**, 605 (2022).

Analytical prediction of scattering properties of non-spherical dust particles with machine learning

X. Chen[1, 2], J. Wang[1, 2, 3], J. Gomes[1], O. Dubovik[4], Ping Yang[5, 6], Masanori Saito[5]

[1]*Department of Chemical and Biochemical Engineering and Iowa Technology Institute, The University of Iowa, Iowa City, IA 52242, USA.*
[2]*Center for Global and Regional Environmental Research, The University of Iowa, Iowa City, IA 52242, USA.*
[3]*Department of Physics and Astronomy, The University of Iowa, Iowa City, IA 52242, USA.*
[4]*Laboratoire d'Optique Atmosphérique, CNRS–Université de Lille, Lille, 59655, France.*
[5]*Department of Atmospheric Sciences, Texas A&M University, College Station, TX 77843, USA.*
[6]*Department of Oceanography and Department of Physics & Astronomy, Texas A&M University, College Station, TX 77843, USA.*

Dust particles affect both solar and terrestrial radiative transfer, but whether they cool or warm the climate is currently an open question in the literature. Accurate estimation of dust scattering and absorption properties, while critical for climate studies, is hindered by the fact that dust particles have irregular shapes and large size ranges; hence, no single method can be applied for all particle sizes and shapes. Often, a comprehensive look-up-table of these properties is created by combining multiple methods. The application of such databases, however, is cumbersome and inaccurate due to the need for multi-variable interpolation. Furthermore, look-up-table approach lacks mathematical rigor needed to determine the sensitivity (Jacobians) of the single-scattering properties to the dust size, shape, and refractive index that are needed in the remote sensing algorithms. These challenges are tackled here by developing a novel approach within the neural network (NN) framework.

A neural network (NN) model is trained with a database widely used in the aerosol remote sensing community to rapidly predict the single-scattering optical properties of non-spherical dust particles. Analytical solutions for their Jacobians with respect to microphysical properties are derived based on the functional form of the NN. The Jacobian predictions are improved by adding Jacobians from a linearized T-matrix model into the training. Out-of-database testing implies that NN-based predictions perform better than the business-as-usual method that interpolates optical properties from the database. Independent validation further demonstrates the efficacy of the NN-based predictions by reducing computational costs while maintaining accuracy. This work represents the first use of machine learning-based function approximation to computationally expedite the application of the existing non-spherical dust properties database; the resultant NN model can be implemented in atmospheric models and satellite retrieval algorithms with high accuracy, computational efficiency, and the rigor of analytical solutions.

A Markov Chain Solution to Polarized Infrared Radiative Transfer in an Optically Anisotropic Media

Feng Xu[1,*], Congcong Qiao[1], Braxton C. Gosvener[1], Benting Chen[1], Lan Gao[1], Olga V. Kalashnikova[2], Anthony B. Davis[2], David J. Diner[2], W. Reed Espinosa[3], Jie Gong[3], and Zhao-Cheng Zeng[4]

[1]*School of Meteorology, University of Oklahoma, Norman (OK), USA (fengxu@ou.edu)*

[2]*Jet Propulsion Laboratory, California Institute of Technology, Pasadena (CA), USA*

[3]*NASA Goddard Space Flight Center, Greenbelt (MD), USA*

[4]*Institute of Remote Sensing and GIS, Peking University, Beijing, China*

The polarization state of atmospheric radiation contains abundant information about aerosol and cloud particle properties. To assist in the combined use of reflected and emitted radiation for dust and cloud remote sensing, we extended our shortwave Markov chain approach towards modeling polarized infrared radiative transfer in an optically isotropic or anisotropic plane-parallel atmosphere. A multi-steam scheme is adopted to resolve the angular dependence of total radiance and polarized radiance. Our model accounts for atmospheric emission, scattering, and absorption, as well as directional surface emission and reflection. Non-spherical particles with random and preferred orientations are considered. A comparison of numerical outcomes with those obtained from the adding-doubling method shows a high degree of agreement for both intensity and linear polarization. Using several MODIS infrared channels as references, simulation is performed for mid-latitude summer reference atmospheres which contain dust particles, water droplets, and ice particles of preferred or random orientations. These reference atmospheres are overlaid on either ocean or land surfaces. Numerical simulations demonstrate that particle orientation and non-sphericity significantly affect the vertically and horizontally polarized components of infrared signals, which could have potential applications in remote sensing. By contrast, infrared radiances, which are often measured in terms of brightness temperature, are less affected.

[1] R. P. Feynman, M. Gell-Mann, and G. Zweig, Phys. Rev. Lett. **13**, 678 (1964).

[2] D. F. Edwards, "Silicon (Si)", p. 547 in *Handbook of optical constants of solids*, ed. E. D. Palik (Academic, 1997).

[3] F. Ladouceur and J. Love, *Silica-based buried channel waveguides and devices* (Chapman & Hall, 1995), Chap. 8.

[4] Author(s), "Title of paper", p. 12 in *Title of Proceeding* (Institute of Electrical and Electronics Engineers, 2023).

Effect of complex refractive index on the scattering matrix of dust aerosols with narrow particle size distributions

Julia Martikainen[1,*], Olga Muñoz[1], Juan Carlos Gómez Martín[1], María Passas Varo[1], Teresa Jardiel[2], Marco Peiteado[2], Yannick Willame[3], Lori Neary[3], Tim Becker[4], and Gerhard Wurm[4]

[1] *Instituto de Astrofísica de Andalucía (IAA), CSIC – Granada, Spain (*juliamar@iaa.es)*

[2] *Instituto de Cerámica y Vidrio– Madrid, Spain*

[3] *Belgian Institute for Space Aeronomy (IASB-BIRA) – Brussels, Belgium*

[4] *University of Duisburg-Essen, Faculty of Physics – Duisburg, Germany*

The optical properties of aerosols play a crucial role in radiative transfer and atmospheric modeling, particularly for planetary atmospheres such as that of Mars. We investigate the effect of the complex refractive index on the scattering matrix of Martian analog aerosols as a function of particle size. We conducted measurements on three well-characterised Martian dust simulants —JSC Mars-1, MGS-1, and MMS-2—each with narrow particle size distributions. The scattering matrix elements were obtained using a nephelometer at the IAA Cosmic Dust Laboratory (CODULAB) in Granada, Spain [1]. Measurements were performed at two wavelengths, 488 nm and 640 nm, covering a broad scattering angle range.

To complement our experimental results, we used the TAMUdust2020 single-scattering property database [2], which is based on hexahedral particle models, to simulate the scattering behavior of Martian dust analogs. This approach allowed us to assess the influence of particle shape and complex refractive index on the polarisation and phase function characteristics observed in our measurements. Our findings highlight the sensitivity of the scattering matrix elements to both size and composition, providing new insights into the scattering patterns of dust aerosols. These results contribute to refining radiative transfer models and improving our understanding of dust-related atmospheric processes on Mars.

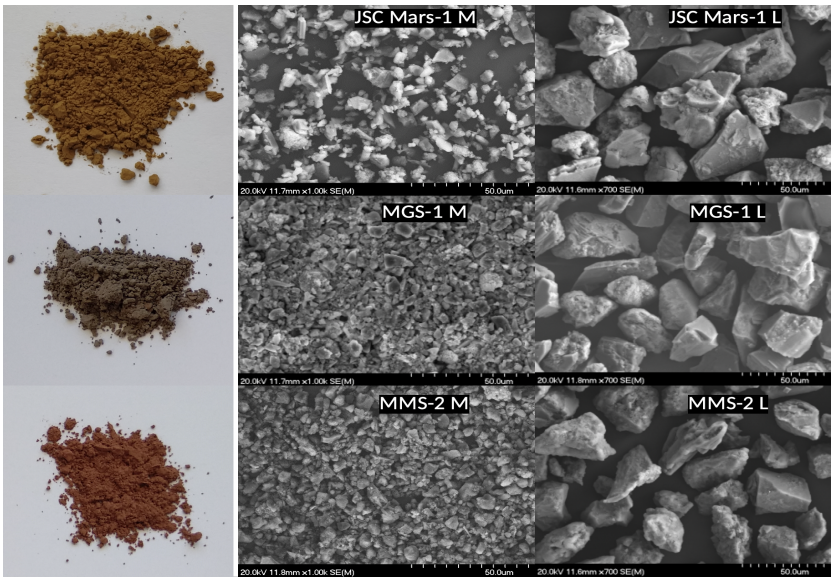

Figure 1: The images of the JSC Mars-1 (top), MGS-1 (middle), and MMS-2 (bottom) analog, along with the SEM images of their L and M narrow size distributions [3].

[1] O. Muñoz et al., 2025, Journal of Quantitative Spectroscopy and Radiative Transfer, 331, 109252

[2] M. Saito et al., 2021, Journal of the Atmospheric Sciences, 78, 2089

[3] J. Martikainen et al., 2025, Monthly Notices of the Royal Astronomical Society, Accepted

ScIce: Light Scattering Database for Ice Crystals of Cirrus Clouds

Alexander Konoshonkin,[1,2,3]* Ilia Tkachev,[1] Natalia Kustova,[1] Dmitriy Timofeev,[1] and Zhenzhu Wang [3]

[1] *V.E. Zuev Institute of Atmospheric Optics – Tomsk, Russia (*a.kon@iao.ru)*
[2] *Dept. of Engineering, Tomsk State University – Tomsk, Russia*
[3]Anhui Institute of Optics and Fine Mechanics, HFIPS, CAS – Hefei, China

Cirrus clouds have a significant impact on the planet's climate by affecting the radiative balance[1,2]. However, their optical properties are not well understood due to the unresolved issue of light scattering by large non-spherical particles[3]. This poses challenges in interpreting experimental data obtained through remote sensing instruments and hinders the development of an accurate optical model for cloud assimilation into radiation transfer models.

Until recently, the problem of light scattering by large non-spherical particles could not be solved due to the limitations of rigorous numerical methods for such particles[4]. On the other hand, the solution obtained using the geometrical optics approximation for ice crystal particles contains a singularity in the backscattering direction. Only recently the physical optics method has been developed, allowing us to address the light scattering problem for large non-spherical particles commonly found in cirrus clouds, taking into account the particle orientation.

This report presents a database of light backscattering matrices calculated for all typical ice crystal shapes of cirrus clouds, excluding particle aggregates. A unique feature of this database, apart from existing ones, is that it provides solutions for the entire range of particle sizes from 0.1 to 10000 μm for all three most commonly used lidar wavelengths: 0.355, 0.532, and 1.064 μm. Such a database is crucial for developing algorithms to interpret laser sounding data of cirrus clouds using both ground-based and space-borne lidars. The database is available in open access in a simple text format to facilitate its utilization by a broad spectrum of scientists.

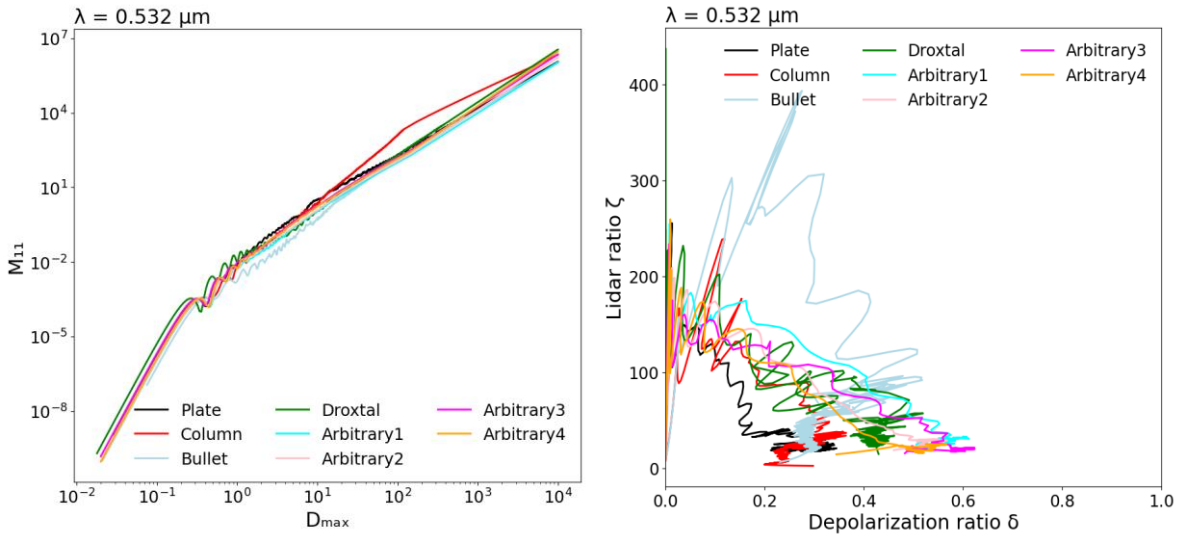

Figure 1: The example of the database (left) and the lidar properties calculated based on the database (right).

[1] K. N. Liou, "Influence of Cirrus Clouds on Weather and Climate Processes: A Global Perspective," Mon. Weather Rev., 114(6), 1167–1199, (1986).

[2] The Intergovernmental Panel on Climate Change, *Climate change 2007 – The Physical Science Basis* (Cambridge University Press, 2007).

[3] K.-N. Liou, P. Yang, Light Scattering by Ice Crystals (Cambridge University Press, 2016).

[4] A. J. Baran, "A review of the light scattering properties of cirrus," J. Quant. Spectr. Radiat. Transfer 110(14-16), 1239–1260, (2009).

Scattering and absorption of light synoptically modeled for particulate planetary surfaces

Karri Muinonen,[1]* Antti Penttilä,[1] Anne Virkki,[1,2] Yehor Surkov,[1] Zuri Gray,[1] Ari Leppälä,[1]Vesa Björn,[1]
Mikko Vuori,[1] Hanna Pentikäinen,[1] Olga Munoz,[3] Elisa Frattin,[3]
Julia Martikainen,[3] Francisco Garcia-Izquierdo,[3] Johannes Markkanen,[4]
Yuriy G. Shkuratov,[5] and Gorden Videen[6]

[1]*Dept. of Physics, University of Helsinki, Finland (*karri.muinonen@helsinki.fi)*
[2]*Finnish Geospatial Research Institute FGI, National Land Survey of Finland, Espoo, Finland*
[3]*Instituto de Astrofisica de Andalucia, Glorieta de la Astronomia, Granada, Spain*
[4]*Institut für Geophysik und Extraterrestrische Physik, Technische Universität Braunschweig, Germany*
[5]*Institute of Astronomy, Kharkiv National University, Kharkiv, Ukraine*
[6]*Space Science Institute, Boulder (CO), USA*

Introduction: Scattering and absorption of light in macroscopic discrete random media of densely packed particles constitutes a computational challenge in electromagnetics described by the Maxwell equations. As a remedy, a computational pipeline is outlined, consisting of a number of separate computational steps. As a starting point, it is advantageous to make use of ensemble-averaged scattering and absorption characteristics, including experimentally measured or numerically computed scattering matrices. This is enabled by the recently extended radiative-transfer and coherent-backscattering methods [RT-CB; 1, 2] and by presenting the scattering matrices in a parameterized empirical form (Muinonen & Leppälä, in preparation).

Methods and models: In more detail, first, empirical scattering matrix models are systematically derived for the measured scattering matrices in the Granada-Amsterdam Light Scattering Database [3]. Second, concerning particles in the wavelength scale or smaller, the empirical matrices are transformed into first-order incoherent volume-element matrices. This is accomplished with the help of the Mie scattering and absorption characteristics for the particle size distributions of the database samples. Third, utilization of asymptotically exact computations (like those with the Discrete-Dipole Approximation codes) for particulate media and volume elements described by using the Voronoi tessellation allows for more fundamental theoretical studies. Fourth, scattering and absorption by particles large compared to the wavelength can be incorporated by using their characteristics computed in the geometric optics approximation. Finally, fifth, the volume porosity and surface roughness of the particulate medium can be accounted for by tracing rays in explicit geometric models for the particulate media.

Results: Example modeling is highlighted for the single and multiple scattering of feldspar samples by using the Granada-Amsterdam [4] and Kharkiv measurements [5], respectively. Finally, lunar photometry and polarimetry is addressed by using the pipeline described above [see also, 6].

[1] K. Muinonen, A. Penttilä, JQSRT **324**, 109058, 8 pp. (2024).
[2] K. Muinonen, A. Leppälä, J. Markkanen, JQSRT **330**, 109226, 12 pp. (2025).
[3] O. Munoz, F. Moreno, D. Guirado, D. D. Dabrowska, H. Volten, J. W. Hovenier, JQSRT **113**, 565-574 (2012).
[4] H. Volten, O. Munoz, E. Rol, J. F. de Haan, W. Vassem, J. W. Hovenier, K. Muinonen, T. Nousiainen, JGR **106**, D15, 17375-17401 (2001).
[5] Y. Shkuratov, S. Bondarenko, A. Ovcharenko, C. Pieters, T. Hiroi, H. Volten, O. Munoz, G. Videen, JQSRT **100**, 340-358 (2006).
[6] Y. Shkuratov, G. Videen, V. Kaydash, *Optics of the Moon* (Elsevier, 2025).

Microwave scattering by rough polyhedral particles on a surface

Anne K. Virkki,[1,2,*] and Maxim A. Yurkin[3]

[1]*University of Helsinki – Helsinki, Finland (*anne.virkki@helsinki.fi)*
[2]*Finnish Geospatial Research Institute, National Land Survey – Espoo, Finland*
[3]*Université Rouen Normandie, INSA Rouen, CNRS, CORIA UMR 6614 – Rouen, France*

Background: The electromagnetic (EM) scattering by non-symmetric wavelength-scale particles on a planar surface has numerous applications in the remote sensing of planetary bodies, both in planetary and geosciences. Here, we simulate microwave scattering by regolith surfaces of planetary bodies by assuming wavelength-scale particles laying on top of a substrate of fine-grained regolith that forms a homogeneous, semi-infinite volume with a planar interface. The primary goal is to inform the interpretation of microwave-remote-sensing observations through a better understanding of the roles of the various physical properties of the surface, including the material, shape, and size-frequency distribution (SFD). Although the focus of the study is on the microwave regime, the results may be of interest at optical wavelengths as well. The presentation is based on [1].

Methods: We conducted numerical simulations of EM scattering by rough polyhedral particles (with 12 or 20 faces) using the discrete-dipole approximation (ADDA code) and contrast the results to that of spheres. The particles have refractive indices (m) corresponding to common minerals in the microwave regime (from 2.17 + 0.004i to 2.79 + 0.0155i), and an SFD consistent with the observed scattering properties: a power-law distribution of size parameters ($x = 2\pi r/\lambda$, where r and λ are respectively the radius and wavelength) between 0.5 and 8 with a power-law index from –2.5 to –3.5. The assumed substrate refractive index 1.55 + 0.004i corresponds to powdered regolith. The simulations were conducted from incidence angle $\theta_i = 0°$ to $\theta_i = 60°$. Example results for the scattering matrix element F_{11} when $x = 3$ and 6 are shown in Fig. 1. The results also include contrasting the scattering properties of surface particles to those in free space to quantify the role of the particle–surface interaction.

Results: The particle roundness and SFD have a clearly observable effect on the polarimetric properties, while the role of permittivity is relatively minor (in the studied range). Among various backscattering observables, the circular polarization ratio is the least sensitive to the decrease of the upper boundary (down to a size parameter of 3) and the index of the SFD. The particles in free space display similar polarimetric properties as those on a surface at incidence angles near 40°–50°. We also find that at high incidence ($\theta_i \geq 60°$), the average scattering profiles of rounder particles do not fully follow the symmetries known to exist for ensembles of particles in free space.

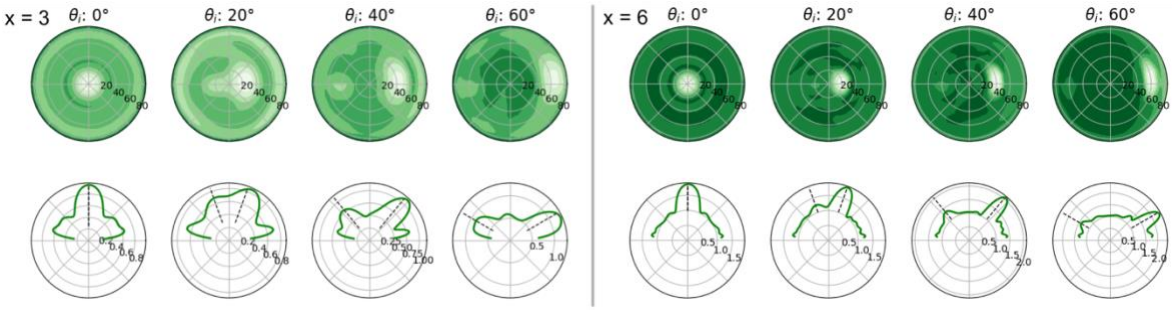

Figure 1: The angular distribution of $\log_{10}\mathrm{F}_{11}$ in the zenith view for azimuthally and ensemble-averaged scattering matrices of 12-face polyhedrons with $\mathrm{m} = 2.17 + 0.004\mathrm{i}$, when $x = 3$ (on the left) or 6 (on the right) and the incidence angle increases from 0° to 60° (columns from left to right as labeled). The top row shows the zenith view, and the bottom row shows the vertical scattering plane, which corresponds to the horizontal middle line in the zenith view. The incidence approaches from the left for all $\theta_i > 0°$. The values by each concentric circle in the zenith view display the angular extent: [0°,80°] from the zenith. The lighter shades depict larger values.

[1] A. K. Virkki and M. A. Yurkin, 2025, In review. ArXiv: http://arxiv.org/abs/2501.10019.

Recent developments of the ADDA code

Maxim A. Yurkin,[1,*] Dmitry A. Smunev,[2] Stefania A. Glukhova,[3] Alexander A. Kichigin,[4] Alexander E. Moskalensky,[5] Konstantin G. Inzhevatkin,[6] Clément Argentin,[1] and Paul Bouillon[1]

[1] *Université Rouen Normandie, INSA Rouen Normandie, CNRS, CORIA UMR 6614 – Rouen, France* (*yurkin@gmail.com)

[2]Clixarea – *Warsaw, Poland*

[3]*Victoria University of Wellington – Wellington, New Zealand*

[4]*Institute of Micro- and Nanostructure Research (IMN) & Center for Nanoanalysis and Electron Microscopy (CENEM), Friedrich-Alexander-Universität Erlangen-Nürnberg, IZNF – Erlangen, Germany*

[5]*Novosibirsk State University – Novosibirsk, Russia*

[6]*JSC Upstream Solutions – Novosibirsk, Russia*

The open-source code ADDA (https://github.com/adda-team/adda) is based on the discrete dipole approximation (DDA) – a numerically exact method derived from the frequency-domain volume-integral formulation of Maxwell's equations [1]. It can simulate the interaction of electromagnetic fields (scattering and absorption) with finite 3D objects of arbitrary shape and composition. Besides standard sequential execution on a single CPU or GPU, ADDA can run on a multiprocessor distributed-memory system, parallelizing a single DDA calculation. This, combined with the almost linear scaling of computational complexity with the number of dipoles (discretization voxels), allows large system sizes and/or fine discretization levels.

ADDA is written in C99 and is highly portable. It provides full control over the scattering geometry (particle morphology and orientation, incident beam) and allows users to calculate a wide variety of integral and angle-resolved quantities. In addition to far-field scattering by various beams (including built-in Gaussian and Bessel beams), this includes near fields as well as excitation by a point dipole or a fast electron. Moreover, ADDA can rigorously and efficiently simulate the scattering by particles near a plane homogeneous substrate or embedded in a homogeneous absorbing host medium. It also incorporates many DDA improvements aimed at increasing both accuracy and computational speed.

In this talk we will focus on the recently implemented ADDA features, either incorporated into the main codebase or available in separate development branches. These include a wide range of built-in Bessel beams [2] and simulations of electron energy-loss spectroscopy (EELS) and cathodoluminescence [3]. The latter two can be computed in an arbitrary passive host medium, even when the electron emits the Cherenkov radiation, or for particles on top of a semi-infinite substrate (under certain approximations). These capabilities also generalize the concept of the Purcell factor (i.e., the enhancement of a point-dipole emitter), which ADDA can rigorously compute in free space or near a substrate [4].

Next, we will discuss the analytical approximations of Green's-tensor integrals for the corresponding DDA formulation, known as IGT, as well as various enhancements to the iterative solvers. These enhancements include block- or shifted iterative methods to accelerate computations for multiple incident beams (e.g., particle orientations) or refractive indices, as well as the use of specialized initial guesses for large particles [5]. Finally, many of these features are accessible through a graphical user interface and we are actively working on integrating ADDA with Spack – a package manager that facilitates installation on a wide range of systems, including supercomputing environments.

[1] M. A. Yurkin and A. G. Hoekstra, J. Quant. Spectrosc. Radiat. Transfer **112**, 2234 (2011).

[2] S. A. Glukhova and M. A. Yurkin, Phys. Rev. A **106**, 033508 (2022).

[3] A. A. Kichigin and M. A. Yurkin, J. Phys. Chem. C **127**, 4154 (2023).

[4] A. E. Moskalensky and M. A. Yurkin, Phys. Rev. A **99**, 053824 (2019).

[5] K. G. Inzhevatkin and M. A. Yurkin, J. Quant. Spectrosc. Radiat. Transfer **277**, 107965 (2022).

Implementation of the weighted discretization in the ADDA code

Paul Bouillon,[1,*] Maxim A. Yurkin,[1]

[1]*Université Rouen Normandie, INSA Rouen Normandie, CNRS, CORIA UMR 6614, Rouen, 76000, France*
(*paul.bouillon@coria.fr)

The discrete dipole approximation (DDA) is widely used to describe scattering and absorption of electromagnetic waves by an arbitrary particle [1]. It is based on the discretization of the particle volume as a set of dipoles (Figure 1a). Thus, internal electric fields $\mathbf{E}_i$ are determined from a linear system of equations expressed in terms of interactions $\overline{\mathbf{G}}_{ij}$ of one voxel (dipole) with another or with the incident field $\mathbf{E}_i^{\mathrm{inc}}$:

$$\mathbf{E}_i = \mathbf{E}_i^{\mathrm{inc}} + \sum_{j\neq i} \overline{\mathbf{G}}_{ij} V_j \chi_j \mathbf{E}_j + \left(\overline{\mathbf{M}}_i - \bar{\mathbf{L}}_i\right) \chi_i \mathbf{E}_i, \tag{1}$$

where $\bar{\mathbf{L}}_i$ is the self-term dyadic, $\overline{\mathbf{M}}_i$ is a finite-size correction to it, and χ_i is the voxel susceptibility.

For most of the particles, there exist shape errors due to the mismatch of cuboid voxels with the boundary (staircase effect) [2]. A weighted discretization (WD) aims to reduce shape errors without changing the regular rectangular grid. The simplest option is to use the effective medium approximation [3] to tune the susceptibility of boundary dipoles, while a more advanced method was proposed by Piller [4]. The boundary voxels are divided into two parts (Figure 1b) : a principal part (p), which contains the voxel center $\mathbf{r}_i$, and a secondary one (s). The corresponding electric fields are related through the boundary-condition tensor $\bar{\mathbf{T}}_i$ as $\mathbf{E}_i^{\mathrm{s}} = \bar{\mathbf{T}}_i \mathbf{E}_i^{\mathrm{p}}$. In addition, χ_i is replaced by an effective susceptibility $\overline{\boldsymbol{\chi}}_i^{\mathrm{e}}$ in (1) while $\left(\overline{\mathbf{M}}_i - \bar{\mathbf{L}}_i\right) \chi_i \mathbf{E}_i$ becomes $\left[\left(\overline{\mathbf{M}}_i^{\mathrm{p}} - \bar{\mathbf{L}}_i^{\mathrm{p}}\right) \chi_i^{\mathrm{p}} + \left(\overline{\mathbf{M}}_i^{\mathrm{s}} - \bar{\mathbf{L}}_i^{\mathrm{s}}\right) \chi_i^{\mathrm{s}} \bar{\mathbf{T}}_i\right] \mathbf{E}_i$.

$$\overline{\boldsymbol{\chi}}_i^{\mathrm{e}} = \frac{V_i^{\mathrm{p}}}{V_i} \chi_i^{\mathrm{p}} \bar{\mathbf{I}} + \frac{V_i^{\mathrm{s}}}{V_i} \chi_i^{\mathrm{s}} \bar{\mathbf{T}}_i \tag{2}$$

Moreover, $\bar{\mathbf{L}}_i$ can be explicitly albeit cumbersomely evaluated [5] for both parts (p) and (s).

Unfortunately, this weighted discretization is not yet available in any open-source code, so we are working on implementing it in ADDA [6]. The results will be presented at the conference.

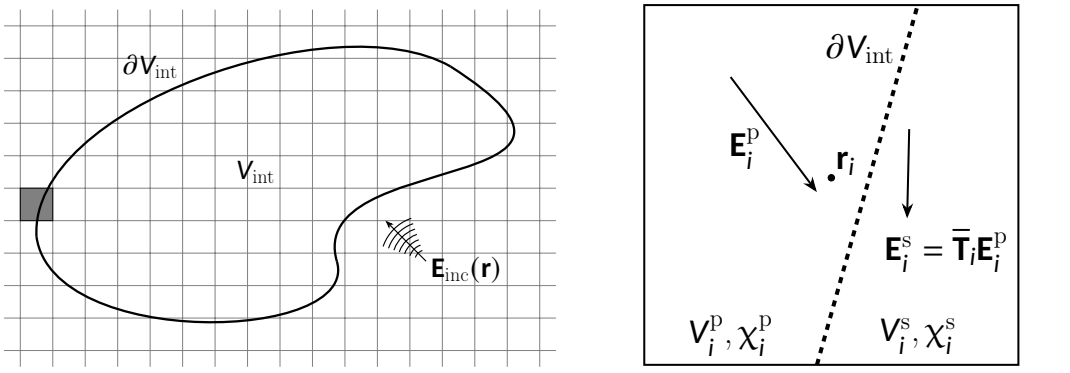

(a) Discretization of the particle

(b) Weighted discretization of a boundary dipole

Figure 1: Weighted discretization applied to the particle

[1] M. A. Yurkin, "Discrete Dipole Approximation", p. 167–198 in *Light, Plasmonics and Particles*, ed. M. P. Menguc and M. Francoeur (Elsevier, 2023).

[2] M. A. Yurkin, V. P. Maltsev, and A. G. Hoekstra, J. Opt. Soc. Am. A **23**, 2578 (2006).

[3] Y. Zhu, C. Liu, and M. A. Yurkin, Opt. Express **31**, 43401 (2023).

[4] N. B. Piller, Opt. Lett. **22**, 1674 (1997).

[5] A. A. Manina, *Use of weighted discretization in the discrete dipole approximation [in Russian]*, BSc thesis, Novosibirsk State University, 2022.

[6] M. A. Yurkin and A. G. Hoekstra, J. Quant. Spectrosc. Radiat. Transfer **112**, 2234 (2011).

Glare points of spheroidal microparticles – simulation study

Jonas Gienger,[1,*] and Alexander Putz[1]

[1]*Physikalisch-Technische Bundesanstalt (PTB) – Berlin, Germany (*jonas.gienger@ptb.de)*

Glare points are bright spots appearing on the surface of a (usually spherical) particle, when the particle is illuminated from one direction and is observed or imaged at an angle (e.g. 90°) to that direction. For macroscopic particles, the effect can be explained using geometrical optics. The different glare points can be attributed to rays interacting a different number of times with the particle surface – either by external reflection or by transmission and internal reflection(s). For smaller particles in the Mie regime (microparticles), a rigorous scattering theory has to be employed and combined with a mathematical model of the imaging process – in the simplest case a Fourier transform of the angular distribution of the scattered far-field. The theoretical discussion of glare points is usually restricted to spherical particles, employing Lorenz-Mie-Theory to describe the scattering [1, 2]. Discussions of spheroidal or other non-spherical particles are scarce in the literature [3] and to the authors' knowledge, no simulation study for spheroidal particles with sizes in the Mie regime has been presented yet.

We have recently presented results from a combined experimental and simulation study for glare points observed on single polymer microparticles ("beads") in the context of flow cytometry [4], with relatively small particle size parameters $x = \pi D/\lambda \lessapprox 100$. Here – for the sake of optical resolution – the aperture of the detection optics is too large to employ the paraxial approximation that is often used in the mathematical modeling of glare points. Consequently, the mathematical model for the image formation is based on a non-paraxial lens model combined with diffraction integrals for field propagation from the lens plane to the image plane.

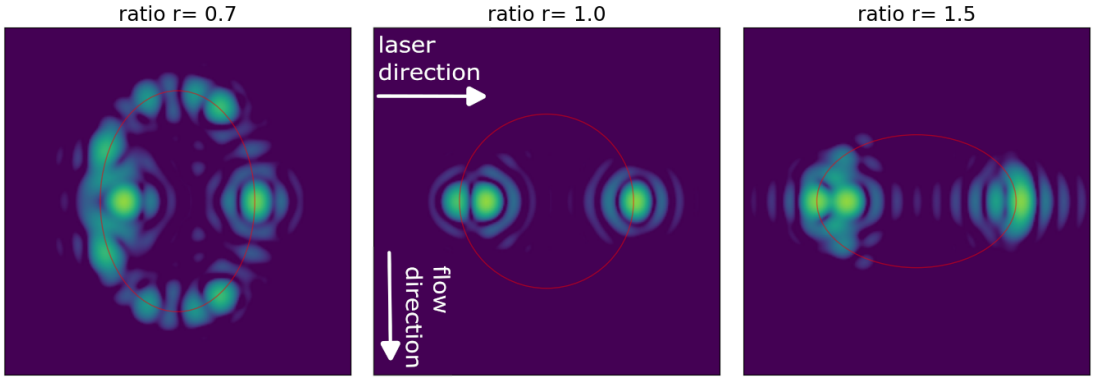

Figure 1: Simulated glare point images for spheroids of different aspect ratios r (ratio vertical to horizontal; vertical axis = symmetry axis). Left to right: r = 0.7 (prolate), r = 1 (spherical), r = 1.5 (oblate). Particle outlines indicated by red lines. Volume-equivalent diameter 5 µm (x = 52), 405 nm laser, polystyrene particles (refractive index 1.6263) in water (refractive index 1.3431).

In the present study we combine the numerical simulation of the image formation process with light scattering simulations from the Discrete Dipole Approximation (DDA; using the ADDA code [5]) to obtain glare-point images of non-spherical (here: spheroidal) particles. These images exhibit several typical features that are not observed for spherical particles, see Fig. 1. We discuss the influence of different parameters such as refractive index, aspect ratio and orientation of the spheroidal particles.

[1] J. A. Lock, Appl. Opt. **26**, 5291 (1987).

[2] H. C. van de Hulst, and R. T. Wang, Appl. Opt. **30**, 4755 (1991).

[3] J. Lock, and M. Selmke, "Glare Points and Near-Zone Sagittal Caustic for Scattering of a Plane Wave by a Spherical or Spheroidal Bubble Floating in Air", p. 42 in *Laser-light and Interactions with Particles (LIP2022)* (Institute of Physics, Polish Academy of Sciences, Warsaw, Poland, 2022).

[4] A. Putz, M. Hussels, and J. Gienger. "Glare Points in Laser Flow Cytometry", p. 1043 in *2023 Photonics & Electromagnetics Research Symposium (PIERS)* (Institute of Electrical and Electronics Engineers, 2023).

[5] M. A. Yurkin, and A. G. Hoekstra, Journal of Quantitative Spectroscopy and Radiative Transfer **112**, 2234 (2011).

Photopolarimetric Journey Through the Diverse World of Solar System Dust

Ludmilla Kolokolova[1,*], Johannes Markkanen[2]

[1]*University of Maryland – College Park(MD), USA (*lkolokol@umd.edu)*
[2] *Technische Universität, Braunschweig, Germany*

Comets and asteroids are the primary sources of dust in the Solar System. Recent space missions have provided close-up views of dust near their parent bodies and even collected samples from some asteroids. These advances have significantly improved our understanding of the physical properties of cosmic dust particles, including their structure and size distribution. A new classification of cometary dust particles, based on Rosetta dust experiments, was summarized in [1], identifying aggregates (agglomerates) of varying porosities as well as solid irregular particles. Ground-based observations and another mission, DART, have provided data on dust potentially originating from asteroids. These objects can also produce agglomerated particles, but with different structures and monomer sizes compared to those found in comets. Another recent discovery is that cometary and asteroidal dust contains, and in some cases is even dominated by, large particles reaching sizes in the centimeter range.

In this talk, we will describe the most popular computational and laboratory modeling tools used to simulate the photopolarimetric properties of different types of cosmic dust particles. We will present some results obtained with MSTM5 [2], FASTMM [3], and SIRIS4[4] computational techniques and by Granada Cosmic Dust Laboratory [5]. We will demonstrate that integrating multiple observational techniques with modeling is essential for obtaining realistic dust properties and understanding the changes particles undergo after their release. This approach is illustrated through the simultaneous analysis and modeling of observed images, color maps, and polarization data for three cases: a comet Schwartz[6], an active asteroid QN173 [7], and the DART impact ejecta [8].

[1] C. Güttler, et al. "Synthesis of the morphological description of cometary dust at comet 67P/Churyumov-Gerasimenko." Astronomy & Astrophysics 630 (2019): A24.

[2] D. Mackowski, and L. Kolokolova. "Application of the multiple sphere superposition solution to large–scale systems of spheres via an accelerated algorithm." Journal of Quantitative Spectroscopy and Radiative Transfer 287 (2022): 108221.

[3] J. Markkanen, and A. J. Yuffa. "Fast superposition T-matrix solution for clusters with arbitrarily-shaped constituent particles." Journal of Quantitative Spectroscopy and Radiative Transfer 189 (2017): 181-188.

[4] K. Muinonen et al. "Light scattering by Gaussian particles with internal inclusions and roughened surfaces using ray optics." Journal of Quantitative Spectroscopy and Radiative Transfer, 110(2009), 1628-1639.
K. Muinonen, et al. "Light scattering by Gaussian random particles: ray optics approximation." Journal of Quantitative Spectroscopy and Radiative Transfer 55.5 (1996): 577-601.

[5] O. Muñoz, et al. "Update Granada–Amsterdam Light Scattering Database." *Journal of Quantitative Spectroscopy and Radiative Transfer* 331 (2025): 109252.

[6] O. Ivanova, et al. "Quasi-simultaneous photometric, polarimetric, and spectral observations of distant comet C/2014 B1 (Schwartz)." Astronomy & Astrophysics 672 (2023): A76.

[7] O. Ivanova, et al. "Long-lasting activity of asteroid (248370) 2005 QN173." Monthly Notices of the Royal Astronomical Society 525.1 (2023): 402-414.

[8] L. Kolokolova et al. "Characterization of the DART ejecta using computer modeling of the ground-based and HST photopolarimetric data." Planetary Science Journal, submitted

Photometric and Polarimetric Modeling for the Galilean Satellite Europa

Ari Leppälä,[1,*] Karri Muinonen,[1] Antti Penttilä,[1] and Anne Virkki[1]

[1]*Department of Physics, University of Helsinki, Finland (*ari.leppala@helsinki.fi)*

Airless Solar System objects' photometric phase curves exhibit a distinctive opposition effect, marked by nonlinear brightening as phase angles approach the backscattering direction. In addition to phase angles below approximately 20 degrees, polarimetric phase curves predominantly show a negative degree of linear polarization, with scattered light polarized parallel to the Sun-object-observer plane of scattering. These phenomena arise from electromagnetic wave scattering in discrete media composed of small particles, due to the interference between reciprocal rays that traverse identical optical paths in opposite directions. As such, this coherent backscattering effect makes the opposition phenomena dependent on specific properties of the medium, particularly the particle size, refractive index, shape, and the packing density of the medium. Incorporating coherent backscattering (CB) into radiative transfer (RT) models provides a comprehensive modeling solution. In addition to coherent backscattering, nonspherical particles contribute to the negative degree of linear polarization.

In prior research, we modeled polarimetric phase curves for Jupiter's satellites Europa, Ganymede, and Io [1, 2]. We employ radiative-transfer coherent-backscattering (RT-CB, [3, 4]) modeling with an ensemble-averaged scattering matrix. This approach utilizes parameterized matrix elements to replicate the observed small-phase-angle polarimetric phase curves for these objects [1]. Decomposing the ensemble-averaged scattering matrix into polarization-conserving Mueller matrices [4] enables RT-CB computations for discrete random media with nonspherical particles [5]. This decomposition facilitates conclusions about near-surface structure and composition by comparing the RT-CB model results with observations [6].

In this study, we replace the previously used ensemble-averaged scattering matrices with those derived from a near-surface composition model characterized by physically described properties, including a size distribution of randomly shaped and oriented particles. These particle geometries are generated using a 3-D Voronoi diagram, with monomers of effective sizes ranging from 0.1 to 0.5 microns. These geometries are then used as inputs for Advanced Discrete Dipole Approximation (ADDA) [7] simulations and complemented by larger Gaussian particles created with the SIRIS-4 [8, 9] code, resulting in an ensemble-averaged scattering matrix that reflects a physically motivated near-surface composition.

Simulating light scattering from a near-surface composition model with specified physical properties and comparing the results with an ensemble-averaged scattering matrix can provide insights into compositional characteristics on icy satellites, including particle size distribution, packing density, and mineral composition. The RT-CB model, combined with photometric and polarimetric measurements at small phase angles, offers a tool for modeling icy satellites and other airless objects based on ground-based observations. This approach enables modeling without costly in-situ measurements, given that Solar System geometry often restricts ground-based observations to small phase angles.

[1] N. Kiselev et al., "New Polarimetric Data for the Galilean Satellites : Europa Observations and Modeling" Planet. Sci. J. **3**, 134 (2022)

[2] N. Kiselev et al., "New Polarimetric Data for the Galilean Satellites: Io and Ganymede Observations and Modeling," Planet. Sci. J. **5**, 10 (2024)

[3] K. Muinonen et al., "Coherent Backscattering Verified Numerically for a Finite Volume of Spherical Particles," ApJ **760**, 118 (2012)

[4] K. Muinonen, A. Penttilä, "Scattering matrices of particle ensembles analytically decomposed into pure Mueller matrices," JQSRT **324**, (2024)

[5] K. Muinonen et al., "Coherent backscattering in discrete random media of particle ensembles," JQSRT **330**, (2025)

[6] A. Leppälä et al., in preparation, (2025)

Probing Dust Properties of Protoplanetary Disks through ALMA's High-Resolution Polarization

Zhe-Yu Daniel Lin,[1,*] Alycia Weinberger,[1] and Gorden Videen[2]

[1]*Earth & Planets Laboratory, Carnegie Science – Washington, USA (*zlin@carnegiescience.edu)*
[2]*US Army Research Laboratory – Adelphi, USA*

Protoplanetary disks the birthplaces of planets, have long been studied to understand the processes of planet formation. Recent high-resolution observations of dust polarization in these disks using sub-millimeter radio interferometry with the Atacama Large Millimeter/submillimeter Array (ALMA) have revealed patterns that challenge our previous understanding. This talk introduces the mechanisms behind these perplexing polarization observations. I will first show that dust scattering in inclined disks can explain some of the polarization. However, the morphological change in the multiwavelength polarization cannot be fully explained by scattering alone. I demonstrate that scattering of aligned prolate grains can account for the polarization transition for HL Tau using the T-matrix method to model elongated dust grains and properly treating scattering of aligned non-spherical grains with a plane-parallel slab model. Scattering dominates the polarization at shorter wavelengths when the disk is optically thick, while polarization from the thermal emission of aligned grains dominate at longer wavelengths when the disk is optically thin. The highest resolution polarization image (5 au) at 870 micron of HL Tau shows intricate polarization patterns between the disk's rings and gaps which can also be explained by optical depth effects of scattering, aligned prolate grains. These results demonstrate the unique perspectives that polarization can provide in studying planet formation.

3D-Printed Dust analogs for Protoplanetary Disk Studies

François Ménard[1,*], J.-M. Geffrin[2], A. Maalouf[3], R. Tazaki[1,4], R. Zerna[1], E. Samara[2], A. Aguila[5], V Tobon-Valencia[1]

[1]*Univ. Grenoble Alpes, CNRS, IPAG, 38000 Grenoble, France (*francois.menard@univ-grenoble-alpes.fr)*
[2]*Aix Marseille Univ, CNRS, Centrale Med, Institut Fresnel, Marseille, France*
[3]*Lab-STICC UMR CNRS 6285, Université de Bretagne Occidentale, Brest, France*
[4]*Department of Earth Science and Astronomy, The University of Tokyo, Japan*
[5]*Interac'Sciences, St-Martin d'Hères, France*

Astrophysical Context: Small dust particles in planet-forming circumstellar disks must grow by several orders of magnitude to form planetary embryos. The exact processes by which this happens remain unclear today. Information is known about the dust sizes and their rough chemical composition in disks, as measured via, e.g., spectral energy distribution measurements and fitting and near- and mid-infrared spectroscopy. However, particle shapes also hold important clues to the elusive dust-growth mechanisms, a better understanding of which is needed to advance our knowledge of the first stages of planet formation. Although rarely studied, particle shapes can be investigated via high resolution imaging of disks and the measurements of scattering phase functions in intensity and linear polarisation, from the optical to the millimeter wavelength range. To reveal the meaning of these phase functions, a comparison is necessary with a database of "measured" or "calculated" scattering properties of complex dust particles of known shapes, sizes, and composition. I will present our recent efforts to measure such scattering properties of complex dust particles from Laboratory Experiments.

Microwave analogy and additive manufacturing: Taking profit of the recent improvements of 3D printers, we built cm-sized analogs of small circumstellar dust particles with a variety of complex shapes and refractive index. The shapes include fractal aggregates with fractal dimensions, D_f , in the range 1.5-2.8, particles with rough surfaces, CAI inclusions and chondrules from meteorites, random Gaussian spheres, etc… See Figure 1. The scattering properties of these analogs were measured in the frequency range 3-18 GHz (size parameters in the range 0.5-35) to mimic their behavior in the visible and/or millimeter range [1,2]. The refractive indices of various printing materials were measured and carefully selected to mimic the properties of relevant astronomical silicates and carbonaceous compounds at near-infrared and mm wavelengths.

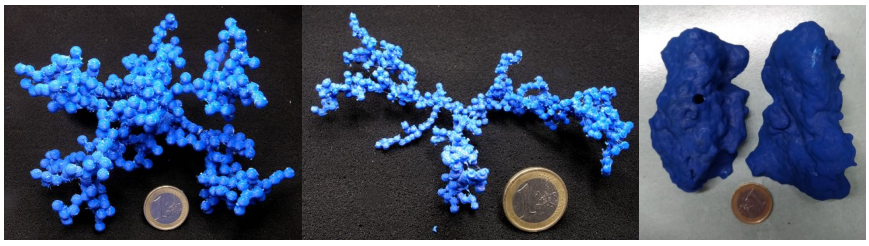

Figure 1: Printed analogs: (left) Fractal aggregate with 500 monomers, $D_f = 2.0$. (Middle) Fractal aggregate with 500 monomers, $D_f = 1,7$. (Right) Copy of a Calcium-Aluminum Rich inclusion. Exact geometry obtained via X-ray tomography. Real size of CAI inclusion = 0.77mm.

Results: The measurement protocol is described [3, 4] who presented results for small fractal aggregates and rough spheres. New measurements are available for larger aggregates, Random Gaussian Spheres, and aggregates made of irregular monomers recently printed [5]. Their relevance to understand the evolution of dust in protoplanetary disks will be discussed.

Acknowledgments: This project has received funding from the European Research Council (ERC) under the European Union's Horizon Europe research and innovation program (grant agreement No. 101053020, project Dust2Planets).

[1] H Saleh *et al*, IEEE Transactions on Antennas and Propagation, Volume: 69, Issue: 2, February (2021)
[2] R Vaillon, J-M Geffrin, Journal of Quantitative Spectroscopy and Radiative Transfer, Vol. 146, Oct. (2014)
[3] Tobon-Valencia *et al.*, *Astronomy & Astrophysics*, *666*, A68 (2022)
[4] Tobon-Valencia *et al.*, *Astronomy & Astrophysics*, *688*, A70 (2024)
[5] Zerna et al., 2025, *Astronomy & Astrophysics*, in preparation

Polarimetry and spectroscopy of regolith simulants at different illumination and observation geometries

Hanna Pentikäinen,[1,*] Antti Penttilä,[1] Karri Muinonen,[1] Ari Leppälä,[1] and Mikko Vuori [1]

[1]*Dept. of Physics, University of Helsinki – Helsinki, Finland (*hanna.pentikainen@helsinki.fi)*

Atmosphereless Solar System objects (SSO), such as asteroids, exhibit special features in the way they scatter unpolarized incident sunlight: mainly, the nonlinear increase in brightness at small phase angles (the angle between the Sun and the observer seen from the object, α) and the negative surge in the degree of linear polarization at $\alpha \leq 30^\circ$. The phenomena are likely due to the surface regolith consisting of closely packed small particles. Another phase angle dependence occurs in the spectra of SSOs: generally, the spectral slopes increase and the absorption band depths vary with increasing phase angle.

To resolve the effects of illumination and observation directions on scattering, and therefore allow for improved retrieval of surface structures and compositions of atmosphereless SSOs, first we examined how the linear polarization phase curves depend on the measurement geometry. Consequently, we measured the intensity and the linear polarization of a flat surface of the dark lunar regolith simulant JSC-1A at zenith incidence angles 0° to 70° and zenith emergence angles -60° to 60° with the University of Helsinki spectrogoniometer. We found that the degree of linear polarization for unpolarized incident light mainly depends on the phase angle only, not the angles of incidence and emergence.

We will similarly measure a rough controlled surface of the lunar regolith simulant, as well as a brighter substance for the purpose of mimicking a higher-albedo asteroid. Additionally, the spectra of the SSO simulating materials will be measured in the different observing geometries to study the effects of phase reddening.

Furthermore, we will model the intensity and linear polarization features with a novel radiative-transfer coherent-backscattering (RT-CB) algorithm developed by Muinonen et al. (presented at this conference, see also [1]) using the empirical scattering matrices from the Granada-Amsterdam Light Scattering Database [2], for which the matrix elements have been parametrized [3].

[1] K. Muinonen, A. Leppälä, J. Markkanen, JQSRT **330**, (2025).

[2] O. Munoz, F. Moreno, D. Guirado, D.D. Dabrowska, H. Volten, J.W. Hovenier, JQSRT **113**, 565-574 (2012).

[3] K. Muinonen, A. Leppälä, in preparation, (2025).

Planetary Atmospheric Profile Inversion through Curved Path Occultation

Bingqiang Sun,* Han Dou, and Chenxu Gao

*Department of Atmospheric and Oceanic Sciences, Fudan University, Shanghai 200438, China (*bingqsun@fudan.edu.cn)*

Based on the principle of atmospheric extinction, the Martian atmospheric profile can be obtained by inverting the occultation data from the Mars rovers. Previous studies have treated the propagation path of electromagnetic radiation in the Martian atmosphere as a straight line. The propagation direction of radiation in the atmosphere is usually deflected, however, due to the vertical gradient of the atmospheric refractive index. Moreover, ignoring the refraction effect could lead to noticeable errors in inversion.

In this study, a new inversion algorithm is proposed to account for the curved path of radiation using occultation. Radiation is handled to be deflected layer-by-layer in the stratified atmosphere, and Snel's law of refraction is applied to construct the path integral of extinction. Using solar occultation data provided by ExoMars 2016/NOMAD, we have inverted the vertical distribution of CO_2 number density in the lower layers of the Martian atmosphere. Moreover, the influence of the refraction effect on the atmospheric profile under different scenarios is analyzed in terms of the Mars Climate Database(MCD) from the Mars Global Climate Model (MGCM). The results show that the overestimation of the CO2 profile can be reduced by applying the refraction correction, especially in the case of cold scenarios.

Circular polarisation scattering from chiral aerosols

Antonio Di Noia,[1,*] Fabio Del Frate,[1] and Giovanni Schiavon[1]

[1]*Rome Tor Vergata University – Rome, Italy (*antonio.di.noia@uniroma2.it)*

Despite its longstanding relevance in planetary science [1], atmospheric circular polarisation has long been an understudied subject as a consequence of the challenging detection of the weak signals associated to it. Recent advances in instrument technology have now made it possible to detect circularly polarised scattered light with high accuracy [2]. This, in principle, opens up new possibilities for exploiting circular polarisation measurements in cloud and aerosol studies [3].

An interesting property of biogenic aerosols is that they may contain chiral material [4, 5], which in principle may enable them to generate circularly polarised light upon single scattering of unpolarised incident light [6]. However, no wide observational basis exists for aerosol chirality parameters and the related scattering properties such as the F_{14} phase matrix element, and only a limited number of radiative transfer models account for light propagation in media containing chiral scatterers [7, 8]. As a result, there is considerable uncertainty around the circular polarisation signals that would be measured by an instrument in presence of chiral aerosols and around the dependency of such signals on aerosol load, size and chirality.

We have developed a Python program that extends M. Mishchenko's Mie scattering code [9] to chiral spheres with arbitrary size distribution. The code computes scattering and extinction efficiencies and scattering phase matrices for large chiral spheres, alongside their ten generalized spherical function expansion coefficients, which makes it suitable for use in multiple scattering calculations. In this presentation we will discuss the variation of relevant scattering parameters as a function of the aerosol chirality parameter for particle size distributions typical of real bioaerosols, with particular emphasis on the F_{14} phase matrix element. The ultimate goal is carry out a first-order evaluation of the intensity of the circular polarisation signals that can be expected as a function of scattering angle in presence of chiral aerosols, and to investigate the conditions under which aerosol chirality can be quantified from remote sensing measurements.

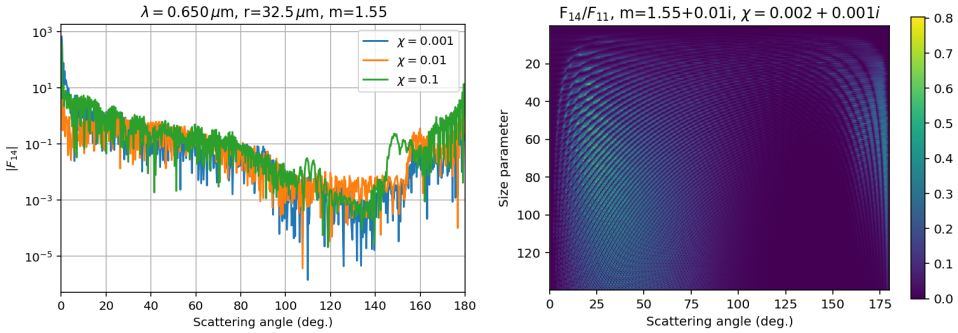

[1] J. C. Kemp, R. D. Wolstencroft, and J. B. Swedland, Nature **231**, 169-170 (1971).

[2] C. H. L. Patty, I. L. ten Cate, W. J. Buma, R. J. M. van Spanning, G. Steinbach, F. Ariese, and F. Snik, Astrobiol. **19**, 1221-1229 (2019).

[3] S. Gassó, and K. Knobelspiesse, Atmos. Chem. Phys. **22**, 13581-13605 (2022).

[4] I. S. Martinez, M. D. Peterson, C. J. Ebben, P. L. Hayes, P. Artaxo, S. T. Martin, and F. M. Geiger, Phys. Chem. Chem. Phys. **13**, 12114, (2011).

[5] N. Zannoni, D. Leppla, P. I. Lembo Silveira de Assis, T. Hoffman, M. Sà, A. Araùjo, and J. Williams, Commun. Earth Environ. **1**, 4 (2020).

[6] L. Nagdimunov, L. Kolokolova, and D. Mackowski, J. Quant. Spectrosc. Rad. Transfer **131**, 59-65 (2013).

[7] A. A. Kokhanovsky, Phys. Rev. E **60**, 4899 (1999).

[8] M. G. Kuzmina, L. P. Bass, and O. V. Nikolaeva "Polarized radiative transfer in optically active light scattering media", p. 1-53 in *Springer Series in Light Scattering*, ed. A. A. Kokhanovsky (Springer, 2017).

[9] M. Mishchenko, L. D. Travis, and A. A. Lacis, *Scattering, absorption and emission of light by small particles* (Cambridge University Press, 2002), Chap. 5.

Nano-particle Transition Matrix code: a parallel implementation of the T-matrix formalism

Giovanni La Mura,[1,*] Giacomo Mulas,[1] Maria Antonia Iatì,[2] Cesare Cecchi-Pestellini,[3]

Shadi Rezaei,[4,2] and Rosalba Saija[4]

[1]*INAF – O. A. Cagliari, Via della Scienza 5, Selargius, 09047, Italy*
[2]*CNR – Ist. per i Processi Chimico-Fisici, Viale F. Stagno d'Alcontres 37, Messina, 98158, Italy*
[3]*INAF – O. A. Palermo, Piazza del Parlamento 1, Palermo, 90134, Italy*
[4]*Univ. di Messina - MIFT, Viale F. Stagno D'Alcontres 31, Messina, 98166, Italy*

Abstract: The study of scattering and absorption of radiation by non spherical particles finds application in many fields of scientific research, ranging from the detection of polluting particles in the atmosphere to the investigation of dust in the interstellar medium and to optical trapping. The Transition Matrix (T-matrix) [1] is an analytical and numerical method in which the scattering process is modeled by directly solving the Helmholtz equations in the regions inside and outside the particle and by imposing the boundary conditions on the fields across the particle surface. Essentially, the T-matrix is the matrix representation of a linear operator that, acting on the multipole amplitudes of the incident field in a suitable basis set, gives the multipole amplitudes of the scattered field. The elements of the T-matrix contain all the information about the scattering process. The T-matrix can be used to derive scattering and absorption cross-sections, as well as to calculate the dynamic effects descending from the exchange of energy and momentum between particle and radiation fields [2,3]. One of the key features of T-matrix is the cluster model that has proven to be very suitable for describing light scattering by non spherical particles due to the fact that particles with arbitrary geometry and composition can be modeled as aggregates of spherical monomers [3,4]. However, applications of this approach have been so far limited by the high computational costs required to model particles made by large numbers of spherical components, solved at a high accuracy level. A possible solution to this problem is the implementation of the T-matrix formalism in high performance parallel algorithms that can greatly reduce computational time, using multi-thread / multi-process hardware technologies, such as GPUs and computing farms. Here we present the Nano-particle Transition Matrix code (NP_TMcode), a parallel implementation of the T-matrix, that uses GPU acceleration, together with optimized linear algebra libraries and multi-process management systems, to reduce the time needed for the calculation of high complexity particle models. We show how this new tool can be applied to explore the spectral and polarimetric footprints left by models of dust grains in interstellar extinction curves and in dust emission features. Finally, we discuss the effects of particle complexity, such as asymmetry and layering, on the distribution and orientation of dust particles.

We acknowledge financial support from the European Union (NextGeneration EU), through the MUR-PNRR projects PRIN2022 "EXO-CASH" (grant No. 2022J7ZFRA).

[1] Waterman, P. C. (1971), "Symmetry, Unitarity, and Geometry in Electromagnetic Scattering", Phys. Rev. D, 3(4), 825–839.

[2] Mishchenko, M.I., Travis L.D., and Lacis A.A (2002). "Scattering, absorption, and emission of light by small particles", Cambridge University Press

[3] Borghese, F., Denti, P., and Saija, R. (2007). "Scattering from model nonspherical particles: Theory and applications to environmental physics", Berlin: Springer

[4] Saija, R. et al. (2001). "Beyond Mie Theory: The Transition Matrix Approach in Interstellar Dust Modeling", ApJ ,249 559(2), 993–1004

Stable Computation of the Electromagnetic T-matrix for High Aspect Ratio Cylinders

Eric C. Le Ru,[1,*] and Matt Majic[1]

[1]*The MacDiarmid Institute for Advanced Materials and Nanotechnology, School of Chemical and Physical Sciences, Victoria University of Wellington, PO Box 600, Wellington 6140, New Zealand*

The T-matrix/Extended Boundary Condition Method (EBCM) is widely used for electromagnetic scattering by simple objects where it is much faster than alternative numerical methods. However, it suffers from numerical instability, especially for larger and/or elongated particles. For spheroids, part of the instability has been attributed to numerical cancellations when computing the integrals required for the T-matrix [1,2] and implementations overcoming them lead to improved stability at high aspect ratios [3,4].

We here re-examine this problem for the special case of finite cylinders. We show that similar issues occur. In the simpler limiting case of long-wavelength/electrostatics, the problematic integrals can be calculated analytically [5]. In the full-wave solution, we show that the integrals almost, but do not exactly, vanish. To compute them without numerical cancellations, we expand the integrands in powers of the size parameter and find that the negative powers integrate to zero exactly when the surface is extended to infinity, hence the cancellations. This is similar to the approach of Waterman in the acoustic case [6] and to that introduced for spheroids [2]. Implementations overcoming this issue are presented and discussed. We show that this results in stable computation of the matrix integrals and stable methods of matrix inversion are also explored. The proposed resulting implementation is validated and compared to the existing approach (see Fig. 1 below). Overall, it provides stable computation of the T-matrix and physical properties such as optical cross sections over a much wider range of aspect ratios.

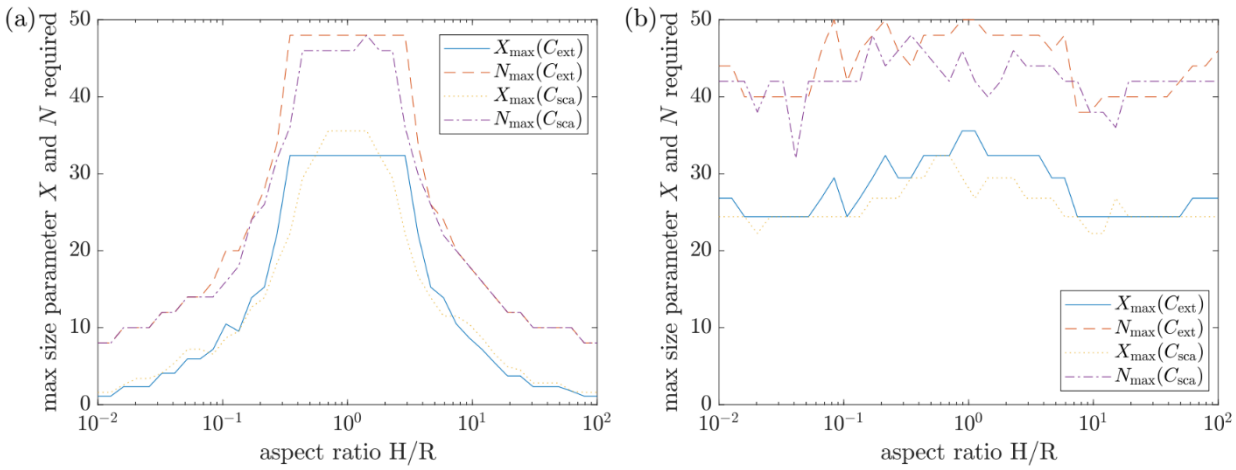

Figure 1: Maximum size parameter for stable computation using the standard EBCM (a) and the proposed new implementation (b) for cylinders of varying aspect ratio and relative refractive index s=1.3+0.2i.

[1] W. R .C. Somerville, B. Auguie, and E. C. Le Ru, *Severe loss of precision in calculations of T-matrix integrals*, J. Quant. Spectrosc. Rad. Transfer **113**, 524 (2012).

[2] W. R. C. Somerville, B. Auguie, and E. C. Le Ru, *A new numerically stable implementation of the T-matrix method for electromagnetic scattering by spheroidal particles*, J. Quant. Spectrosc. Rad. Transfer **123**, 153 (2013).

[3] W. R. C. Somerville, B. Auguie, and E. C. Le Ru, *Accurate and convergent T-matrix calculations of light scattering by spheroids*, J. Quant. Spectrosc. Rad. Transfer **160**, 29 (2015).

[4] W. R. C. Somerville, B. Auguie, and E. C. Le Ru, *SMARTIES: User-friendly codes for fast and accurate calculations of light scattering by spheroids*, J. Quant. Spectrosc. Rad. Transfer **174**, 39 (2016).

[5] M. Majic and E. C. Le Ru, *Analytic results for the electrostatic T-matrix and polarizability of finite cylinders*, J. Quant. Spectrosc. Rad. Transfer **330**, 109227 (2025).

[6] P. Waterman, *T-matrix methods in acoustic scattering*, J. Acoust. Soc. Am. Transfer **125**, 42 (2009).

Simple empirical approximation for integrated reflected intensity of particulate surfaces in geometric optics regime

Antti Penttilä,[1,*] Julia Martikainen[2], Mikko Vuori[1], and Karri Muinonen[1]

[1]*Department of Physics, University of Helsinki, Finland (*antti.i.penttila@helsinki.fi*)*
[2]*Instituto de Astrofísica de Andalucía, CSIC, Granada, Spain*

Introduction: Modeling the brightness of a surface consisting of particulate material is a problem we often face in planetary science, but it is also present in many other fields from Earth remote sensing to material science and industrial applications. The forward problem depends on particle sizes, shapes, packing, and the optical properties of the materials. In the inverse problem, we want to estimate some of the mentioned properties from the scattering characteristics of the material.

In general, the forward problem can be difficult if the particulate material has rough structure in many size scales including the scale of the wavelength considered, in which case the Maxwell equations need to be solved for the wavelength scale. However, if the particles are large compared to the wavelength, we can employ a geometric optics approximation to calculate average single-scattering properties of the grains in the material, and a radiative transfer approximation to consider the response of the particulate material.

We have employed the abovementioned modeling to study the effect of particle size and complex refractive index $m = n + ik$ on the reflected intensity of particulate surfaces. The direct application of this method is the inversion of m, and especially the extinction coefficient k, from reflectance measurements with known particle shapes and sizes.

Method: We will simulate the forward problem in a grid of input parameters (size, n and k) and create a library of reflectance values that are integrated over the backward scattering hemisphere of a particulate surface when illuminated directly from above. Particle shape is fixed to a random convex polyhedral shape. Single-particle scattering properties are simulated using the SIRIS4[1] geometric optics code, and multiple scattering and the backward hemispherical reflectance with RT-CB[2] code using only the radiative-transfer part as the coherent backscattering effects are not important here.

Results: We will present the results of these simulations and show how the received reflectance can be approximated with a simple, logistic-type function with the size parameter of the particles (size in relation to the wavelength) and the extinction coefficient combined into a single parameter, and the real part n not having any significant role in this approximation. The analytical approximation can be used for quick inversion of reflectance measurements for the extinction coefficient k with known size or to the size with known extinction coefficient [3].

[1] Muinonen et al. (2009). Light scattering by Gaussian particles with internal inclusions and roughened surfaces using ray optics. Journal of Quantitative Spectroscopy & Radiative Transfer 110, 1628–1639.

[2] Muinonen et al., present meeting

[3] Penttilä et al. (2024). Modeling linear polarization of the Didymos-Dimorphos system before and after the DART impact. The Planetary Science Journal, 5(1), 27.

Fast surface integral equation method for scattering by homogeneous particles with rough surfaces

Johannes Markkanen,[1,*]

[1]*Institut für Geophysik und Extraterrestrische Physik, TU Braunschweig, Germany*
(*j.markkanen@tu-braunschweig.de)

I present the Fast Surface Integral Equation Method FaSIEM program designed to compute the light scattering characteristics of homogeneous particles with rough surfaces. FaSIEM solves the Poggio-Miller-Chang-Harrington-Wu-Tsai surface integral equation [1] using the Galerkin method with the Rao-Wilton-Glisson basis and testing functions [2]. This discretization results in a system of linear equations, which is solved using the GMRES iterative solver. The matrix-vector multiplication in each iteration step is accelerated by the high-frequency Multilevel Fast Multipole Algorithm (MLFMA) [3].

The program is implemented in a modern Fortran and is parallelized with the shared-memory OpenMP library. The source code with the BSD-3 lisence, is available at [4]. The particle shapes are represented as triangular surface meshes in Object file format (OFF), with their composition defined by a complex refractive index. For accurate and efficient solutions, the element size should be approximately $\lambda/10$ where λ is the wavelength in the background medium. Since FaSIEM is based on surface formulation, its computational complexity scales with the surface area of the particle, offering a significant advantage over volumetric methods such as the discrete dipole approximation or finite-element methods, which scale with the particle's volume.

In this presentation, I will provide a brief overview of surface integral equation methods and demonstrate FaSIEM's capabilities by applying it to investigate impacts of microscale surface roughness on light scattering characteristics. In particular, I will focus on the analysis of particles much larger than the wavelength that exhibit multiscale surface roughness, a feature commonly observed in many natural particles [5].

[1] A. Poggio, E. Miller, Chapter 4 - integral equation solutions of three-dimensional scattering problems, in: R. Mittra (Ed.), Computer Techniques for Electromagnetics, International Series of Monographs in Electrical Engineering, Pergamon, 1973.

[2] S. Rao, D. Wilton, A. Glisson, Electromagnetic scattering by surfaces of arbitrary shape, IEEE Transactions on Antennas and Propagation 30 (3) (1982) 409–418

[3] W. Chew, E. Michielssen, J. M. Song, J. M. Jin, Fast and Efficient Algorithms in Computational Electromagnetics, Artech House, Inc., USA, 2001.

[4] `https://bitbucket.org/planetarysystemresearch/sie`.

[5] B. Mandelbrot, The Fractal Geometry of Nature, Einaudi paperbacks, Henry Holt and Company, 1983.

Accelerating iterative solvers in the discrete dipole approximation using dedicated initial guesses

Clément Argentin[1,*] and Maxim A. Yurkin[1]

[1] *Université Rouen Normandie, INSA Rouen Normandie, CNRS, CORIA UMR 6614 – Rouen, F-76000, France (*argentic@coria.fr*)*

The Discrete Dipole Approximation (DDA) [1] is a versatile and widely used method for simulating light scattering by particles with arbitrarily shapes and internal structure, ranging in sizes from much smaller than to several tenths of a wavelength. Its flexibility, coupled with open-source implementations like ADDA, DDSCAT, and IF-DDA, has enabled applications in biology, nanotechnology, and climate studies. However, the high computational cost of solving the underlying large-scale linear systems remains a significant limitation.

This work focuses on accelerating the iterative solvers within the DDA by improving their initialization strategies. Previous works on DDA implementations, have explored preconditioning, block iterative methods, and initial guesses to enhance efficiency. While these approaches have yielded modest gains, achieving acceleration factors of 2–3 for block methods and up to 50% improvement for initial guesses, they leave significant room for enhancement. We aim to optimize initial guesses to improve solver convergence, particularly for soft particles.

We build on existing studies [2,3] that demonstrated promising results using scalar solutions or approximate methods as initial guesses and compared several iterative solver methods. Our approach aims to extend these strategies by incorporating multiple approximations, theory, and geometric optics. For specific particle shapes, such as spheres and spheroids with refractive indices and sizes consistent with previous study [4], these advanced approximations are expected to yield substantial improvements.

We also plan to benchmark these advanced initial guess strategies by directly integrating initial guesses produced by IF-DDA [2,3], such as scalar fields (e.g., uGu), into the iterative solvers available in ADDA. This approach will allow us to compare the performance of iterative methods across both codes, providing a comprehensive evaluation of their efficiency under different configurations. Additionally, by exploring the interoperability between ADDA and IF-DDA, we aim to bridge their formulations, contributing to open-source development and fostering broader adoption within the DDA community.

Our results aim to provide a comparative analysis of initial guesses used with already established optimized iterative solvers, highlighting scenarios where these advanced strategies significantly reduce computational costs. Furthermore, initial guesses can be combined with preconditioning techniques and block iterative methods to enhance solver performance. These approaches are also extendable to particles with more complex geometries, broadening the applicability of our methods across diverse scattering problems. By refining solver initialization, this study paves the way for more efficient DDA simulations across diverse applications.

[1] Purcell, E. M. and Pennypacker, C. R., Astrophys. J., **186**, p. 705, 1973.

[2] Chaumet, P. C., J. Quant. Spectrosc. Radiat. Transfer, **312**, 108816, 2024.

[3] Chaumet, P. C., Maire, G., and Sentenac, A., J. Quant. Spectrosc. Radiat. Transfer, **298**, 108505, 2023.

[4] Inzhevatkin, K. G. and Yurkin, M. A., J. Quant. Spectrosc. Radiat. Transfer, **277**, 107965, 2022.

Imaging Polarimetry of the Tail and Coma of the Comet C/2023 A3 (Tsuchinshan-ATLAS)

Mirza Arnaut,[1,*] Christian Wöhler,[1] Pritish Halder,[2] Goldy Ahuja,[3] Shashikiran Ganesh[3]

[1]*Image Analysis Group, TU Dortmund University, 44227 Dortmund, Germany*
*(*mirza.arnaut@tu-dortmund.de)*
[2]*Dept. of Physics and Astronomy, University of Nebraska-Lincoln, Lincoln, NE, 68588-0299, USA*
[3]*Astronomy and Astrophysics Section, Physical Research Laboratory, Ahmedabad, 380009, India*

In this study we present preliminary results of a recent observation campaign focusing on polarimetric imaging of the comet C/2023 A3 (Tsuchinshan-ATLAS) conducted between October 23rd and December 29th, 2024, at 15 different phase angles between 85.5° and 16.4°. We used a Newton reflector of 150 mm aperture and 600 mm focal length located near Dortmund, combined with a The Imaging Source monochrome polarization camera DZK 33UX250 [1]. Each individual frame of this camera contains four simultaneously acquired subframes corresponding to polarizer directions of 0°, 45°, 90° and 135°, at a scale of 2.4 arcseconds per pixel. While previous studies focus on the spectropolarimetry of cometary comae (e.g., [2]), our images were taken in panchromatic mode (peak response at 600-650 nm [1]) in order to access as faint parts of the tail as possible. For each observation, tens to hundreds of frames were acquired with the maximum possible exposure time of 4 s, aligned and stacked in order to increase the signal-to-noise ratio. Here we focus on our observation of October 23rd, 2024, from 18:02 to 19:12 UT at elevations between 24° and 15° above the horizon. The increasing airmass was not an issue as it affected all polarizer directions in exactly the same way. The (faint) sky background was determined by subtracting from each subframe the average over a region of blank sky next to the comet. We derived a DoLP of 0.68 for the faintest detectable part of the tail and 0.30 for the brightest part of the coma (Fig. 1).

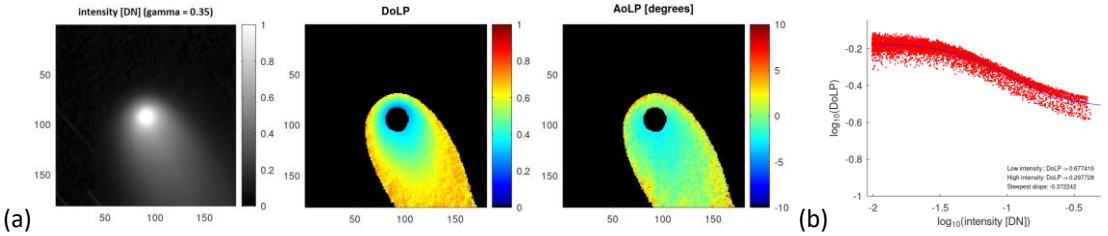

Figure 1: (a) Images of the intensity (contrast-enhanced by gamma transformation), DoLP and AoLP of C/2023 A3 at 85.5° phase angle. The field of view is 7.1 x 7.1 arcminutes. (b) Double-logarithmic scatterplot of DoLP vs. intensity. The DoLP values of the tail and coma were obtained from the maximum and the minimum of the fitted tanh function (blue curve).

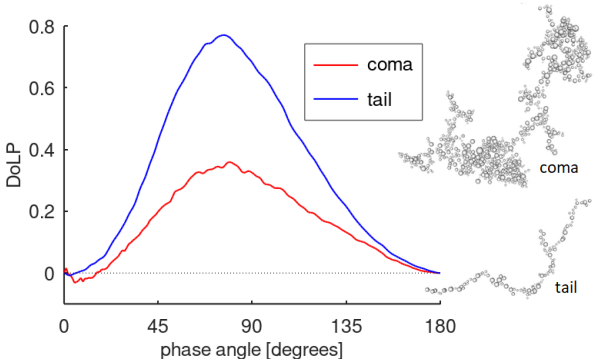

Figure 2: DoLP at 600 nm simulated with MSTM4 [3] for olivine agglomerates consisting of 1024 (coma) and 128 (tail) monomers of 100 nm mean radius, with fractal dimensions of the agglomerates of 1.8 and 1.4, respectively.

Color images of the comet taken with a cooled CMOS camera on October 22nd, 2024, do not show any sign of a green C_2 emission, which had been detected easily with the same setup for several other, even much fainter comets. We thus assume a low-carbon composition and predominance of light scattering by dust. Simulation results (Figure 2) show that the coma consists of more compact dust particles than the tail, which are composed of a larger number of monomers. A possible explanation is that the large dust agglomerates in the coma are freshly released from the nucleus and are formed of small agglomerates adhering to each other due to frozen volatiles. While moving into the tail, these dust particles are heated by solar irradiation, leading to sublimation of the volatiles and release of the small agglomerates.

[1] https://www.theimagingsource.com/de-de/product/unique/33u-polarsens/
[2] E. Zubko, G. Videen, D. C. Hines, Y. Shkuratov, Planet. Space Sci. **123**, 63-76 (2016)
[3] D. W. Mackowski, L. Kolokolova, J. Quant. Spectr. Radiat. Transf. **287**, 108221 (2022)

Comparison of scattering properties of meteorite inclusion analogs

Remi Zerna,[1,*] François Ménard,[1] Jean-Michel Geffrin,[2] Amélie Litman,[2] Vanesa Tobon Valencia[1,2]

[1]*Univ. Grenoble Alpes, CNRS, IPAG, F-38000 Grenoble, France (*remi.zerna@univ-grenoble-alpes.fr)*

[2]*Aix Marseille Univ, CNRS, Centrale Med, Institut Fresnel, Marseille, France*

To better understand proto-planetary disks images obtained with telescopes like ALMA or JWST, it is essential to have a good understanding of the scattering properties of the different objects that compose them. Asteroids and meteorites in our Solar System are made of abundant chondrules (typically mm-sized pebbles) and matrix (fine, sub-micron dust). This is reminiscent of the dust expected in much younger proto-planetary disks where asteroids and planets are yet to form. Here, we wish to investigate the capacity of solar-system chondrules to match the scattering properties observed in young disks. As a first experiment, we performed X-ray tomography of real objects — 3 chondrules and 1 Calcium Aluminum rich Inclusion (CAI) — found in a carbonaceous chondrite, assuming it is representative of rather unprocessed early solar system material. We then 3D-printed them on a centimeter scale with materials whose refractive index is close to that of astronomical silicates. Finally, to measure their scattering properties, we rely on the microwave analogy, using the CCRM facility in Marseille (see [1,2] for details).

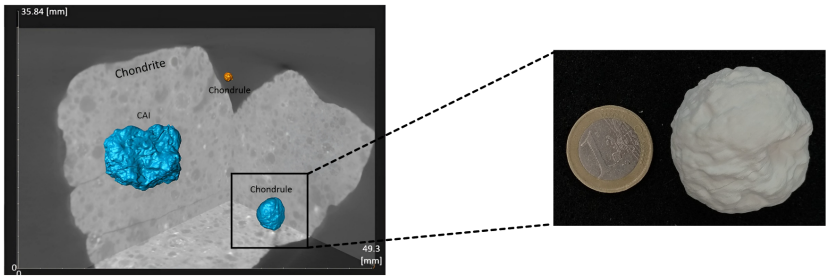

Figure 1: **Left:** X-Ray tomography of the inside of a meteorite. On this figure, we can observe that the CAI is less spherical than the selected chondrules. **Right:** One of the three chondrules 3D-printed.

We measured the scattering properties of three chondrules and one CAI analogs. For each, we present the scattering phase function (SPF) and the degree of linear polarization (DLP). For the SPF, a comparison with Mie theory shows that the chondrules and the CAI behave roughly like spheres of equivalent mass. However, in terms of DLP, the CAI differs from Mie with a much lower polarization fraction, likely due to its more irregular nature [3].

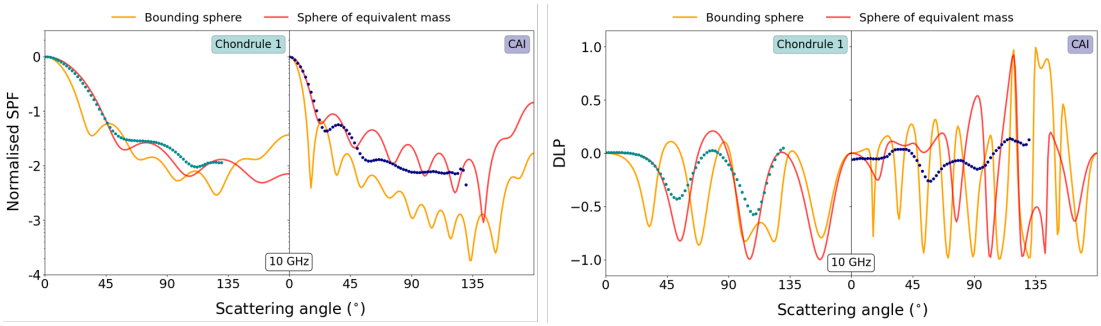

Figure 2: Scattering properties of one chondrule and the CAI analogs at 10 GHz (X∼5 and X∼13, resp.): SPF on the left panel and DLP on the right panel. The blue dashed curves trace the data while the orange and red curves correspond to Mie theory, respectively for the bounding sphere and sphere of equivalent mass [3].

Acknowledgments: This work was supported by the Dust2Planets ERC-ADG-101053020 project DUST2PLANET. We also thanks Yves Marrocchi (CRPG, Nancy) for the X-ray tomography and the analogs morphology. Finally, we would like to thank Azar Maalouf (LAbSTIC, Brest) and Jean-Marie Felio (IUSTI, Marseille) for the 3D printing.

[1] V. Tobon Valencia et al, A&A 666, A68 (2022)
[2] V. Tobon Valencia et al, A&A 688, A70 (2024)
[3] R. Zerna, F. Ménard, J-M. Geffrin et al, in prep.

The scattering properties of distant comet C/2020 V2 (ZTF)

Oleksandra Ivanova[1,2,*], Johannes Markkanen[3], Anhelina Voitko[1], and Igor Luk'yanyk[4]

[1]*Astronomical Institute of the Slovak Academy of Sciences – Tatranská Lomnica, Slovak Republic (*oivanova@ta3.sk)*

[2]*Main Astronomical Observatory of the National Academy of Sciences of Ukraine – Kyiv, Ukraine*

[3]*Institute für Geophysik und Extraterrestrische Physik – Braunschweig, Germany*

[4]*Astronomical Observatory of Taras Shevchenko National University of Kyiv– Kyiv, Ukraine*

Introduction: Comets are key bodies in the Solar System. According to current models, many planetesimals were ejected into the Oort cloud during planetary formation [1]. Gravitational perturbations, such as passing stars, can alter their orbits, sending them inward or even capturing them in other systems [2]. As a result, some interstellar or Oort-cloud objects follow hyperbolic trajectories. Such comets will cross through the inner Solar System only once, making it crucial to study them in detail as long as possible even at large heliocentric distances. Thanks to technical capabilities, the number of active comets–detected beyond 20 au is increasing, including C/2017 K2 (PANSTARRS), C/2010 U3 (Boattini), C/2014 UN271 (Bernardinelli-Bernstein), and C/1995 O1 Hale-Bopp [3]. Here, we present observations of the hyperbolic comet C/2020 V2 (ZTF) (hereafter 2020V2) based on spectroscopic, polarimetric, and photometric data. According to the JPL Small-Body Database, 2020V2 has a perihelion of 2.228 au, eccentricity of 1.001, inclination of 131.61°, and reached perihelion on May 8, 2023.

Observations: We observed comet 2020V2 from February 13 to June 2, 2022, using four telescopes over 16 epochs. Photometric observations were conducted during all the epochs, with the comet at 5.148–4.256 au from the Sun and 4.495–4.579 au from Earth, at phase angles of 8.8°–12.5°. However, on the last observational night, we have additionally obtained simultaneous polarimetric and spectroscopic data on the comet. Most telescopes used Johnson-Cousins or Bessell, while 6-m telescope BTA on June 2 equipped by SDSS g-sdss and r-sdss filters. Long-slit spectroscopic data were acquired on June 2, 2022, using the VPHG1200@540 grism and a 6.93' × 1.007" slit, covering 3650–7250 Å with a dispersion of 0.87 Å/pixel. Polarimetric observations were conducted with the SDSS r-sdss filter using a dichroic polarization analyzer.

Modelling. Using our photometric and polarimetric observations of this comet, we attempted to model the physical characteristics of its dust environment. We utilized the state-of-art modeling tools such as Fast superposition T-matrix method [4] and Radiative transfer with reciprocal transactions [5], in combination with the dynamical dust model, to characterize dust properties and their evolution in the coma.

Results. Spectroscopy post-monitoring shows no significant gas emissions, allowing a focus on the dust environment. Photometric data from winter-spring 2022 reveal stable apparent magnitude. The average dust production level Afρ is ~3800 cm, consistent with other distant comets. Near-nucleus polarization is deeper than typically observed for comets inside 2 au. Dust color varied from red to neutral on 3 and 6 March. BTA data show dust color shifts from neutral to red with cometocentric distance, stabilizing beyond ~19000 km. Morphological analysis using multiple filters indicates a stable dust coma with a persistent ejection and tail, varying slightly daily.

[1] **A. Higuchi and E. Kokubo,** "*Hyperbolic Orbits in the Solar System: Interstellar Origin or Perturbed Oort Cloud Comets?"*, MNRAS, Vol. 492, 1, pp. 268-275 (2020).

[2] **S. Torres et al.,** "*Galactic tide and local stellar perturbations on the Oort cloud: creation of interstellar comets"*, A&A, Vol. 629 (2019).

[3] **E. Lellouch et al.,** "*Size and albedo of the largest detected Oort-cloud object: Comet C/2014 UN271 (Bernardinelli-Bernstein)",* A&A, Vol. 659 (2020).

[4] J. Marrkanen and A. Yuffa, "Fast superposition T-matrix solution for clusters with arbitrarily-shaped constituent particles", JQSRT 189, pp. 181-188 (2017)

[5] Muininen et al., "Multiple scattering of light in discrete random media using incoherent interactions", Opt. Lett. 43, pp.683-686 (2018)

Modeling the surface properties of asteroid (3200) Phaethon using CY-chondrite meteorites

Mikko Vuori,[1,*] Antti Penttilä,[1] Karri Muinonen,[1] Eric MacLennan,[1] Mikael Granvik[1,2]

[1]*Dept. of Physics, University of Helsinki – Helsinki, Finland (*mikko.vuori@helsinki.fi)*
[2]*Asteroid Engineering Laboratory, Luleå University of Technology – Kiruna, Sweden*

(3200) Phaethon is an active near-Earth asteroid that diffuses dust as it comes close to the Sun, and is the likely parent body of the annual Geminid meteor shower. Phaethon has been hypothesized to be connected to, for example, main-belt asteroid (2) Pallas. The two asteroids could be remnants of a common parent body or Phaethon could be an ejected piece of Pallas. Thermal models of Phaethon show heterogeneity between its northern and southern hemispheres either in the surface grain size, porosity, or both [1]. Recently, Yamato-type (CY) carbonaceous chondrite meteorites have been connected to Phaethon and the CY meteorites are now believed to be originated from the asteroid [2]. Using CY meteorites, a light scattering model is created for the surface of Phaethon to study its surface properties and heterogeneity.

Samples of 6 different CY meteorites are studied at the University of Helsinki Astrophysical Scattering Laboratory. The samples spectra and polarization properties are measured. Modeling the measurements from the meteorite samples has been started using the method described in Martikainen et al. [6]. The mineralogy of the samples have been studied with XRD by King et al. [3]. Utilizing the knowledge of the composition, light scattering simulations with SIRIS4 (geometric optics with diffuse scatterers framework) [4], RT-CB (radiative transfer and coherent backscattering code) [5; Muinonen et al., present meeting], and Mie calculations are combined to recreate the measured spectral and polarization properties for the samples. Mie scattering is used to calculate single scattering properties of nano-scale inclusions in regolith particles. The particles are simulated with SIRIS4 and finally the regolith media with RT-CB. From the simulations a model is created that explains the scattering properties of the samples. The model for the meteorites is then extrapolated to Phaethon. Particle size, composition, and porosity are optimized against Phaethon's spectra and polarization data, especially focusing on explaining the surface heterogeneity between the hemispheres. The model can also be used to study the connection between Phaethon and Pallas by fitting it to spectral data from Pallas.

Results from the study will be presented at the conference. Destiny+, a space mission by JAXA planned to be launched in 2028, will do a fly-by of Phaethon and image its surface properties giving us an answer to our derived hypothesis.

[1] E. MacLennan, S. Marshall, Mikael Granvik, "Evidence of surface heterogeneity on active asteroid (3200) Phaethon", *Icarus*, Volume 388, 2022.

[2] E. MacLennan, M. Granvik, "Thermal decomposition as the activity driver of near-Earth asteroid (3200) Phaethon", *Nature Astronomy*, **8**, 60–68, 2024

[3] A.J. King, H.C. Bates, D. Krietsch, H. Busemann, P.L. Clay, P.F. Schofield, S.S. Russell, "The Yamato-type (CY) carbonaceous chondrite group: Analogues for the surface of asteroid Ryugu?", *Geochemistry*, Volume 79, Issue 4, 2019.

[4] K. Muinonen, T. Nousiainen, H. Lindqvist, O. Muñoz, G. Videen, "Light scattering by Gaussian particles with internal inclusions and roughened surfaces using ray optics", *Journal of Quantitative Spectroscopy and Radiative Transfer Volume* 110, 2009.

[5] K. Muinonen, "Coherent Backscattering of Light by Complex Random Media of Spherical Scatterers: Numerical Solution", *Waves in Random Media* 14(3), 2004.

[6] J. Martikainen, A. Penttilä, M. Gritsevich, H. Lindqvist, K. Muinonen, "Spectral modeling of meteorites at UV-vis-NIR wavelengths", *Journal of Quantitative Spectroscopy and Radiative Transfer*, Volume 204, 2018.

Optical trapping and light scattering from single particles

Chuji Wang,[1,2]* Haifa Alali,[1] Yukai Ai,[1] Yon-Le Pan,[3] and Gorden Videen[2,3]

[1]*Mississippi State University, Starkville (MS), USA (*cw175@msstate.edu)*
[2]*Space Science Institute, Boulder (CO), USA*
[3]*Devcom Army Research Lab, Adelphi (MD), USA*

Optical trapping–enabled single-particle study represents an emerging field that allows in situ, substrate-free interrogation of individual particles ranging from submicron to tens of microns in size under controlled conditions. In this talk, I will present the integration of optical trapping with Raman spectroscopy (OT-RS) as a powerful platform technique for probing the chemical and surface properties of individual particles suspended in air or a controlled reactive environment. The universal optical trap (UOT) enables non-contact, near real-time analysis of a wide variety of particles—including solid and liquid, transparent and absorbing, and both homogeneous and heterogeneous structures—under atmospherically relevant conditions.

I will highlight several examples from our recent studies using OT-RS on diverse particle types, such as biological aerosols (e.g., pollen, bacteria, fungi), mineral dust (e.g., black carbon, terrestrial, and extraterrestrial materials), and liquid droplets (e.g., sea spray aerosols). By trapping particles over extended periods, OT-RS enables time-resolved observation of surface dynamics and the investigation of heterogeneous chemistry as particles interact with ambient air or chemical reagents.

These studies include the acquisition of fluorescence-free Raman spectra of bioaerosols, observation of particle surface dynamics, monitoring of real-time particle growth and nucleation, and investigation of heterogeneous surface chemistry. Together, these case studies demonstrate the capability of OT-RS to characterize chemical composition, monitor time-evolving processes, and reveal multiphase microchemistry in near real time at the single-particle level. I will also discuss future perspectives and opportunities for advancing this rapidly evolving technique.

This work was supported by the NASA Emerging Worlds NNH22ZDA001N-EW, grant 80NSSC23K0788 and by the NASA Interdisciplinary Research in Earth Science NNH22ZDA001N-IDS, grant 80NSSC24K0851.

Limits of direct optical measurement of optical forces and torques

Timo A. Nieminen,[1,2]* Prathan Buranasiri,[1], Mark L. Watson,[2] Alexander B. Stilgoe,[2] and Halina Rubinsztein-Dunlop[2]

[1]*Department of Physics, Faculty of Science, King Mongkut's Institute of Technology Ladkrabang, Bangkok, Thailand (*timo@physics.uq.edu.au)*

[2]*ARC Centre of Excellence in Quantum Biotechnology, School of Mathematics and Physics, The University of Queensland, Brisbane, Australia*

At the fifth ELS conference in Halifax, in 2000, we suggested that direct optical measurement of the momentum flux of the trapping beam, with and without a particle in the trap, would be an effective and useful way to measure optical forces in optical tweezers [1]. Since then, there have been multiple implementations of this method, and it has indeed been effective and useful [2,3]. As we noted originally [1], this is not a ``universal'' technique that will always work – multiple conditions need to be met sufficiently well. Fortunately, typical cases of trapping in optical tweezers usually satisfy these conditions. Chief among these is that enough of the light that produces the forces can be collected and measured. It is straightforward to design optically-driven devices that violate this condition, for example by deflecting light at an angle too great to be collected [4] (and in the process producing a high force efficiency). In figure 1, we can see that such a situation can arise simply with a spherical particle in an optical trap.

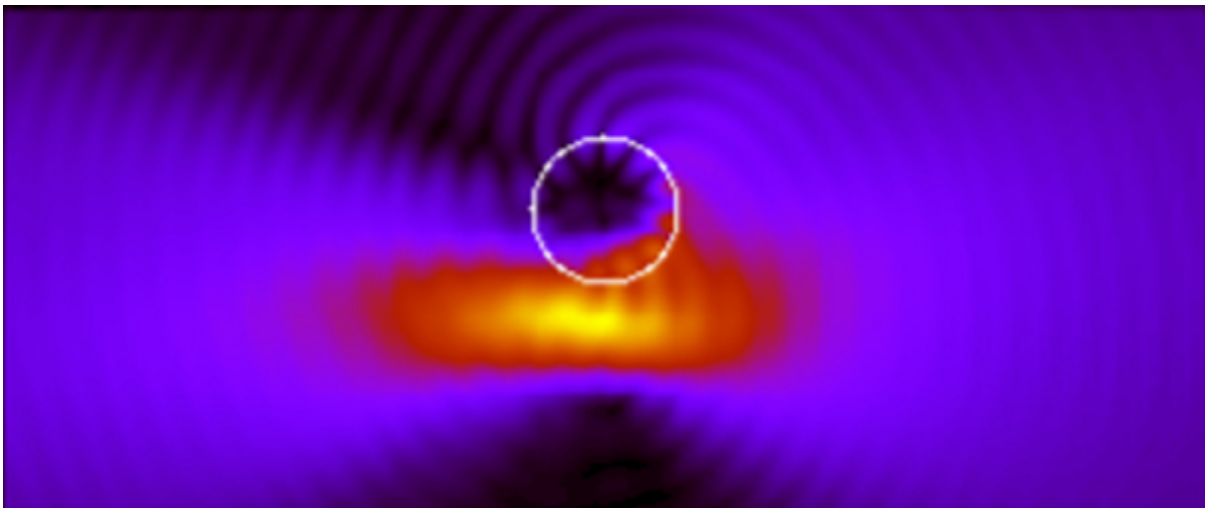

Figure 1: An optically trapped particle deflecting part of the beam (incident from the left) at a large angle (upward), preventing collection by the condenser [5].

Similarly, direct optical measurement of the spin angular momentum flux has proven highly effective for torque measurements. However, we can again find examples where the method fails, such as with radially birefringent objects [6,7]. For both force and torque, we can find cases where not only is the wrong magnitude of the force or torque given by the measurement, but even the direction is wrong.

We review these methods and the requirements for their validity, and explore their limits for force and torque measurements in optical tweezers.

[1] T. A. Nieminen, H. Rubinsztein-Dunlop, and N. R. Heckenberg, J. Quant. Spectrosc. Radiat. Transfer **70**, 627 (2001).

[2] G. Thalhammer, L. Obmascher, and M. Ritsch-Marte, Opt. Express 23, 6112 (2015).

[3] A. A. M. Bui, A. V. Kashchuk, M. A. Balanant, T. A. Nieminen, H. Rubinsztein-Dunlop, and A. B Stilgoe, Sci. Rep. **8**, 10798 (2018).

[4] G. A. Swartzlander Jr, T. J. Peterson, A. B. Artusio-Glimpse, and A. D. Raisanen, Nat. Photonics 5, 48 (2011).

[5] I. C. D. Lenton, A. B. Stilgoe, H. Rubinsztein-Dunlop, and T. A. Nieminen, Eur. J. Phys. **38**, 034009 (2017).

[6] L. Marrucci, C. Manzo, and D. Paparo, Phys. Rev. Lett. **96**, 163905 (2006).

[7] T. A. Nieminen, M. L. Watson, V. L. Y. Loke, A. B. Stilgoe, and H. Rubinsztein-Dunlop, J. Opt. **24**, 124001 (2022).

On relationships between EM and acoustical scatterings

Gérard Gouesbet,[1]*Leonardo A. Ambrosio,[2] and Jianqi Shen[3]

[1]*Normandie Université, CORIA, CNRS, INSA de Rouen, France* (*gouesbet@coria.fr)
[2]Sao *Carlos School of Engineering, Sao Paulo University, Brazil*
[3]University *of Shanghai for Science and Technology*

On one hand, the radial component E_r of the electric field of an EM wave may be written as [1]:

$$E_r = E_0 \sum_{n=0}^{\infty} \sum_{m=-n}^{+n} c_n^{pw} g_{n,TM}^m n(n+1) \frac{j_n(kr)}{r} P_n^{|m|}(cos\theta) \exp(im\varphi) \quad (1)$$

with usual notations, and $g_{n,TM}^m$ being transverse magnetic beam shape coefficients (BSCs) which encode the structure of the EM wave. There is a similar relation for the radial magnetic component H_r of the magnetic field.

On the other hand, an acoustical wave propagating in a linear lossless medium may be written as [2]:

$$\psi_A = \psi_{A0} \sum_{n=0}^{\infty} \sum_{m=-n}^{+n} c_{n,A}^{pw} g_{n,A}^m j_n(kr) P_n^{|m|}(cos\theta) \exp(im\varphi) \quad (2)$$

again with usual notations, the subscript "A" standing for "Acoustical", and $g_{n,A}^m$ being acoustical BSCs which encode the structure of the acoustical wave.

The strong obvious analogy between Eqs. (1) and (2) suggests that the arsenal developed since decades to evaluate the EM BSCs may be adapted to the case of acoustical BSCs. Indeed, a technique used to evaluate EM BSCs, known as the localized approximation, has been adapted to the evaluation of acoustical Gaussian BSCs [3], [4], with the case of Bessel beams discussed in [5]. Another technique in the EM framework, known as the finite series technique, has been adapted as well to the case of acoustical waves [6]. Other approaches to be discussed are as follows:

(1) The localized approximation technique for acoustical fields, for the present time valid for Gaussian and Bessel beams, can be generalized to the case of a large class of arbitrary acoustical shaped beams by using a method named the N-beam method which has been successful in the case of EM fields

(2) Expressing the EM fields in terms of one or two vector potentials, it is possible to express the EM BSCs in terms of the acoustical BSCs. Because there are two sets of EM BSCs (one for transverse magnetic field and one for transverse electric field) and only one set of acoustical BSCs, this approach allows one to essentially divide the computational time by a factor 2.

[1] G. Gouesbet and G. Gréhan. Generalized Lorenz-Mie theories, Springer, 2023..
[2] G. Gouesbet, L.A. Ambrosio and J. Shen. Journal of Quantitative Spectroscopy and Radiative Transfer. 333, 109329, 2025.
[3] G. Gouesbet and L.A. Ambrosio. Journal of the Acoustical Society of America, 55 (2), 2024.
[4] G. Gouesbet and L.A. Ambrosio. Journal of the Acoustical Society of America, 2156 (1), 2024.
[5] L.A. Ambrosio and G. Gouesbet. Acta Acustica. 8, 26, 2024.
[6] L.A. Ambrosio and G. Gouesbet. Journal of Sound and Vibration. 585, 118461, 2024.

Acoustic and optical Raman tweezers as a tool to manipulate and analize cosmic dust analogues

Melissa Infusino[1,2 *], John R. Brucato[3] , Luigi Folco[4,5] , Alessandra Rotundi[6] ,Maria A. Iatì[1] , Antonino Foti[1] , Pietro G. Gucciardi[1] , Andrea Mandanici[7] ,Onofrio M. Maragò[1] , Maria G. Donato[1]

[1] CNR-IPCF, Istituto per i Processi Chimico-Fisici, Messina, Italy
[2] Colegio de Ciencias e Ingeniera, Universidad San Francisco de Quito, Quito, Ecuador
[3] INAF-Osservatorio Astronomico di Arcetri, Firenze, Italy
[4] Dipartimento di Scienze della Terra, Università di Pisa, Pisa, Italy
[5] CISUP, Centro per la Integrazione della Strumentazione dell'Università di Pisa, Pisa, Italy
[6] Ist. di Mat., Fis. e Appl., Università "Parthenope", Napoli, Italy
[7] Dipartimento di Scienze Matematiche e Informatiche, Università di Messina, Messina, Italy
*(*melissa.infusino@ipcf.cnr.it)*

Meteorites and cosmic dust hold crucial information about the origin and evolution of the Solar System. Identifying their composition and assessing the presence of organic matter on their surfaces,while minimizing alteration or contamination, is essential for planetary science. Recently, Acoustic andOptical Raman Tweezers (ARTs and ORTs) have been successfully used to trap, manipulate, and analyzespectra coming from micrometeorites and cosmic dust.In this work, we explore ARTs and ORTs as tools for detecting the presence of extraterrestrial organicsand biosignatures in cosmic dust. The minerals under study were selected because they have been identified in both rover-based missions and orbital data from Mars, such as smectite clays and magnesium sulfate. These minerals are particularly important because they are linked to the hydrological history of the planet and have a well-established affinity for organic molecules[5]. Smectite clays and magnesium sulfate have been artificially doped in laboratory facilities with selected organic molecules of interest. ARTs and ORTs combined provide a powerful, contamination-free approach for trapping and analyzing small particles across a wide range of sizes, from tens of nanometers to a few millimeters. The first technique combines Acoustic Levitation (AL) for contactless manipulation of larger grains (up to a few millimeters) with Raman Spectroscopy for molecular identification. The levitator used in this study is the TinyLev device, which consists of two opposing spherical-cap arrays of ultrasonic transducers. In this system, an acoustic standing wave creates multiple trapping sites along the device's symmetry axis,positioning particles at the nodes of the wave. In ORTs, a single-beam optical tweezers setup is employed. Here, a NIR laser beam is tightly focused by a high-NA microscopic objective, allowing both trapping and Raman excitation of single nano- or micro-particles. These approaches offer a promising pathway for the non-invasive study of extraterrestrial materials, preserving their pristine properties while enabling precise spectroscopic analysis.

Acknowledgements: This work has been funded by the PRIN2022 "Cosmic Dust II" (grant No. 2022S5A2N7), the PRIN 2022 "EnantioSelex" (grant. No. 2022P9F79R) and within the Project "Space It Up" funded by ASI and MUR – Contract n. 2024-5-E.0.

[1] E. Jacquet, C. Dullemond, J. Drazkowska, and S. Desch, Space Sci. Rev. 220, 78 (2024).
[2] S. Ferretti, S. Marrara, D. Bronte Ciriza, A. Magazzù, A. Foti, G. Gucciardi, A. Musolino, L. Folco, V. Della Corte,A. Rotundi, R. Saija, A. Mandanici, O. M. Maragò, and M. G. Donato, ApJ 974, 287 (2024)
[3] A. Magazzù,D. Bronte Ciriza, A. Musolino, A. Saidi, P. Polimeno, M. G. Donato, A. Foti, P. G. Gucciardi, M. A. Iatì,R. Saija, N. Perchiazzi, A. Rotundi, L. Folco, and O. M. Maragò ApJ942, 11 (2023)
[4] P. Polimeno, A. Magazzù, M. A. Iatì, et al. Eur. Phys. J. Plus 136, 339 (2021).
[5] A. Alberini, T. Fornaro, C. García-Florentino,M. Biczysko, I. Poblacion, J. Aramendia, J. M. Madariaga, G. Poggiali, Á. Vicente-Retortillo, K. C. Benison, S. Siljeström, S. Biancalani, C. Lorenz, E. A. Cloutis, D. M. Applin, F. Gómez,A. Steele, R. C. Wiens, K. P. Hand, and J. R. Brucato Sci. Rep. 14, 15945 (2024)

A Multipolar method to optimize the opto-mechanical interactions in levitodynamics with complex wavefronts

M. Perrin,[1,*] M. Kleine,[1] Y. Amarouchene [1] Y. Louyer,[1] N. Bachelard [1]

[1]*LOMA, CNRS UMR 5798, University of Bordeaux, F-33400 Talence, France. (* mathias.perrin@u-bordeaux.fr)*

These last years, the study of nano-particle(s) trapped in vacuum by light, has received a great attention [1]. Using such a platform shall permit to realize mechanical quantum states with levitated particles, or classical motion sensors for rotation and translation [2, 3]. A topical issue is now to optimize the trapping potential. For example, one whishes to maximize the trap stiffness, without increasing the beam power (e.g. to avoid melting in vacuum). To do so, we seek for an optimal trapping wavefront.

Using a multipolar expansion of the scattered far field, we compute the force on a particle illuminated by a highly focused beam whose phase profile is imposed by a Spatial Light Modulator (SLM). This permits to find rapidly the optimal phase profile, e.g. to maximize stiffness and avoid the scattering force effect [3] that tends to untrap the particle. Large particles can also be trapped in some complex wavefronts (see Figure 1).

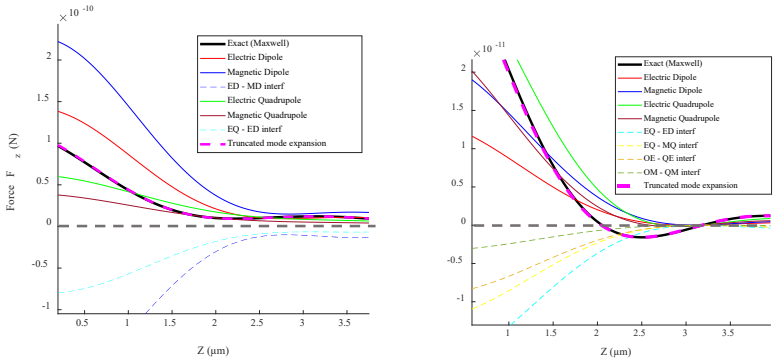

Figure 1: **(Left)** Force from a tweezer beam on a dielectric sphere (no stable trapping occurs). **(Right)** Force from an optimized wavefront : a stable trapping occurs. Particle is a r=0.43 μm radius silica sphere.

At the conference, we will show in detail how to optimize the stiffness for a given power. We shall discuss the underlying mechanism that explains why this is possible, despite the strong index contrast – compared to trapping in liquids [4]–, for which the Born convergence is faster [5]. We will also present new experimental results, where a gain on stiffness by 2.5 has been observed for the first time.

[1] J. Rieser, M. A. Ciampini, H. Rudolph, N. Kiesel, K. Hornberger, B. A. Stickler, M. Aspelmeyer, U. Delic, *Tunable light-induced dipole-dipole interaction between optically levitated nanoparticles*, Science, **377** (2022), no. 6609, 987–990.

[2] L. Bellando, M. Kleine, Y. Amarouchene, M. Perrin, Y. Louyer, *Giant Diffusion of Nanomechanical Rotors in a Tilted Washboard Potential*, Phys. Rev. Lett., **129** (2022), no. 2, 023602.

[3] Y. Amarouchene, M. Mangeat, B. V. Montes, L. Ondic, Th. Guérin, D. Dean, Y. Louyer, *Nonequilibrium Dynamics Induced by Scattering Forces for Optically Trapped Nanoparticles in Strongly Inertial Regimes*, Phys. Rev. Lett., **122** (2019), no. 18, 183901.

[4] U. G. Būtaitė, C. Sharp, M. Horodynski, G. M. Gibson, M. J. Padgett, S. Rotter, J. M. Taylor, D. B. Phillips, *Photon-efficient optical tweezers via wavefront shaping*, Science Advanced (2024), **10** eadi7792.

[5] F. Gruy, V. Rabiet, M. Perrin, *Fourier Transform of the Lippmann-Schwinger Equation: Solving Vectorial Electromagnetic Scattering by Arbitrary Shapes*, Mathematics (2023), **11**, 4691.

Nonequilibrium dynamics of levitated nanoparticles

Pavel Zemánek,[1,*] Oto Brzobohatý[1], Stephen Simpson[1], Martin Duchaň[1], Vojtěch Liška[1], Tereza Zemánková[1], Martin Šiler[1], Petr Jákl[1]

[1]*Czech Academy of Sciences, Institute of Scientific Instruments, Královopolská 147, 612 00 Brno, Czech Republic (*zemanek@isibrno.cz)*

The recent experimental progress in control of the mechanical motion of a single levitated particle opens new ways to investigate more complex configurations in more dimensions or with more levitated and interacting objects. An optical levitation offers relatively easy tunability of the key system parameters (oscillating frequency, the strength of the optical coupling between particles, damping, effective temperature, etc.) over several orders of magnitude. Similarly, the forces acting upon the particles can be tuned between conservative and non-conservative, and various examples of nonequilibrium multidimensional dynamics can be demonstrated.

We provide a few experimental examples along this direction to demonstrate nonequilibrium dynamics of a single optically levitated object with optically coupled degrees of freedom [1,2] and of more levitated objects where their optical coupling (referred to as optical binding) leads to the formation or synchronization of limit cycles [3,4] and their cooling [5,6]. Finally, we present a protocol for a nanomechanical state amplifier that amplifies and squeezes the motional state of a levitated nanoparticle in a stroboscopic sequence of switched potentials [7].

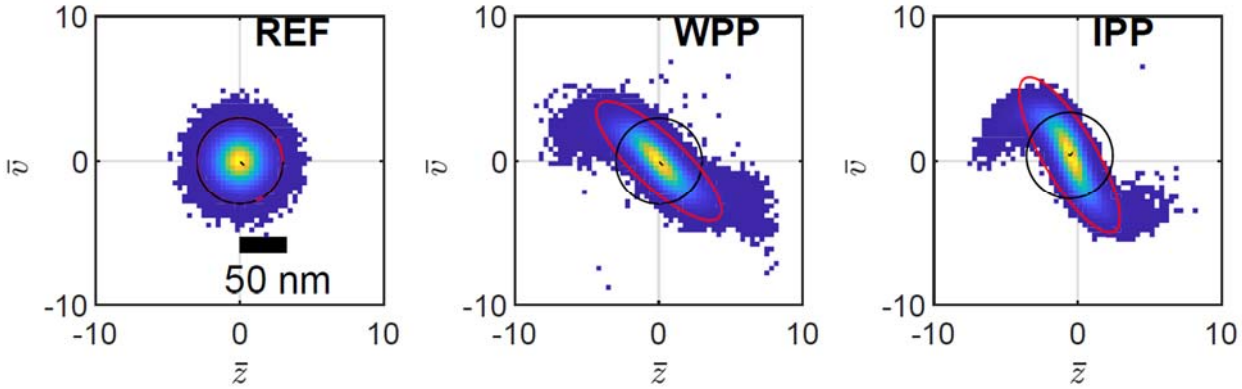

Figure 1: Examples of the reconstructed phase space probability distributions from 165 000 repetitive measurements of the same levitating particle in parabolic potential (PP) without any potential change (REF) and after a three-step stroboscopic sequences PP-weak parabolic potential (WPP)-PP and PP-inverted parabolic potential (IPP)-PP. Axes are normalized to the square root of the corresponding initial variance. The black circle of radius 3 denotes the area of three initial standard deviations and the red ellipses obtained from the eigenvectors of the covariance matrix denote the area corresponding to three standard deviations [7].

The authors acknowledge support from The Czech Science Foundation (GA23-06224S), Czech Academy of Sciences (Praemium Academiae), and Ministry of Education, Youth and Sports of the Czech Republic (CZ.02.01.01/00/22 008/0004649).

[1] V. Svak, O. Brzobohatý, M. Šiler, P. Jákl, J. Kaňka, P. Zemánek, S. Simpson, Nature Commun. **9**, 5453 (2018)
[2] Y. Arita, S. Simpson, G.D. Bruce, E.M. Wright, P. Zemánek, K. Dholakia Commun. Physics **6**, 238 (2023).
[3] O Brzobohatý, M. Duchaň, P. Jákl, J. Ježek, P. Zemánek, S. H. Simpson, Nature Commun. **14**, 5441 (2023).
[4] V. Liška, T. Zemánková, V. Svak, P. Jákl, J. Ježek, M. Bránecký, S.H. Simpson, P. Zemánek, O. Brzobohatý, Nature Physics **20**, 1622 (2024)
[5] V. Liška, T. Zemánková, V. Svak, P. Jákl, J. Ježek, M. Bránecký, S.H.Simpson, P. Zemánek, O. Brzobohatý. Optica **10**, 1203–1209 (2023)
[6] Y. Arita, G.D. Bruce, E.M. Wright, S.H. Simpson, P. Zemánek, K. Dholakia. Optica **9**, 1000 (2022).
[7] M. Duchaň, M. Šiler, P. Jákl, O. Brzobohatý, A. Rakhubovsky, R. Filip, P. Zemánek, arXiv:2403.04302 (2024)

Boron-Doped Diamond and the Discovery of New Properties in an Old Material

Souvik Bhattacharya,[1] Jonathan Boyd,[2] Sven Reichardt,[3], Valentin Allard,[4] Amir Hossein Talebi,[3] Nicolò Maccaferri,[5] Olga Shenderova,[6] A. L. Lereu,[4] Ludger Wirtz,[3] R. Mohan Sankaran*[1], and Giuseppe Strangi*[2,7]

[1]*Department of N.P and R. Engineering, University of Illinois Urbana-Champaign, Champaign, IL, U.S.A.;*
[2]*Department of Physics, Case Western Reserve University, Cleveland, OH, U.S.A.;*
[3]*Department of Physics and Materials Science, University of Luxembourg, Luxembourg;*
[4]*Aix Marseille Univ, CNRS, Centrale Med, Institut Fresnel, Marseille, France;*
[5]*Department of Physics, Umeå University, Sweden;*
[6]*Adamas Nanotechnologies, Raleigh, NC, U.S.A.;*
[7]*Department of Physics, NLHT Labs, University of Calabria, Rende, Italy*

Diamond is well-known for its extraordinary mechanical, thermal, and optical properties. The introduction of impurity dopants can further tune and transform diamond. For example, boron, a p-type dopant, has been used to enhance electronic conductivity[1] and produce superconductivity[2]. In recent years, a whole host of other impurity atoms in combination with vacancies have been found to create color centers with unique spin properties that have potential for quantum technologies.[3] In this talk, we will discuss our recent discovery of low energy (<0.5 eV) plasmonic excitations emerging from the valence subbands as a result of boron doping of diamond.[4] Our study was made possible by recent advancements in characterization techniques including scanning transmission electron microscopy-valence electron energy loss spectroscopy (STEM-VEELS) and near-field infrared (IR) spectroscopy. Applying these techniques to boron-doped diamond, we obtain complementary information about the material response in terms of the energy loss and absorption.

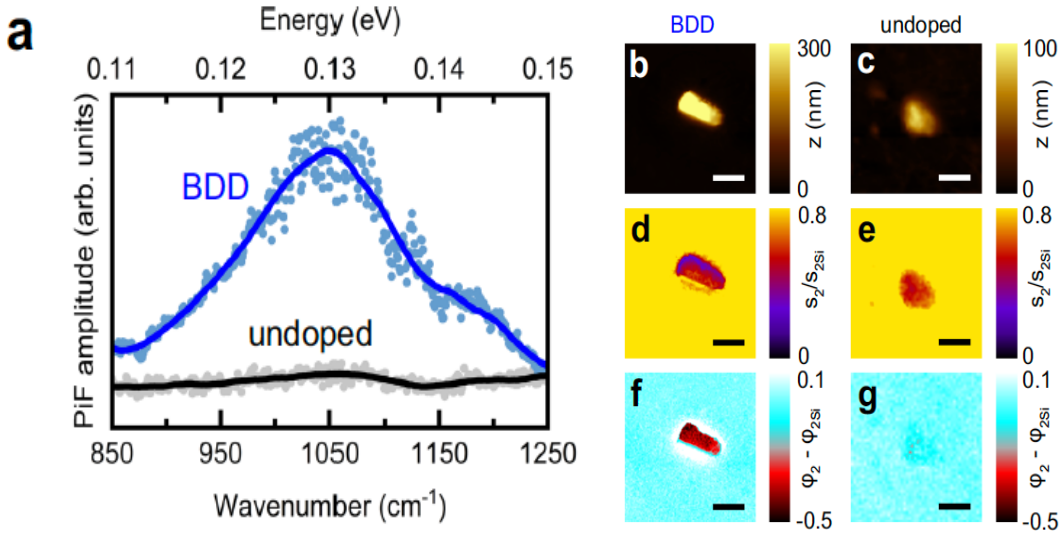

***Figure 1**: Near-field infrared spectroscopic characterization of BDD. **a)** Representative photo-induced force microscopy (PiFM) spectra collected from BDD and undoped diamond. **b–g)** s-SNOM images collected from BDD and undoped diamond.*

A theoretical treatment based on first-principles calculations is then carried out to elucidate the fundamental band origin of the response. We show that boron doping leads to emptying of valence subbands, opening up intervalence band (IVB) transitions. Further analysis of the real dielectric

component of the calculated response function reveals a resonance and zero-crossing that blue shift with increasing carrier density, indicating the emergence of metallicity and plasmonic behavior. This mechanism is notably distinct from the collective Drude-like intraband excitations that are reported in traditional metals and other doped semiconductors. The possibility of plasmonic properties in diamond is yet another insight into this remarkable material that could be combined to for example, enhance the fluorescence of color centers for quantum sensing applications.

1. Y. Einaga, **Accounts of Chemical Research 55** (24), 3605-3615 (2022).
2. E. A. Ekimov, V. A. Sidorov, E. D. Bauer, N. N. Mel'nik, N. J. Curro, J. D. Thompson and S. M. Stishov, **Nature 428** (6982), 542-545 (2004).
3. B. C. Rose, D. Huang, Z.-H. Zhang, P. Stevenson, A. M. Tyryshkin, S. Sangtawesin, S. Srinivasan, L. Loudin, M. L. Markham, A. M. Edmonds, D. J. Twitchen, S. A. Lyon and N. P. de Leon, **Science 361** (6397), 60-63 (2018).
4. S. Bhattacharya, J. Boyd, S. Reichardt, V. Allard, A. H. Talebi, N. Maccaferri, O. Shenderova, A. L. Lereu, L. Wirtz, G. Strangi* and R. M. Sankaran*, **Nature Communications 16** (1), 444 (2025).

Extracting cross-sections from partially measured electromagnetic scattered fields of single particles

A.E. Adane[1], F. Malaval[1], A. Litman[1,*], H. Tortel[1], J-M Geffrin[1] and C. Rockstuhl[2]

[1]*Aix Marseille Univ, CNRS, Centrale Med, Institut Fresnel, Marseille, France (*amelie.litman@fresnel.fr)*
[2]*Institute of Nanotechnology, Karlsruhe Institute of Technology, Karlsruhe, Germany*

Context Light scattering measurements are conducted by illuminating a collection of unknown particles with a given impinging light wave. These multi-bistatic measurements $\mathbf{E}_{sca}(r_s; r_r; r_o; \lambda)$ are acquired with different illumination angles r_s, different collection angles r_r, several orientations of the particles r_o, and different size parameters/wavelengths. While exploiting these measurements, our aim here is two-fold. First, we would like to deduce as many of the particles' optical properties as possible, such as the Jones matrices, the phase function, the degree of linear polarization as well as integrated quantities such as the scattering cross-section C_{scat} and the extinction cross-section C_{ext}. Second, we would like to come up with a data processing chain that allows us to minimize the number of measurements, while keeping a similar level of accuracy in the derived particles' optical properties.

Methodology The first step of the proposed processing chain is to project the measured $\mathbf{E}_{sca}$ fields onto the vector spherical harmonics (VHS) by solving the following minimization problem [1]

$$\underset{a_{nm},b_{nm}}{argmin}\left\| E_{sca}(r_s,r_r) - \sum_n \sum_m a_{nm}(r_s) M_{nm}(r_r) + b_{nm}(r_s) N_{nm}(r_r) \right\|$$

Once the associated a_{nm} and b_{nm} VSH coefficients are retrieved, it is possible to compute the integrated quantities in two different ways:

- By interpolating the electromagnetic field for any point in space thanks to the VSH, particularly in the forward direction to extract C_{ext}, but also on quadrature rules integration points on a sphere surrounding the particles to compute C_{scat} [2].
- By directly computing C_{ext} and C_{scat} from the coefficients a_{nm} and b_{nm} [1].

Results The results of the developed processing chain will be benchmarked thanks to signals measured and/or simulated in the microwave frequency range to mimic their behavior in the visible or millimeter range (or radiowave range) [3] [4].

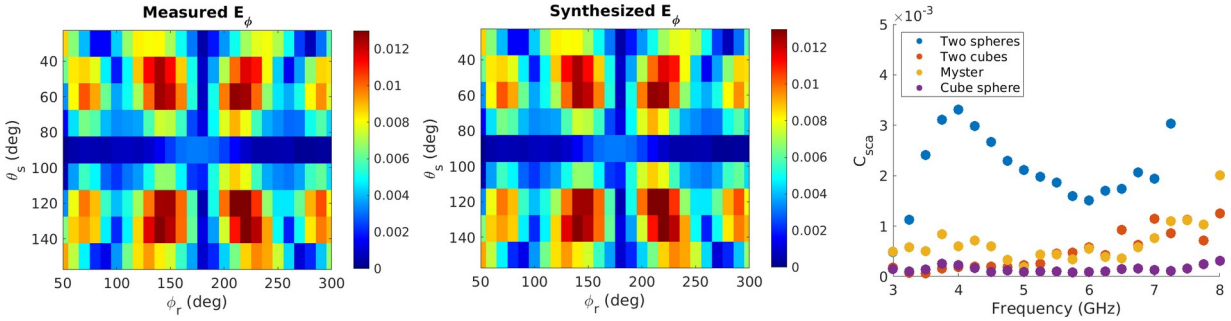

(Left) Measured $\mathbf{E}_{sca}(r_s; r_r)$ – (Middle) Simulated $\mathbf{E}_{sca}(r_s; r_r)$ with extracted VSH coefficients – (Right) Extracted C_{scat}

Acknowledgements This work was supported by the French National Research Agency in the framework of the Investissements d'Avenir program (ANR-15-IDEX-02); and by the Dust2Planets ERC-ADG-101053020 project. A.E. Adane acknowledges the support of the Erasmus+: Erasmus Mundus programme of the European Union under Convention n° 101128124 — EUROPHOTONICS — ERASMUS-EDU-2023-PEX-EMJM-MOB.

[1] M. Nieto-Vesperinas, "Fundamentals of Mie scattering", p. 39-72, in *Dielectric Metamaterials: Fundamentals, Designs and Applications*, ed. I Brener et al (Woodhead, 2020)
[2] A. Pentilla, K. Lumme, J. Quant. Spectrosc. Radiat. Transf., 112, 1741-1746 (2011)
[3] R Vaillon, J-M Geffrin, J. Quant. Spectrosc. Radiat. Transf., 146, 100-106 (2014)
[4] J-M Geffrin, P Sabouroux, Inv. Prob., 25(2), 024001 (2009)

Analysis and engineering of scattering from multiple cylinders in the presence of planar PECs

Tommaso Isernia,[1,*] Renat Abdullin[1] , Giada Battaglia[1], Andrea Morabito[1], Lorenzo Crocco[2], and Roberta Palmeri[1]

[1]*DIIES, Università Mediterranea di Reggio Calabria – Reggio Calabria, Italy (tommaso.isernia@unirc.it)*

[1]*Istituto per il Rilevamento Elettromagnetico dell'Ambiente (IREA/CNR), Napoli, Italy (crocco.l@irea.cnr.it)*

Scattering from cylinders lying above (and parallel to) a planar Perfect Electric Conductor is a problem which is of interest in many different applications, including the analysis and synthesis of metagratings [1,2] as well as of Reconfigurable Intelligent Surfaces, which is a very hot topic in electromagnetic engineering [3]. Usually, such a problem is solved either by using full wave analysis or synthesis tools, or even by making some hypothesis on the kind of scatterers (such as their being identical, or smoothly varying, or wire-like)

In this contribution we aim to briefly review our recent activities on the subject, which are essentially based on extensions of the so called 'Scattering Matrix Method' in [4], a method able to accurately solve the problem in an effective fashion (at a 'mesoscale') thanks to proper expansions of the different scattered fields. In particular, we have been able both to extend the basic method (originally meant for the free space case) to new geometries of actual interest, as well as to turn the basic equations into a tool for inverse design [5] of convenient devices.

The method is able to deal with arbitrary cross-section cylinders, and we have been able to generalize it to case of the presence of a planar PEC as well as to all cases where the cylinders (which may be different each from the other) are within a dihedral PEC with an angle of the kind pi/n, with n integer. Examples of properly engineered simple structures able to realize anomalous reflection will also be shown.

[1] Y. Li, X. Ma, X. Wang, G. Ptitcyn, M. Movahediqomi, and S. A. Tretyakov, "All-angle Scanning Perfect Anomalous Reflection by Using Passive Aperiodic Gratings," IEEE Trans. Antennas Propag., vol. 72, no. 1, pp. 877-889, 2023, doi: 10.1109/TAP.2023.3329665.

[2] A. Epstein and O. Rabinovich, "Unveiling the properties of metagratings via a detailed analytical model for synthesis and analysis," Phys. Rev. Appl., vol. 8, no. 5, November 2017, Art. no. 054037, doi: 10.1103/PhysRevApplied.8.054037.

[3] *IEEE Transactions on Antennas and Propagation* special issue on Smart Radio Environments, October 2022

[4] D. Felbacq, G. Tayeb, and D. Maystre, "Scattering by a random set of parallel cylinders," J. Opt. Soc. Am. A, vol. 11, no. 9, pp. 2526-2538, Sept. 1994, doi: 10.1364/JOSAA.11.002526.

[5] R. Palmeri, M. T. Bevacqua, A. F. Morabito, and T. Isernia, "Design of artificial-material-based antennas using inverse scattering techniques," IEEE Trans. on Antennas and Propagation, 66(12), pp. 7076-7090, 2018.

[1] R. P. Feynman, M. Gell-Mann, and G. Zweig, Phys. Rev. Lett. **13**, 678 (1964).

[2] D. F. Edwards, "Silicon (Si)", p. 547 in *Handbook of optical constants of solids*, ed. E. D. Palik (Academic, 1997).

[3] F. Ladouceur and J. Love, *Silica-based buried channel waveguides and devices* (Chapman & Hall, 1995), Chap. 8.

[4] Author(s), "Title of paper", p. 12 in *Title of Proceeding* (Institute of Electrical and Electronics Engineers, 2023).

Torsional mechanical modes in acousto-plasmonic antennas

Antonio Garcia-Martin,[1,*] B. Castillo López de Larrinzar,[1] J.M. Garcia,[1] C. Xiang,[2] and N.D. Lanzillotti-Kimura,[2]

[1]*Instituto de Micro y Nanotecnología IMN-CNM, CSIC (CEI UAM+CSIC), Tres Cantos, Madrid, Spain (*a.garcia.martin@csic.es)*

[2]*Centre de Nanosciences et de Nanotechnologies, Université Paris-Saclay, Palaiseau, France*

Metallic nanoantennas have been studied as efficient coherent phonon generators and detectors, harnessing their characteristic optical absorption and polarization dependence of the optical modes [1-2]. The ability to control the excitation of phononic modes depends on the properties of the multiple optical resonances of the system. Lately, it has been made possible to optimally excite and detect phonon modes via plasmon resonances at the same optical frequency using chiral nanostructures and circularly polarized light [3]. However, torsional modes remain elusive in nanophononic studies. In this work we present two different approaches, one consisting in a twisted single nanostructure (toroidal propeller) [4] the second being composed of two coupled bars [5]. In both cases torsional mechanical modes are excited using light with null angular momentum. The twisting of the phononic mode is provided by the peculiar geometry of the nano-nanoantenna, either intrinsic in the case of the toroidal propeller or as a result of the interaction of the bars though the substrate.

We will present a complete theoretical analysis of the phononic and plasmonic modes, as well as their surface deformation field profiles.

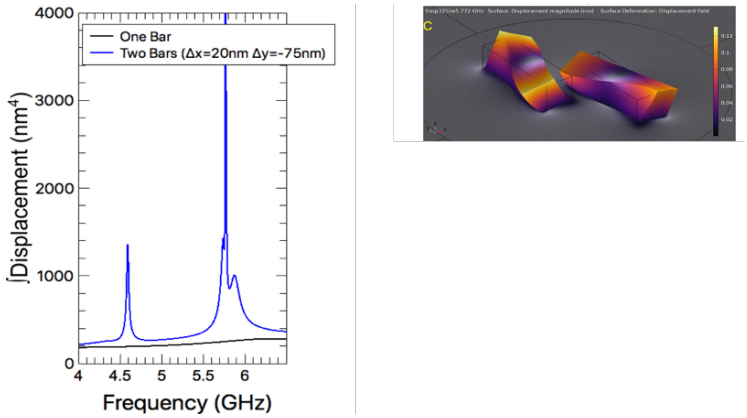

Figure 1: Left: Integral of the displacement, showing the resonances occurring for interacting bars. Right. Deformation profile depicting the torsional nature of the mechanical modes.

[1] K. O'Brien, et al. Nature communications, 5, 4042 (2014).

[2] N.D. Lanzillotti-Kimura, et al. Pysical Review B, 97, 235403 (2018).

[3] B. Castillo López de Larrinzar, C. Xiang, E.R. Cardozo de Oliveira, N.D. Lanzillotti-Kimura, and A. García-Martín. Nanophotonics 12, 1957-1964 (2023).

[4] B. Castillo López de Larrinzar, J.M. Garcia, N.D. Lanzillotti-Kimura, and A. García-Martín, Nanomaterials, 14, 1276 (2024)

[5] B. Castillo López de Larrinzar, J.M. Garcia, C. Xiang, N.D. Lanzillotti-Kimura, and A. García-Martín, Nanophotonics (in press 2025)

The Geometry Matrix Formalism for Gain Assisted Plasmonic Resonators

A. Veltri,[1,2]* A. Aradian,[3] K. Caicedo,[4] M. Mora,[1] N. Recalde,[1]
M. Infusino,[1,2] M. A. Iatì,[2] R. Saija,[5] O. M. Maragó[2]

[1]*Colegio de Ciencias e Ingenieria, Universidad San Francisco de Quito, Ecuador (*e-mail: aveltri@usfq.edu.ec)*
[2]*Institute of Chemical and Physical Processes (IPCF-CNR), Messina, Italy*
[3]*Université de Bordeaux, CNRS, CRPP,UMR5031, F-33600 Pessac, France*
[5]*Università degli Studi di Messina, Messina, Italy*
[4]*Institute of Applied Sciences and Intelligent Systems (ISASI-CNR), Napoli, Italy*

We introduce a new dynamical formalism, the *Geometry Matrix approach*, for modeling the emission dynamics of gain-assisted plasmonic nanostructures. This framework provides a systematic and modular method to analyze the optical response of both metallic nanospheres and nanoshells, handling both the quasi-static approximation and full Mie scattering regimes. The Geometry Matrix formalism enables a direct and efficient calculation of the threshold gain, emission regimes, and stability conditions, offering an advanced theoretical foundation for integrating quantum gain media into plasmonic systems.

This new approach extends previous theoretical models of gain-assisted plasmonic nanoparticles [1, 2] by unifying the description of nanoshell and nanosphere emission dynamics. In [2], the formalism was successfully applied to describe the emission properties of gain-assisted nanoshells in the quasi-static regime. More recently, numerical simulations in [3] have validated our model by reproducing similar gain threshold and emission characteristics in a full Mie scattering framework. By incorporating nonlinear interactions and a precise modal decomposition of the plasmonic response, the Geometry Matrix approach allows us to investigate key features such as gain-driven modal instabilities and the transition from amplified spontaneous emission to coherent spasing.

Beyond its theoretical significance, the Geometry Matrix formalism has direct applications in designing plasmonic computing elements. Its predictive power enables the optimization of nanoscale plasmonic logic gates, offering a viable pathway toward computational architectures that merge the speed of photonics with the miniaturization capabilities of plasmonics. This novel framework establishes a foundation for energy-efficient, high-speed plasmonic processing units that could surpass traditional electronic and photonic computing architectures.

We acknowledge financial support from the European Union (NextGeneration EU), through the MUR-PNRR projects PE0000023-NQSTI and SAMOTHRACE (ECS00000022), the PRIN2022 "Cosmic Dust II" (2022S5A2N7), and carried out within the Project “Space It Up” funded by ASI and MUR – Contract n. 2024-5-E.0 - CUP n. I53D24000060005.

[1] A. Veltri, A. Chipouline, A. Aradian, “Multipolar, time-dynamical model for plasmonic nanoparticle spasers,” *Scientific Reports* **6**, 33018 (2016).

[2] A. Aradian, K. Caicedo, A. Cathey, M. Mora, N. Recalde, M. Infusino, A. Veltri, “Emission dynamics and spectrum of a nanoshell-based plasmonic nanolaser spaser,” *Nanophotonics*, 2024.

[3] N. Recalde, D. Bustamante, M. Infusino, A. Veltri, “Dynamic multi-mode Mie model for gain-assisted metal nano-spheres,” *Materials*, **16**(5), 1911 (2023).

Cloaked quasi-bound states in the continuum in out-of-plane symmetry broken Si nanodisk metasurfaces

J. A. Sánchez-Gil,[1,*] L. Hidalgo-Arteaga, [1] B. Castillo López de Larrinzar,[1,2] D. R. Abujetas,[3] A. García-Martín [2]

[1] *Instituto de Estructura de la Materia IEM, CSIC, Madrid, Spain (*j.sanchez@csic.es)*
[2] *Instituto de Micro y Nanotecnología IMN-CNM, CSIC, CEI UAM+CSIC, Madrid, Spain*
[3] *Departamento de Matemáticas, Universidad de Castilla-La Mancha, Toledo, Spain*

Brewster quasi-bound states in the continuum (qBICs) have been observed in all-dielectric metasurfaces operating in the microwave regime [1]. These states arise from a symmetry-protected BIC linked to a strong, spectrally isolated vertical magnetic dipole resonance. They emerge when the out-of-plane symmetry is disrupted by tilting the meta-atoms, which are centimeter-sized disks with an exceptionally high refractive index. These qBICs exhibit distinctive features: they remain dark at specific Brewster-like angles, $\theta = \pm\phi$ (where ϕ is the tilt angle), are highly asymmetric, and exhibit a large but finite Q-factor.

In this work, we show that similar Brewster qBICs can also be realized in the optical domain using Si nanodisk metasurfaces, in spite of the spectral overlap between in-plane and out-of-plane dipolar resonances within these meta-atoms [2]. By employing a coupled electric/magnetic dipole model [3], we reveal that optical Brewster qBICs occur in tilted nanodisks at modified Brewster angles, which can significantly deviate from the nanodisk tilt angles ($\theta \neq \phi$). This deviation arises due to the hybridization of in-plane and out-of-plane dipolar resonances and is observed for both magnetic and electric dipole resonances. In particular, for one of the Brewster-like angles, the qBIC is indeed excited despite the fact that the metasurface remains fully transparent, thereby being termed “cloaked” qBIC [2]. Numerical simulations confirm the asymmetric nature of these qBICs in their near-field and absorption (extinction) profiles. Furthermore, we propose a practical metasurface design to support cloaked qBICs, achievable through oblique epitaxial growth to fabricate inclined cylinder arrays rather than merely tilted ones. Other configurations based on dimer meta-atoms that may support Brewster qBICs will be discussed too. The diverse phenomena associated with cloaked qBICs make them ideal for tuning or switching nano-optical devices between on/off qBIC states [4], presenting exciting opportunities for enhanced light-matter interactions at the nanoscale.

The authors acknowledge the financial support from the grants BICPLAN6G (TED2021-131417B-I00) and LIGHTCOMPAS (PID2022-137569NB-C41), funded by the Spanish MCIN/AEI/10.13039/501100011033, “ERDF A way of making Europe”, and European Union NextGenerationEU/PRTR.

[1] D. R. Abujetas, Á. I. Barreda, F. Moreno, J. J. Sáenz, A. Litman, J.-M. Geffrin, and J.A. Sánchez-Gil, Sci. Rep. **9**, 16048 (2019).

[2] L. Hidalgo-Arteaga, B. Castillo López de Larrinzar, D. R. Abujetas, A. García-Martín, J. A. Sánchez-Gil, “Dark asymmetric quasi bound states in the1 continuum in semiconductor metasurfaces with2 out-of-plane symmetry breaking,” Optica Open. Preprint. https://doi.org/10.1364/opticaopen.28163375.v1.

[3] D. R. Abujetas, J. Olmos-Trigo, J. J. Sáenz, J. A. Sánchez-Gil, Phys. Rev. B 102, 125411 (2020).

[4] D. R. Abujetas, N. de Sousa, A. García-Martín, José M. Llorens, J. A. Sánchez-Gil, Nanophotonics 10, 4223–4232 (2021).

Light scattering by plasmonic and dielectric nanostructures: Biomedical applications

Pablo Albella,[1,*] J. González-Colsa,[1] G. Serrera,[1] F. González,[1] F. Moreno,[1] A. Franco,[1] D. Ortiz,[1] J.M. Saiz,[1] F. Bresme,[2] and F. González,[1]

[1]*Dep. of Applied Physics (Group of Optics), University of Cantabria, Santander, Spain (*pablo.albella@unican.es)*

[2]*Dept. of Chemistry (Molecular Sciences Research Hub), Imperial College London, London, U.K.*

Optical nanoantennas can efficiently convert freely propagating light waves into highly localized excitations that strongly interact with matter. Specifically, those made of metals, so-called plasmonic, have been utilized to achieve strong light-matter interactions at deep subwavelength scales. Their ohmic losses can cause temperature increases in the nanoantenna and its surroundings, a well-known thermoplasmonic effect [1,2] that is being exploited for a wide range of biomedical applications, such as cancer therapies, biosensing or drug delivery. On the other hand, this thermoplasmonic effect shows an impact on the emission properties of nearby targets, limiting its efficiency when used for applications such as sensing or surface enhanced spectroscopies (Raman or Fluorescence), making necessary to find alternatives to plasmonic nanoantennas. A recent proposal has been based on high index dielectrics [3].

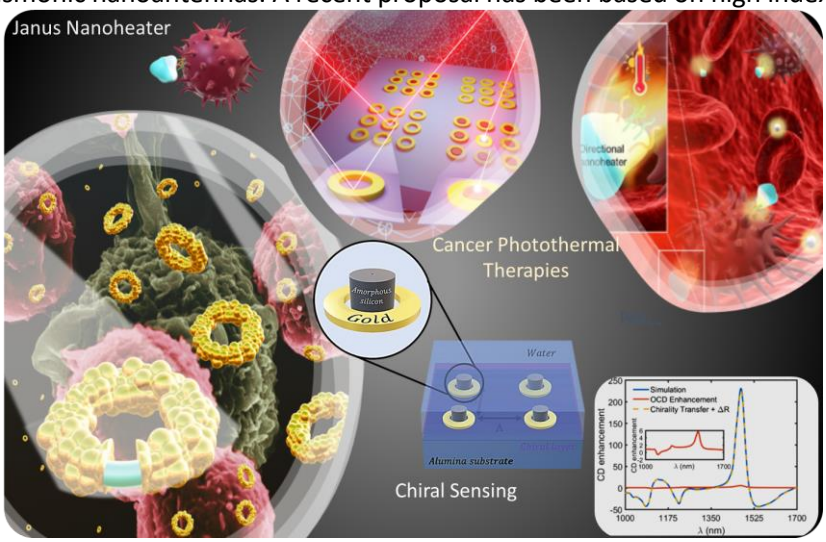

Figure 1: A simple illustration of the topics that will be discussed in the talk: plasmonic and non-plasmonic nanoantennas for biomedical applications

Here, we will first revisit and highlight the properties and strengths of plasmonic nanoantennas, focusing on our recent developments of novel nanoheaters capable of delivering **heat asymmetrically**, a desirable effect in photothermal cancer therapies and drug delivery [4-6]. The rest of the talk will be centered on non plasmonic nanoantennas and its capability not only to provide significant near-field enhancement and excellent scattering efficiencies under low losses but also exhibit remarkable optical properties, such as the ability to excite nanoscale displacement currents, leading to magnetic optical hot spots [7]. This capability is paving the way for the development of the next generation of nanoantennas with the potential to improve SERS and SEF [8], light guiding [9,10], non-linear phenomena [11] or sensing applications, including chiral enantiomer separation [12].

[1] A. O. Govorov, H. H. Richardson, Nano Today 2007, 2, 30.
[2] G. Baffou, R. Quidant, Laser Photonics Rev. 2013, 7, 171.
[3] A. Barreda, J. M. Saiz, F. González, F. Moreno and P. Albella. AIP Advances 2019, 9, 040701.
[4] J. González-Colsa et al. Opt. Express 2022, 30(1), 125.
[5] J. González-Colsa, A. Franco, F. Bresme, F. Moreno and P. Albella. Sci. Rep 2022, 12(1), 14222.
[6] J. González-Colsa, A. Kuzyk and P. Albella. Small Structures 2024, 2300523.
[7] P. Albella, A. M. Poyli, M. Schmidt, S. A. Maier, F.Moreno, J. J. Sáenz and J. Aizpurua. JPCC 2013, 117, 13573.
[8] M. Caldarola, P. Albella et al. Nature Comms 6:7915, (2015).
[9] P. Albella, T. Shibanuma and Stefan A. Maier. Sci. Reports 5, 18322 (2015)
[10] T.Shibanuma, T.Matsui, T.Roschuk, J.Wojcik, P.Mascher, P.Albella & S.A. Maier. ACS Photonics 2017, 4, 489
[11] T. Shibanuma, G. Grinblat, P. Albella and S. A. Maier. Nano Lett. 17 (4), 2647–2651, 2017.
[12] G. Serrera, J. González-Colsa and P. Albella. Appl. Phys. Lett. 124, 251701 (2024).

Optical Modelling of Complex Thermoplasmonic Agents in the Context of Advanced Therapies

Javier González-Colsa,[1,*] Anton Kuzyk,[2] and Pablo Albella[1]

[1]*Group of Optics, Department of Applied Physics, University of Cantabria, 39005 Santander, Spain (*Javier.gonzalezcolsa@unican.es)*

[2]*Department of Neuroscience and Biomedical Engineering, Aalto University School of Science, Espoo, Finland*

Toroidal nanostructures have gained attention as exceptional candidates for photothermal applications due to their unique thermal properties, spectral adaptability, and functional versatility [1, 2]. Our recent computational studies revealed that gold toroids surpass other geometries, such as nanodisks and nanorods, in achieving higher temperatures. These structures also offer advantages like rotational symmetry and extensive heating areas, making them particularly interesting for biomedical use [3].

However, toroidal nanostructures present challenges in terms of fabrication in colloid due to its particular geometry such as material uniformity, roughness control and scalability. However, recent advances in the DNA-origami technique provide a promising framework for their assembly [4]. This technique uses DNA strands as programmable building blocks to create nanoscale templates with the desired shapes, including toroidal structures. The DNA templates are then coated with metal, such as gold, to create the final plasmonic structure: a hybrid DNA/metal nanotoroid.

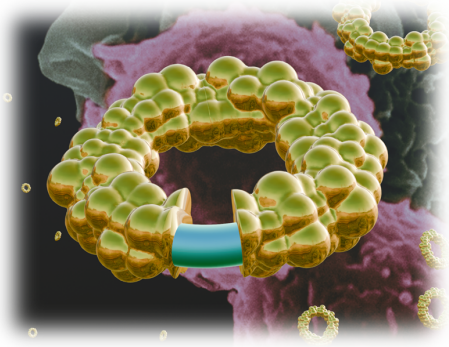

Figure 1: Illustration of a DNA/Gold core-shell.

In our work, we computationally investigated DNA/Au core-shell toroids revealing significant improvements compared to solid counterparts [5]. These hybrid structures demonstrated enhanced temperature increases and optimal resonance within the NIR-II therapeutic window, enabling larger tissue penetration and improved efficacy in photothermal therapy. Our analyses highlighted experimental factors that typically suppose a fabrication challenge, including asymmetric gold growth, partially uncovered shells and surface roughness.

Additionally, we showed the remarkable stability and minimal sensitivity to rotational variations which further support their suitability for applications beyond the NIR spectrum. This study establishes DNA/Au core-shell toroidal nanostructures as groundbreaking platforms for localized photothermal treatments, offering transformative potential for cancer therapy and other biomedical innovations.

[1] J. González-Colsa; G. Serrera; J. M. Saiz; D. Ortiz; F. González; F. Bresme; F. Moreno and P. Albella, Opex 2022, **30**(1), 125.

[2] J. González-Colsa; J. D. Olarte-Plata; F. Bresme and P. Albella, JPCL 2022, **13**(26), 6230−6235.

[3] J. González-Colsa; A. Franco; F. Bresme; F. Moreno; P. Albella, Sci.Rep 2022, 12(1), 14222.

[4] A. Kuzyk; R. Schreiber; Z. Fan; et al., Nature 2012, **483**, 311–314.

[5] J. González-Colsa; A, Kuzyk; P. Albella, Small Structures 2024, 2300523.

Raman spectroscopy analyses to study the physiological features of a 3D HepG2 model

C. Corsaro,[1,*] M. G. Rizzo,[2] S. Conoci,[2,3,4] S. Marrara,[1] V. Crupi,[1] F. Neri,[1] and E. Fazio [1]

[1]*Department of Mathematical and Computational Sciences, Physical Science and Earth Science, University of Messina, I-98166, Messina, Italy (*ccorsaro@unime.it)*

[2]*Department of Chemical, Biological, Pharmaceutical and Environmental Sciences, University of Messina, I-98166, Messina, Italy*

[3]*CNR-DSFTM, URT LabSens Beyond Nano Messina, I-98166, Messina, Italy*

[4]*Department of Chemistry G. Ciamician, University of Bologna, I-40126, Bologna. Italy*

Three-dimensional (3D) cell culture models, particularly those utilizing the HepG2 human hepatocellular carcinoma cell line, are useful in mimicking in vivo liver physiology. These models offer enhanced cellular interactions and functionality compared to traditional two-dimensional (2D) cultures. Recent studies utilizing Raman spectroscopy have provided insights into the physiological features of these 3D HepG2 models [1]. The integration of advanced imaging techniques like Raman spectroscopy further enhances the capability to study complex biological interactions within these models. Specifically, HepG2 spheroids show a time-dependent suppression of cell division, with a notable accumulation of cells in the G0/G1 phase of the cell cycle. This indicates a shift towards quiescence, which is characteristic of differentiated liver cells. The metabolic activity of HepG2 cells in 3D cultures is significantly enhanced, allowing for better drug metabolism studies. For instance, under dynamic conditions, these cells displayed increased proliferation capacity and functionality compared to static cultures [2].

In this work, Raman analysis has been utilized to assess the biochemical composition and cellular responses within HepG2 spheroids. This technique has allowed a non-invasive monitoring of metabolic states by detecting specific molecular vibrations related to cellular components, paving the way for improved predictive models in toxicology and pharmacology.

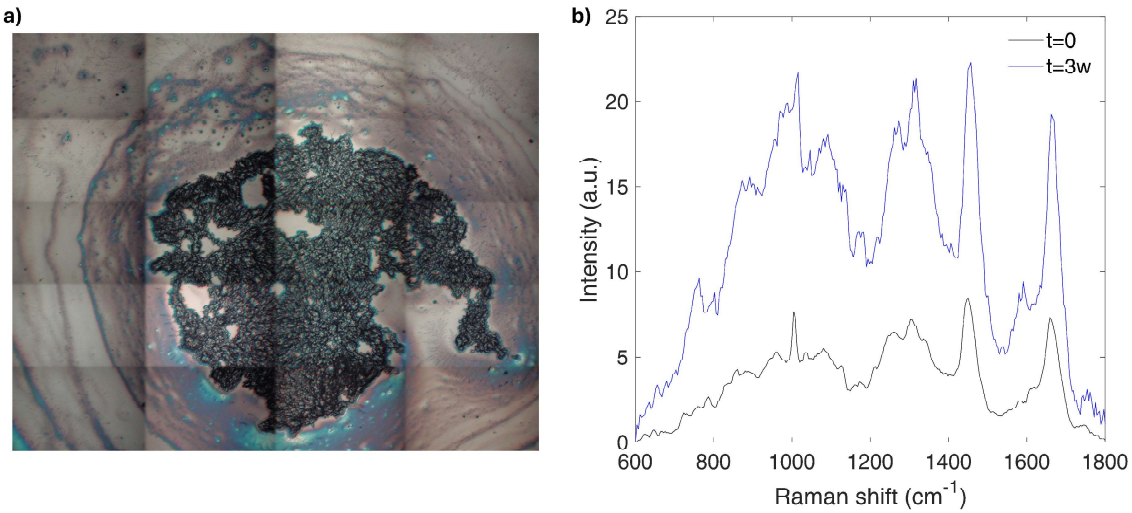

Figure 1: a) Mosaic reconstruction of an optical image of 3D HepG2 cells after 3 weeks of growth. b) Raman spectra of 3D HepG2 cells just incubated and after 3 weeks of growth.

Funding and acknowledgment: This work has been partially funded by the European Union (NextGeneration EU), through the MUR-PNRR project SAMOTHRACE (ECS00000022).

[1] J. Marzi, *et al.*, ACS Applied Materials & Interfaces **14(27)**, 30455-30465 (2022).

[2] H.-H. Tsai, *et al.*, International Journal of Molecular Sciences **20(16)**, 4024 (2019).

Light scattering investigations of Black turmeric (*Curcuma Caesia*) as potent antibacterial agent and its response at different temperatures

Farhana Hussain,[1] Sanchita Roy [2,*]

[1]*Department of Physics, School of Applied Sciences, University of Science and Technology, Meghalaya, District- Ri Bhoi, 793101, Meghalaya, India.*
[2] *Department of Physics, Royal School of Applied and Pure Sciences, The Assam Royal Global University, Guwahati,781035, Assam, India*

The present work explores feasibility of static light scattering to analyze the antibacterial properties of black turmeric (*Curcuma caesia*) against *Escherichia coli* (ATCC-9637) at temperatures of 37°C, 45°C, 55°C, and 65°C. Significant changes in antibacterial activity was observed at different temperatures particularly pronounced at 37°C. The corresponding light scattering profiles observed for samples subjected to different temperatures were also monitored by using a He-Ne laser-based light scattering setup. We measured scattering Mueller matrix elements (D_{11} and D_{12}), which provided insights into its morphological characteristics. By analyzing the scattering profiles of volume scattering function and degree of linear polarization at 632.8 nm, we correlated changes in scattering patterns due to the size, shape, and composition of black turmeric particles due to its interaction with *E. coli*. The results showed a significant alteration in the scattering matrix upon inoculation with *E. coli*, demonstrating that light scattering is a promising, non-invasive technique for assessing both the morphological and antibacterial properties of black turmeric. This research deepens our understanding of how black turmeric's antibacterial activity can be characterized through light scattering methods.

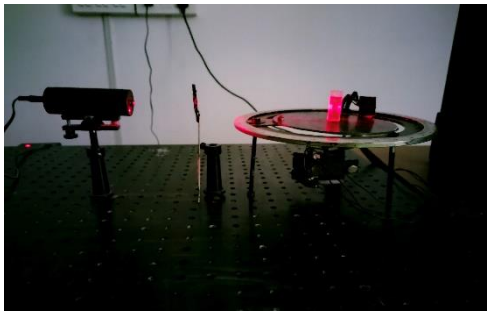

Figure 1. Laboratory-based light scattering setup

References:

[1] Martikainen, Julia, Olga Muñoz, Juan Carlos Gómez Martín, María Passas Varo, Teresa Jardiel, Marco Peiteado, Yannick Willame, Lori Neary, Tim Becker, and Gerhard Wurm. "Database of Martian dust optical properties in the UV-vis-NIR." *Monthly Notices of the Royal Astronomical Society* (2025).

[2] Roy, Sanchita, Nilakshi Barua, Alak K. Buragohain, and Gazi A. Ahmed. "Study of ZnO nanoparticles: Antibacterial property and light depolarization property using light scattering tool." *Journal of Quantitative Spectroscopy and Radiative Transfer* 118 (2013): 8-13.

[3] Hussain F, Roy S. Radiative transfer of Black turmeric and its interpretation of antimicrobial property by light scattering. The European Physical Journal Plus. 2024 Aug 1;139(8):687.

[4] Qian, Shaoyu, and John JJ Chen. "Experimental investigation of liquid foams by polarised light scattering technique via the Mueller matrix." *Chemical Engineering Science* 104 (2013): 189-200.

[5] Muñoz, Olga, E. Frattin, Teresa Jardiel, Juan Carlos Gómez-Martín, Fernando Moreno, J. L. Ramos, D. Guirado et al. "Retrieving dust grain sizes from photopolarimetry: an experimental approach." *The Astrophysical Journal Supplement Series* 256, no. 1 (2021): 17.

The role of cloud microphysical versus cloud macrophysical variability in solar cloud radiative transfer - review and recommendations for future work

Andreas Macke[1,*], Ronald Scheirer[2]

[1]*Leibniz Institute for Tropospheric Research – Leipzig, Germany (*macke@tropos.de)*

[2] *Swedish Meteorological and Hydrological Institute – Norrköping, Sweden*

Numerous studies have demonstrated the importance of spatial variability of clouds for the realistic treatment of radiative fluxes and radiances, mainly in the solar but also to some extent in the terrestrial spectral range [e.g. 1]. Ultimately, the local scattering and absorption properties of a cloud volume are defined by the particle number density and the averaged single scattering and absorption properties within that volume. Intuitively, one would assume that for 3D radiative transfer problems, the spatial variability of the cloud particle density plays a more important role due to multiple scattering than the local details of particle sizes and shapes (and to some extent orientation), which in the end determine the scattering phase matrix and the single-scattering albedo. Thus, the question arises how important the details of cloud microphysical properties are compared to cloud morphology for realistically treating 3d cloud radiative transfer. In fact, even water clouds consisting of spherical droplets exhibit a strong spatial variability of the effective droplet radius along all directions due to growth processes and turbulence. Due to the lack of information about the local hydrometeor sizes and shapes, homogeneity is still the predominant assumption in climate modeling and remote sensing today. The variability of cloud microphysics becomes even more important for mixed-phase clouds, in which water and ice hydrometeors with variable fractions coexist, and finally for optically thin cirrus clouds, in which single scattering and thus the microphysical properties of clouds dominate.

In this article, previous work on the radiative transfer of 1D and 3D solar clouds is reviewed, in which radiative quantities for fixed and variable cloud microphysical properties are compared for different cloud types based on idealized 1D and modeled 3D clouds. As examples, it was shown that solar broadband absorption in 3D clouds is systematically underestimated when the horizontal variability of cloud microphysics is neglected [2]. For cirrus clouds, the shape of the ice crystals is just as important as the optical thickness of the cloud [3]. Further results are discussed in the presentation

Within the German research initiative “Cloud 3D Structure and Climate” (C3SAR) [4], the role of microphysical and macrophysical cloud variability on solar radiation fluxes and radiance at the surface and at the top of the atmosphere is investigated on the basis of long-term ground- and satellite-based observations, specific field campaigns and cloud-resolving models. To separate the role of microphysical and macrophysical cloud properties and variability on the modeled and observed fluxes, we propose intensive radiation closure studies as an operational tool at remote sensing supersites. Here, continuous active ground-based remote sensing together with irradiance and radiance measurements from the ground and space, and high-resolution cloud modeling provide the best possible information to determine the accuracies in all cloud variables required to provide realistic cloud radiative properties. Ultimately, some unresolved cloud variability must be accepted as natural variability and as a limitation of our understanding of the radiative properties of clouds in remote sensing and climate modeling.

[1] A. Marshak, and A. Davies, Eds, 3D radiative transfer in cloudy atmospheres. Springer (2005).

[2] R. Scheirer and A. Macke, J. Geophys. Res., **108**, 4599 (2003).

[3] I. Schlimme, A. Macke, and J. Reichardt, J. Atmos. Sci. **62**, 2274 (2005)

[4] A. Macke and Co-Authors, Cloud 3D Structure And Radiation (C3SAR) - A new initiative to account for 3d effects in climate research, Proceedings of the International Radiation Symposium, Hangzhou, China, 2024 (2025)

Temperatures of dust grains in some circumstellar environments

Juris Freimanis[1,*]

[1]*Ventspils International Radio Astronomy Centre of Ventspils University of Applied Sciences – Ventspils, Latvia (*jurisf@venta.lv)*

Necessity of this study: Temperature of cosmic dust grains is important for grain growth and evaporation, and the growth and evaporation of layered "ice" mantles. Dust temperature determines the observable infrared radiation, as well as speed of multiple chemical reactions on grain surfaces and inside the mantles. Often it is assumed that at the given spatial point dust temperature spans over some narrow interval, or even dust is characterized by a single temperature. This study is devoted to testing such assumptions.

Method of research: Monte Carlo radiative transfer calculations using the code RADMC-3D [1] were performed for models of circumstellar dust clouds containing dust grains of several kinds with some variety of chemical composition and size. Thermal equilibrium between the dust and the local radiation field was assumed. The central star and the interstellar radiation field are assumed to be the primary sources of energy. Morphologies of the dust cloud include homogeneous spherical cloud, spherically symmetric radial outflow with constant speed leading to inverse square dependence of density on radius, and an axisymmetric model of dense torus with rarified bipolar holes.

The results. Dust temperature in circumstellar conditions is primarily, very strongly and very nonlinearly determined by the chemical composition. Temperatures of various kinds of dust particles at one and the same place, inside one and the same radiation field can differ by up to 1000 K, and it is explained by the interplay between the dependence of complex refractive index on wavelength and the spectrum of radiation. Dependence of dust temperature on grain size exists, but it is considerably less significant than that on grain material.

[1] C. Dullemond, *RADMC3D Release 2.0*, Jul 01, 2022. https://www.ita.uni-heidelberg.de/~dullemond/software/radmc-3d/ .

Effect of Surface Roughness and Composition on Scattered Light by Regolith Surfaces

Francisco J. García-Izquierdo[1,*], Elisa Frattin[1], Julia Martikainen[1], Olga Muñoz[1], Fernando Moreno[1], Juan Carlos Gómez Martín[1], Teresa Jardiel[2], Marco Peiteado[2], Amador Caballero[2], Gorden Videen[3], Johannes Markkanen[4], Antti Penttilä[5], and Karri Muinonen[5]

[1]*Insituto de Astrofísica de Andalucía, Glorieta de la Astronomía, Granada, Spain (*fgarcia@iaa.es)*

[2]*Instituto de Cerámica y Vidrio (ICV), CSIC, Madrid, Spain*

[3]*Space Science Institute, Boulder Suite 205, USA*

[4]*Institut für Geophysik und Extraterrestrische Physik, Technische Universität Braunschweig, Mendelssohnstr. Braun-schweig, Germany*

[5]*Department of Physics, University of Helsinki, Finland*

The present work investigates how surface roughness and composition affect light scattered by planetary regolith simulants. Light scattering experiments are conducted at the IAA CoDuLab [1] at two wavelengths, namely 488 nm and 640 nm. Centimeter-sized cylindrical samples with varying porosity and surface roughness were produced at ICV using MMS2 Martian analogue powder (m(488nm) = 1.5+i0.0011 and m(640nm) = 1.5+i0.00035 [2]). The powder, refined to below 20 µm, was mixed with ethyl cellulose for controlled porosity. The samples were isostatically pressed, calcined at low heating rates to remove the cellulose, and sintered below their melting point. The resulting aggregates were cut to expose rough surfaces and designated as MASC (Martian Analogue Synthesized Cylinder) [3]. We have obtained the scattering matrices in an angular range from 94 to 177 degrees of scattering angle, using normal incidence. Figure 1 shows scattering matrix elements for MASC-1 and MASC-4 regolith analogues at 488 nm. The albedos at 170° for MASC-1 and MASC-4 are 0.16±0.04 and 0.06±0.01, respectively, compared to a Spectralon standard (99% reflectance). The F_{11} curves are normalized to their albedos, showing that MASC-4's greater surface roughness causes darkening across most angles. Differences in the scattering matrix elements F_{22}/F_{11}, F_{33}/F_{11}, and F_{44}/F_{11} highlight the impact of surface roughness.

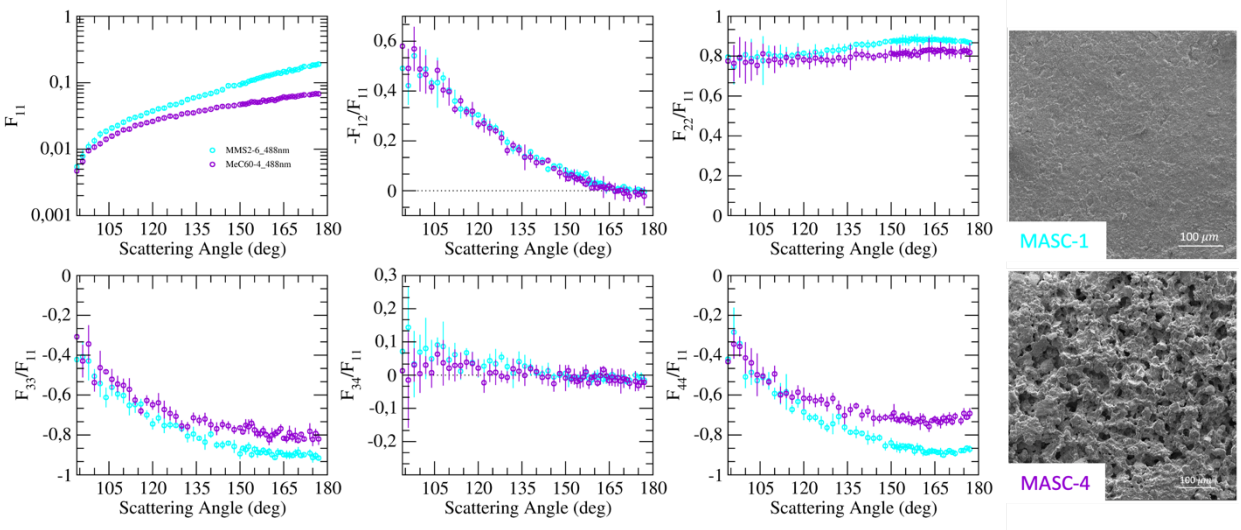

Figure 1: Experimental scattering matrices at 488 nm and SEM images of two Martian analog simulant regolith (MASC-1 in sky-blue and MASC-4 in purple). The F_{11} is normalized to the value $F_{11}(170°)$ of a diffuse reflectance standard, a Spectralon (Labsphere SRT-99-020 AA-00823-000). Matrices are obtained using normal incidence.

[1] Muñoz, Moreno, Guirado et al. JQSRT, 11(1), (2010)

[2] Martikainen, Muñoz, Gómez-Martín et al. ApJ Supp Series, 273 (2) (2024)

[3] Frattin, García-Izquierdo, Muñoz, et al. Submitted to A&A.

Mueller parameters of non-homogeneous scatterers obtained from microwave analogy and additive manufacturing

Jean-Michel Geffrin[1,*], Rémi Zerna[2], Elio Samara[1], Hervé Tortel[1], Amélie Litman[1], François Ménard[2]

[1]*Aix Marseille Univ, CNRS, Centrale Med, Institut Fresnel, Marseille, France*
*(*jean-michel.geffrin@fresnel.fr)*
[2]*Univ. Grenoble Alpes, CNRS, IPAG, 38000 Grenoble, France*

Microwave analogy and additive manufacturing: Taking profit of the recent improvements of 3D printers, we can build non-homogenous analogs of circumstellar dust particles (or asteroids) at the centimeter scale [1]. Thanks to the scale invariance rule of Maxwell equations, we can measure the scattering parameters of such analogs in the microwave frequency range to mimic their behavior in the visible or millimeter range (or radiowave range) [2].

Simulation of ice coverage: In this case, lattices were used to manage the air volume ratio within four different aggregates. The bulk material has a refractive index which is similar to astronomical silicate while the inclusions of air in the lattices allow to reduce the index close to the one of typical water ice properties. These aggregates have been realized by 3D printing and their associated Mueller components have been experimentally acquired. All the measurements were made in an anechoic chamber, exactly as it can be found in [3, 4]

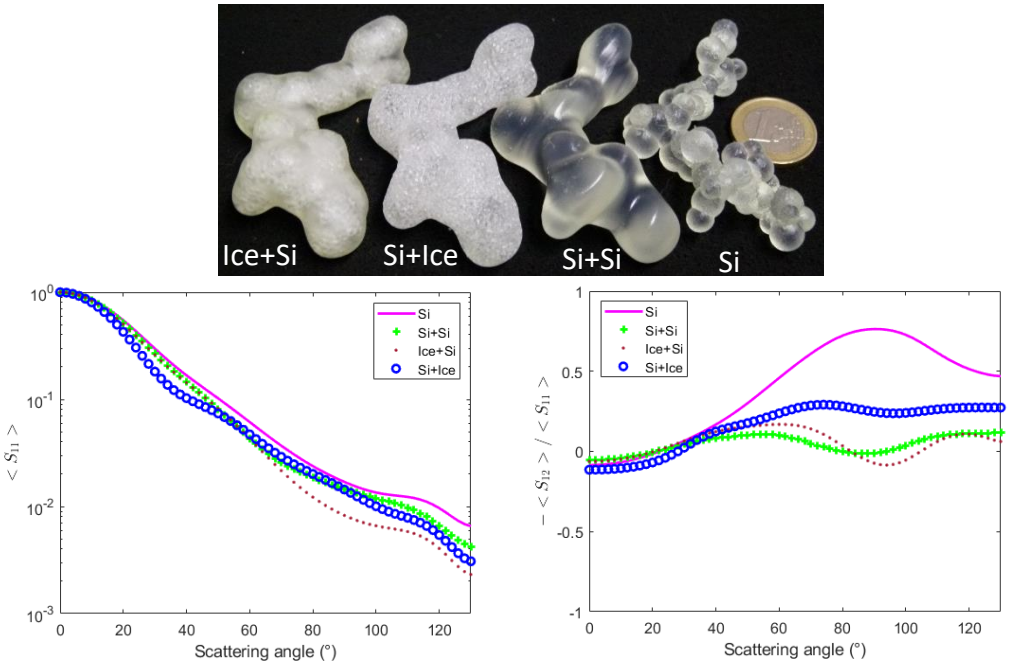

Figure 1: a) Printed analogs (right to left): silicate aggregate without cover (named : "Si"), silicate aggregate covered with silicate (Si+Si), silicate aggregate covered with ice (Si+Ice), ice aggregate covered with silicate (Ice+Si). b) Measured Phase functions, c) Measured degree of linear polarization (size parameter: x=6.6)

Conclusion: Our measurements will be compared to computations considering the design of the analogs, the printing parameters and the measured results will be discussed. Other 3D printing techniques are also under investigation, multi material printers and new materials will be characterized and tested.

Acknowledgments: This work was supported by the French National Research Agency in the framework of the Investissements d'Avenir program (ANR-15-IDEX-02). It was also supported by the Dust2Planets ERC-ADG-101053020 project. We would like to thank J Yon from CORIA for sharing the aggregate geometries with us.

[1] H Saleh *et al*, IEEE Transactions on Antennas and Propagation, Volume: 69, Issue: 2, February (2021)
[2] R Vaillon, J-M Geffrin, Journal of Quantitative Spectroscopy and Radiative Transfer, Vol. 146, Oct. (2014)
[3] V Tobon-Valencia *et al*, *Astronomy & Astrophysics*, *666*, A68 (2022)
[4] V Tobon-Valencia *et al*, *Astronomy & Astrophysics*, *688*, A70 (2024)

The IAA Cosmic Dust Laboratory, 15 years studying scattering by non-spherical particles

Olga Muñoz,[1,*] Jesús Escobar-Cerezo[2], Elisa Frattin[1], Francisco J García-Izquierdo[1,], Juan Carlos Gómez-Martín[1,], Zuri Gray[3], Teresa Jardiel[4], Julia Martikainen[1], Antonio J Ocaña[1], Marco Peiteado[4], Fernando Moreno[1]

[1]*Instituto de Astrofísica de Andalucía (IAA), CSIC – Granada, Spain (*olga@iaa.es)*
[2]*Hospital Universitario Clínico Virgen de las Nieves, – Granada, Spain*
[3] *Department of Physics, University of Helsinki, – Helsinki, Finland*
[4] *Instituto de Cerámica y Vidrio (ICV), CSIC, – Madrid, Spain*

Over the past fifteen years, the Cosmic Dust Laboratory (CODULAB) [1,2] at IAA-CSIC has produced a significant number of scattering matrices for clouds of randomly oriented cosmic dust analog samples. These measurements are conducted at three different wavelengths (448 nm, 520 nm, and 647 nm) and cover a phase angle range from 3° to 177°. Over the years, we have made various modifications to the CODULAB optical train and sample holder to expand the size range of the samples of interest: clouds of randomly oriented micron-sized particles [3]; planetary regolith simulants [4], single sub-mm/mm dust grains in random orientation [5,6].

All experimental data are available in digital form through the Granada-Amsterdam Light Scattering Database that has been recently updated Granada-Amsterdam Light Scattering Database [7].

In this talk, I will summarize the main results obtained over the years at CODULAB on scattering by non-spherical particles with particular emphasis on astronomical applications.

[1] Muñoz, Moreno, Guirado et al. JQSRT, 11(1), (2010)
[2] Muñoz, Moreno, Guirado et al. Icarus, 211(1), (2011)
[3] Martikainen, Muñoz, Gómez-Martín et al. ApJ Supp Series, 273 (2) (2024)
[4] Frattin, García-Izquierdo, Muñoz, et al. Submitted to A&A.
[5] Muñoz, Moreno, Gómez-Martín et al. ApJ Supp Series, 247 (1), (2020)
[6] García-Izquierdo, Frattín, Muñoz, et al. In preparation.
[7] Muñoz, Frattin, Martikainen, et al. JQSRT, 331, (2025)

Aerosol optical centroid height retrieval from hyperspectral measurements in oxygen absorption bands: perspectives from polar orbiting satellite to geostationary satellite constellation

Xi Chen,[1,*] Jun Wang,[1] Zhendong Lu,[1] Xiaoguang Xu,[2] Meng Zhou,[3] and Jim Carr[4]

[1] *The University of Iowa, Iowa City (IA), USA (*xi-chen-4@uiowa.edu)*
[2] *Joint Center for Earth Systems Technology, University of Maryland, Baltimore County, Baltimore (MD), USA*
[3] *Goddard Earth Sciences Technology and Research II, University of Maryland, Baltimore County, Baltimore (MD), USA*
[4] *Carr Astronautics Inc., Greenbelt (MD), USA*

Abstract: Constraint of the vertical distribution of aerosol particles is crucial for the study of aerosol plume structure, aerosol radiative effects, and monitoring surface air pollution. Spaceborne lidars like CALIOP can detect aerosol extinction profiles around the world, but only have less than 0.2% global coverage. The sensitivity of the Earth reflected sunlight in oxygen (O2) absorption band to aerosol layer height provides the possibility to get aerosol layer height information using passive remote sensing technique. The aerosol optical central height (AOCH) was defined to describe the peak height of aerosol extinction profile with a quasi-Gaussian distribution and we developed an algorithm to retrieve AOCH of absorbing aerosols by using the hyperspectral measurements in O2 absorption bands, which is applicable for the TROPOspheric Monitoring Instrument (TROPOMI) onboard a polar orbiting satellite and the Tropospheric Emissions: Monitoring Pollution (TEMPO) observing from geostationary orbit. The narrow-band radiance at several channels ranging from ultraviolet (UV), visible (VIS) to NIR (O2 B or A band) are convolved from TROPOMI or TEMPO hyperspectral measurements. The aerosol optical depth (AOD) is retrieved from blue band and then used in AOCH retrieval from the ratio between O2 absorption band and its close continuum band through a look-up-table approach accounting for AERONET-based dust and smoke optical properties. For TROPOMI measurements, both O2 B and A bands are combined in the optimization while TEMPO only covers O2 B band. The validation with spaceborne lidar CALIOP indicates that adding O2 B band can improve TROPOMI retrieval over land effectively. However, comparing with TROPOMI, the lack of NIR channels in TEMPO may miss some information about cloud and surface, which are also significant for aerosol retrieval. Considering the Advanced Baseline Imager (ABI) onboard another geostationary satellite system, GOES-R, covering VIS and NIR channels, we try to develop an advanced algorithm combining the synergistic measurements of ABI and TEMPO to better constrain surface reflectance used in AOCH retrieval. Furthermore, given their different viewing geometries, the synergistic ABI and TEMPO measurements in the same visible channels (469 and 639 nm) have the potential to provide more information about aerosol model, such as fine mode AOD using dual- or triple-view measurements. As a result, the fine mode fraction and surface reflectance can also be retrieved simultaneously with AOD and AOCH, which will help provide the diurnal variation of aerosol layer height and surface $PM_{2.5}$ pollution in contiguous U.S.

A combined retrieval of mid-visible and thermal infrared dust optical depth and coarse mode particle size from MODIS observation

Jianyu Zheng,[1,2,*] Yaping Zhou,[1,2] Yingxi Shi,[1,2] Hongbin Yu,[2] Zhibo Zhang,[3]

[1]*Goddard Earth Sciences Technology and Research II, University of Maryland Baltimore County, Baltimore, MD 21250, USA (*jzheng3@umbc.edu)*

[2]*NASA Goddard Space Flight Center, Greenbelt, MD 20771, USA*

[3]*Department of Physics, University of Maryland Baltimore County, Baltimore, MD 21250, USA*

Mineral dust aerosol impacts the radiation budget of Earth, cloud formations, ocean and terrestrial biogeochemical processes, visibility, and human health. The quantification of each impact relies on understanding the spatiotemporal variation of dust physicochemical properties, such as dust loading, optically represented by dust aerosol optical depth (DAOD) and dust particle size distribution. Recently, we developed a novel algorithm of retrieving the thermal infrared DAOD and coarse mode effective diameter of dust over ocean (along the CALIPSO track) from MODIS thermal infrared observations with a constraint by CALIOP-derived dust vertical profiles [1]. In this study, we further improve the algorithm to cover off-CALIOP-track MODIS pixels over both ocean and land based and to retrieve dust properties simultaneously in mid-visible and thermal infrared wavelengths leveraging the climatological CALIOP dust vertical profiles. The retrievals are evaluated with AERONET observations, and the multiple in-situ measurements of dust particle size distribution. The algorithm will be used to produce global dust properties at 1 degree resolution for the 20-year MODIS observational record, which can be used to advance the understanding of dust climate impacts.

[1] Zheng, J., Zhang, Z., Yu, H., Garnier, A., Song, Q., Wang, C., Biagio, C. D., Kok, J. F., Derimian, Y., and Ryder, C., "Thermal infrared dust optical depth and coarse-mode effective diameter over oceans retrieved from collocated MODIS and CALIOP observations", *Atmos. Chem. Phys*., 23, 8271–8304, 2023.

Unveiling Hidden Characteristics of Scattering Phase Function: From Spherical to Complex Ice Crystals

Guanglang Xu

Shenzhen University – Shenzhen, Guangdong ,China (gl.xu@szu.edu.cn)

In paper [1], Xu et al. introduced the Cp parameter, derived from the expansion coefficients of the scattering phase function associated with Legendre polynomials. This parameter characterizes the morphological complexity of large ice crystals and has been shown to be strongly correlated with complexity metrics like surface roughness and internal air bubbles. This approach has been recently applied to investigate the microphysical and light scattering properties of bullet rosette ice crystals [2]. In this presentation, building upon our prior work [3], we extend the application of the Cp parameter to a broader range of particle shapes, including spheres and their aggregates. Moving beyond ray tracing methods, we employ more numerically rigorous techniques such as Lorenz-Mie theory and Multiple Sphere T-matrix (MSTM) approaches to accurately account for wave interference effects.

The core of this presentation lies in showcasing novel findings that reveal hidden patterns within scattering phase functions for both spherical and more complex non-spherical particles in light scattering. We have identified a particularly intriguing relationship between the refractive index of a sphere and the Cp parameter. Consistent with prior knowledge, increasing the real part of the refractive index leads to oscillations in scattering efficiency towards higher refractive indices. Notably, we discovered that the Cp parameter also oscillates with increasing refractive index, but in an opposing manner compared to scattering efficiency. Furthermore, increasing the imaginary part of the refractive index results in a decrease in the Cp parameter, mirroring the trend observed in scattering efficiency. These observations suggest deeper connections between the angular distribution of scattered energy and the total scattering cross-section. We will also present preliminary theoretical analyses to support these findings during the talk.

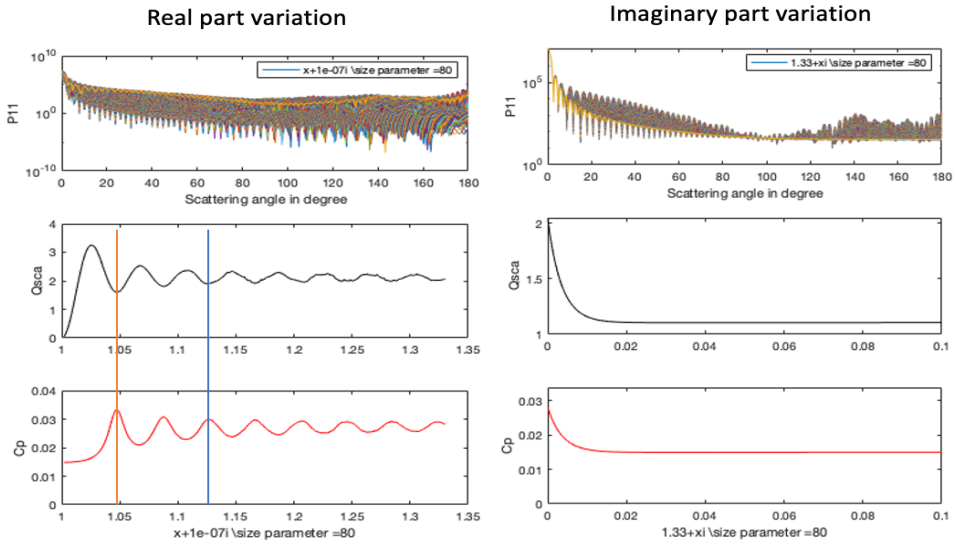

Figure 1: The Cp parameter The Cp parameter reveals hidden correlations between scattering efficiency and scattering phase functions for a spherical particle. **Left Panel:** Variation patterns resulting from increasing the real part of the refractive index. **Right Panel:** Variation patterns resulting from increasing the imaginary part of the refractive index.

[1] G. Xu, F. Waitz, S. Wagner, F. Nehlert, M. Schnaiter and E. Järvinen, "Toward Better Constrained Scattering Models for Natural Ice Crystals in the Visible Region," *Journal of Geophysical Research: Atmospheres,* vol. 128, p. e2022JD037604, 2023..

[2] Wagner, S. W., Schnaiter, M., Xu, G., Nehlert, F., and Järvinen, E.: Light scattering and microphysical properties of atmospheric bullet rosette ice crystals, EGUsphere [preprint], https://doi.org/10.5194/egusphere-2024-3316, 2024.

[3] Xu et al. Some hidden patterns in light scattering phase functions: from sphere to complex non-spherical particles. to be submitted to JQSRT.

Light Scattering by Two-layer Spheroids: Separation of Variable Method in Spheroidal Coordinates

Jiachen Ding[1,*] and Ping Yang,[1,2,3]

[1]*Dept. of Atmospheric Sciences, Texas A&M University – College Station (TX), USA (*njudjc@tamu.edu)*
[2]*Dept. of Physics & Astronomy, Texas A&M University – College Station (TX), USA*
[3]*Dept. of Oceanography, Texas A&M University – College Station (TX), USA*

Many particles in nature have inhomogeneous compositions. For example, mineral dust aerosol can be coated with other chemical compositions during long-range transport. Algae particles have two-layer structures. Accurate simulation of the inhomogeneous particle optical properties is fundamental to remote sensing applications and radiative transfer computations. Advancement of remote sensing instruments and techniques, such as spaceborne multi-angle polarimeters and associated retrieval algorithms, can potentially infer more detailed particle microphysical and optical properties. Knowledge of inhomogeneous particle optical properties will benefit the retrieval of particle composition and inhomogeneity.

Core-shell spheres are widely used to model the effect of particle inhomogeneity, and their optical properties can be computed analytically for arbitrary particle sizes [1]. However, the core-shell sphere model cannot account for the effect of nonsphericity, which is another important characteristic of natural particles. Two-layer spheroids account for both inhomogeneity and nonsphericity, and are expected to be more accurate to model the optical properties of inhomogeneous particles in nature. An illustration of two-layer spheroids is shown in Figure 1.

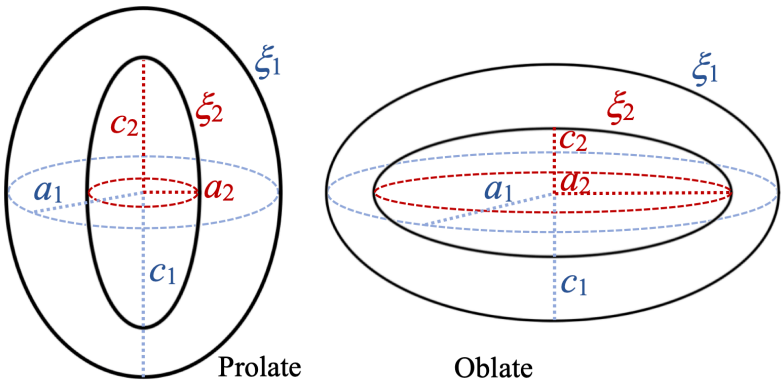

Figure 1: Illustration of two-layer prolate and oblate spheroids

It is challenging to compute the optical properties of two-layer spheroids with small-to-large size parameters and various aspect ratios. Previous studies sought a solution analogous to the counterpart for core-shell spheres [e.g., 2,3], but their methods are only applicable to spheroids with small-to-moderate size parameters (less than ~100). Recently, a Lorenz-Mie type solution [4] has been reported to be applicable to homogeneous spheroids with very large size parameters. Based on the theory and techniques in [4], in this study, we develop an analytical solution to light scattering by two-layer spheroids applicable to small-to-large two-layer spheroids with a wide aspect ratio range. This presentation will introduce the theory and techniques of light scattering by two-layer spheroids, and show the single-scattering properties of two-layer spheroids computed by the developed method.

[1] C. F. Bohren and D. R. Huffman, *Absorption and scattering of light by small particles* (John Wiley & Sons, Inc., 1983), Chap. 8.

[2] I. Gurwich, M. Kleiman, N. Shiloah, and A. Cohen, Appl. Opt. **39**, 470 (2000).

[3] D. G. Turichina, V. B. Il'in, V. G. Farafonov, and S. I. Laznevoi, Astron. Astrophys. Trans. **34**, 129 (2024).

[4] J. Ding and P. Yang, Opt. Express **31**, 40937 (2023).

Decoding the Hazy Mysteries of the Cosmos: Aerosol Remote Sensing from Earth to Exoplanets

Yuk L. Yung

Aerosols—tiny suspended particles in planetary atmospheres—play a pivotal role in shaping climate, weather, and even the potential for life. From the smog-laden skies of Earth to the photochemical hazes of Titan and the ethereal layers of Pluto, these microscopic particles scatter and absorb light in ways that encode vital information about atmospheric composition and dynamics. Over the past decades, advances in remote sensing and radiative transfer modeling have transformed our ability to decode these signals, turning aerosols into powerful tracers of planetary processes. Some advances in aerosol remote sensing are as follows:

1. Earth: CLARS-FTS and the Challenge of Urban Aerosols . High-resolution spectra from CLARS-FTS over Los Angeles reveal how aerosols interact with anthropogenic pollutants, influencing air quality and radiative forcing.

2. Titan: Cassini's Legacy of Hydrocarbon Haze. Cassini/UVIS and ISS observations uncovered fractal aggregates of tholins—complex organic aerosols—floating in Titan's nitrogen-methane atmosphere. These particles act as a planetary-scale UV shield and may seed methane rain, offering a unique analog for early Earth's haze-covered skies.

3. Pluto: New Horizons and the Puzzle of Blue Haze. New Horizons revealed a stunning, multilayered haze extending hundreds of kilometers above Pluto's surface. Alice UV spectroscopy and MVIC/LEISA imaging suggest these aerosols form via methane photochemistry, creating a dynamic, seasonal and interannual haze cycle unlike anything seen in the inner solar system.

4. Exoplanets: The Frontier of Extraterrestrial Aerosols. JWST and future missions aim to detect aerosols in exoplanet atmospheres, where they may obscure molecular features or even create "false positives" for life. Models predict sulfate and photochemical hazes in hot Jupiters, while Earth-like worlds could host organic or sulfur-based aerosols.

Broader Implications include: (1) Atmospheric Evolution: Aerosols influence escape rates, cloud formation, and surface UV flux, altering planetary habitability. (2) Comparative Planetology: By studying aerosols across different worlds, we uncover universal principles in atmospheric physics and chemistry. (3) Future Missions: Upcoming telescopes (HabEx, LUVOIR) and probes will push aerosol remote sensing into new regimes, from icy moons to temperate exo-Earths.

The remote sensing of aerosols has evolved from a niche field into a cornerstone of planetary science, linking Earth's climate to the exotic atmospheres of distant worlds. As we continue to refine our models and expand observational capabilities, these tiny particles promise to reveal even greater secrets about the diversity and dynamics of planetary atmospheres—both near and far.

Light scattering from clusters of helical particles

Yehor Surkov,[1,*] Karri Muinonen,[1] Antti Penttilä,[1] Yuriy Shkuratov,[2] Gorden Videen[3]

[1]*Department of Physics, University of Helsinki, Finland (*yehor.surkov@gmail.com)*
[2]*V.N. Karazin Kharkiv National University, Kharkiv, Ukraine*
[3]*Space Science Institute, Boulder, USA*

We study the light-scattering properties of small clusters composed of chiral and symmetric particles, such as helices, cylindrical capsules, and spheres. Using the ADDA implementation [e.g., 1] of the discrete dipole approximation (DDA) method [2-3], we examine the dependencies of scattering intensity, linear polarization, and circular polarization on the geometric characteristics of the clusters, including interparticle distance and particle number. The objective is to discern the effects of particle shape and arrangement on key light-scattering parameters, with potential implications for remote sensing and the detection of biological components.

The angular dependence of linear polarization, represented by the M_{12} element of the Mueller matrix, provides shape-related information and distinguishes particle types, particularly in the range of 60°–140° scattering angles. Circular polarization, quantified through the circular intensity differential scattering (CIDS) parameter, emerges as a critical diagnostic feature. Symmetric particles, such as spheres and capsules, exhibit oscillatory CIDS patterns around zero when arranged asymmetrically. In contrast, chiral helices display distinct, stable trends in CIDS that persist regardless of interparticle distance. These trends, characterized by the linear regression of CIDS angular dependencies in the range of scattering angles from 90° to 180°, reveals stable slope values at small particle numbers, indicating potential for the estimation of geometric parameters such as particle size and helix turns. However, the slope of the linear regression tends to 0 with increasing number of helical particles.

The findings suggest that angular polarization analysis, particularly the CIDS trends, could enhance the interpretation of scattering measurements for applications in atmospheric studies, planetary exploration, and bioaerosol detection. These results align with experimental studies, where chiral biological components show pronounced CIDS patterns, contrasting with symmetric synthetic particles [e.g., 4-5].

[1] M. A. Yurkin, and A. Hoekstra, J. Quant. Spectrosc. Radiat. Transf. 112, 13 (2011).
[2] E. M. Purcell, and C.R. Pennypacker, Astrophysics 186, 705-714 (1973).
[3] B. T. Draine, and P.J. Fratau, J. Optical Society A 11, 4 (1994).
[4] Y. L. Pan, J. Arnold, L. Beresnev et al., Optics Express 30, 2 (2022).
[5] Y.L. Pan, A. Kalume, L. Beresnev et al., Aerosol Science and Technology 59, 1 (2024).

Recent advances in UV–vis spectroscopy of turbid solutions

Alla Gisich,[1] Eric Le Ru[1], Baptiste Auguié[1]*

[1]*School of Chemical and Physical Sciences,*
Victoria University of Wellington, New Zealand
*(*baptiste.auguie@vuw.ac.nz)*

UV–vis optical spectroscopy is a powerful nondestructive material characterisation technique for micro and nanoparticles in solution, ubiquitous in many fields—including foodstuffs, biochemicals, materials and medical research. The technique however requires that liquid samples cause minimal scattering to the probing light, and absorb sufficiently over the optical pathlength. Furthermore, traditional UV–vis spectroscopy cannot distinguish between scattering and absorption contributions to extinction.

We will describe our recent and on-going efforts using an integrating sphere technique to overcome these limitations [1,2]. Scattering can also be measured in a 90-degree configuration, providing a complementary characterisation to both transmission and absorption. We have applied these three techniques on solutions of Au nanospheres (diameters 20–100 nm), checked the consistency of extinction as the sum of absorption and scattering, and validated the results against Mie theory (Fig. 1).

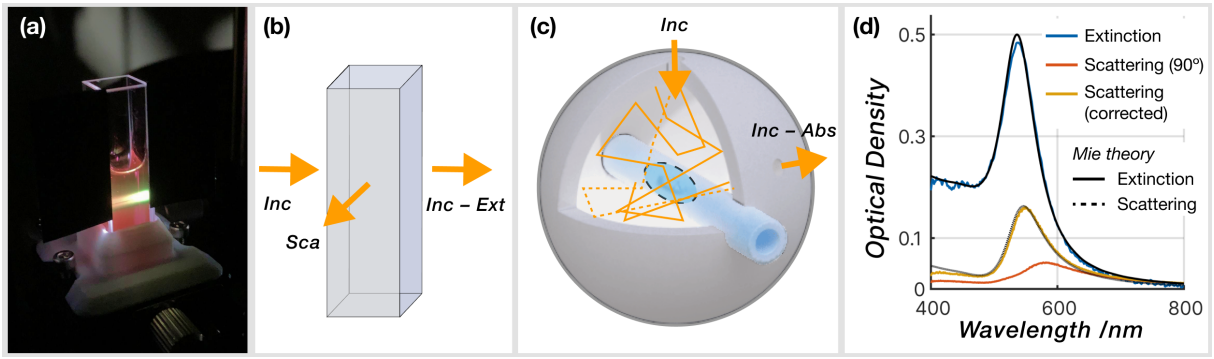

Figure 1: (a) Photograph of a cuvette with a solution of Au nanospheres, showing a strong colour variation along the beam path. (b) Schematic of extinction and scattering measurements of liquid samples in a standard cuvette. (c) Absorption spectroscopy setup enclosing a liquid sample inside an integrating sphere. (d) Extinction and scattering spectra for 60 nm Au spheres in water.

Scattered light measured at 90 degrees requires a calibration factor accounting for the collection geometry, and, more importantly, a non-trivial post-processing for the “inner-filter" effect of light undergoing scattering and absorption along the path [3].

Experimental access to all three types of spectra provides a much richer characterisation tool than extinction alone, and offers therefore a more stringent test of the parameters used in a theoretical fit. Notably, good agreement with Mie theory could only be obtained by considering the size polydispersity of the colloids and an accurate dielectric function for the metal [4].

The integrating sphere technique has also been applied to challenging samples consisting of low-concentration dye molecules in the presence of resonant plasmonic nanoparticles. The method’s key strengths are: i) full angular and spatial averaging; ii) robust non-imaging optics; iii) recycling of scattered light inside the cavity; iv) increased pathlength. This combination enables the measurement of minute changes in absorption against a turbid reference sample [1,5,6].

References

[1] B.L. Darby, B. Auguié, M. Meyer, A. E. Pantoja, and E. C. Le Ru, Nat. Photon. **10**, 40–45 (2016).
[2] J. Grand, B. Auguié, and E. C. Le Ru., Anal. Chem., **91**, 14639–14648 (2019).
[3] N. Micali, F. Mallamace *et al*, Anal. Chem., **73**, 4958–4963 (2001).
[4] A. Djorović, S. J. Oldenburg, J. Grand, and E C. Le Ru, ACS Nano, **14**, 17597–17605 (2020).
[5] S. Lee, H. Hwang, W. Lee, D. Schebarchov, Y. Wy, J. Grand, *et al*, ACS Energy Letters, **5**, 3881-3890 (2020).
[6] A. Stefancu, J. Gargiulo, G. Laufersky, B. Auguié, V. Chiş, E.C. Le Ru *et al* ACS Nano **17**, 3119-3127 (2023).

Wavelength-dependent tuning of thermal and thermo-plasmonic response in aggregates of porphyrins

Claudia Triolo,[1,*] Rosalba Saija,[2] Saveria Santangelo,[1] Luigi Monsù Scolaro,[3] Salvatore Patané [2]

[1]*Department of Civil, Energy, Environmental and Materials Engineering (DICEAM), Mediterranean University – Reggio Calabria, Italy (*claudia.triolo@unirc.it)*

[2]*Department of Mathematical and Computer Sciences, Physical Sciences and Earth Sciences, University of Messina – Messina, Italy*

[2]*Department of Chemical, Biological, Pharmaceutical and Environmental Sciences, University of Messina – Messina, Italy*

The control of nanoscale thermally activated processes aided by plasmonic resonances has emerged as a cutting-edge research area in the plasmonic field, with diverse applications spanning from medicine to material sciences [1-3]. In this study, we present an optical and thermal analysis of a porphyrin aggregate using finite element method (FEM) simulations. The interest in this material is due to the ability to mimic the plasmonic behavior under conditions of strong absorption resonance nearby a spectral region where the real part of the dielectric function is negative. The simulated structure is a 3D right-handed helix, whose geometry reproduces an aggregate of porphyrins, ranging in length from 22,5 to 150 nm. Under illumination by a linearly polarized monochromatic stationary plane wave, the spectral regions of the H- and J-bands are investigated. Due to the different arrangement of transition moments that characterizes the two bands, the optical and thermal behaviors observed in steady-state are quite different. A consistent temperature rise is achieved by exciting the H-band, while heating is poor in the J-region. The cause is attributed to the plasmon-like response, which occurs only in the spectral region corresponding to the J-band, where two relaxation mechanisms can be hypothesized to occur: thermal relaxation and plasmon-related optical relaxation.

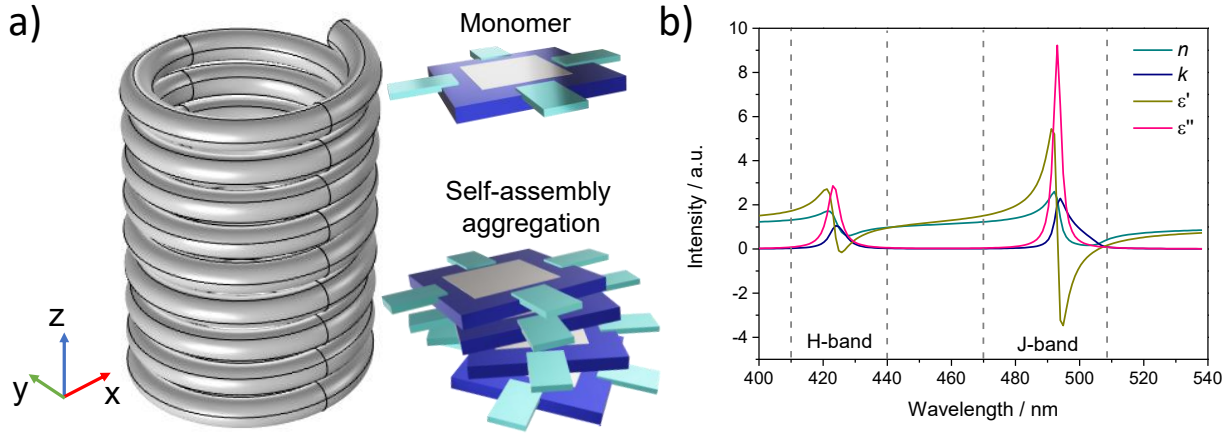

Figure 1: (a) 3D helical structure (turns, N=9) that reproduces a self-assembly aggregate of porphyrins: the thickness of a single turn coincides with those of a single monomer of porphyrin (2 nm), and the self-assembly aggregation determines the formation of the right-handed helix. (b) Refractive index, n, and absorption coefficient, k, and real (ε') and imaginary (ε'') parts of the dielectric function derived from the ellipsometry measurements. The dashed vertical lines delimit the H- and J- band regions, in which the simulations are performed.

[1] G. Baffou, F. Cichos, R. Quidant, Nat. Mater. **19**, 946–958 (2020).

[2] G. Baffou, R. Quidant, F.J. Garcìa de Abajo, ACS Nano **4**, 709–716 (2010).

[3] A. Cacciola, C. Triolo, O. Di Stefano, A. Genco, M. Mazzeo, R. Saija, S. Patané, S. Savasta, ACS Photonics **2**, 971–979 (2015).

Structure factor of fractal aggregates based on pair correlation modeling : comparison with current modeeling and impacts

Jérôme Yon[1], Mijail Littin[1], Guillaume Lefevre[1], Yoran Raynud Diara[1], Marek Mazur[1], Michael Sztucki[2], Romain Ceolato[3], and Andrés Fuentes[4]

[1]*INSA Rouen Normandie, Univ Rouen Normandie, CNRS Normandie Univ, CORIA UMR 6614, F-76000, Rouen, France*

[2]*European Synchrotron Radiation Facility, Grenoble, France*

[3]*ONERA, Université de Toulouse, FR 31055, France*

[4]*Departamento de Industrias, Universidad Técnica Federico Santa María, Valparaíso, Chile*

The characterization of nanoparticle aerosols is of vital importance for many applications, such as nanomaterials synthesis, aircraft engine emissions, pollution, climate change and health impact. Optical techniques based on light scattering have the great advantage of being sensitive, in-situ and capable of covering spatial scales ranging from a few millimeters to a few kilometers. The processing of these collected signals is often based on Mie theory, but it is well known that this is not suitable for fractal aggregates such as soot and black carbon. Cross-sections can be evaluated numerically using T-matrix or DDA approaches, but they are computationally expensive. To overcome these constraints and enable real-time analysis, approximate models that take account of the fractal nature have been developed to directly interpret scattering patterns (Rayleigh Debye Gans theory for fractal aggregates for static light scattering in the visible range, Beaucage unified model [1] for small-angle X-ray scattering (SAXS), both constructed in q reciprocal space). Both models establish a link between size and morphology via Guinier and Porod regimes, which can be repeated at different scales for SAXS measurements (e.g. primary spheres and aggregates for mass fractal aggregates, as is the case in the present study).

However, by definition, the scattered signal corresponds to the Fourier transform of the pair correlation of the particles [2], allowing an alternative model based on the pair correlation function itself [3]. This approach has recently been demonstrated to cover polydisperse aggregates composed of any number of primary spheres, providing a theoretical decomposition of the scaling originally proposed by Beaucage.

In the present study, we aim at comparing the two modeling approaches and explore the impact of the parameters of the analytical pair correlation model on the scattering structure factor. We will study the extent to which the nature of the aggregates can affect the Porod regime at large q and potentially affect the measurement of the primary sphere size distribution with conventional approaches. To this end, both approaches are applied to SAXS data of soot particles in a laminar ethylene diffusion flame measured at the European Synchrotron Radiation Facility (ESRF) [4] and processed via Abel inversion.

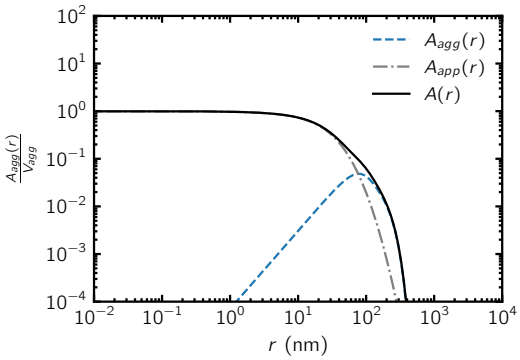

Figure 1: Decomposition and modeling of fractal aggregates pair correlation function in two components.

[1] Beaucage, G. and Schaefer, D.W, Journal of non-crystalline solids, **172**, 797–805 (1994).

[2] Sorensen, C.M, JAerosol Science & Technology, **35**, 648–687 (2001).

[3] Yon, J. and Morán, J. and Ouf, F-X and Mazur, M. and Mitchell, J.B, Journal of Aerosol Science, **151**, 105627 (2021).

[4] T. Narayanan, M. Sztucki, T. Zinn, J. Kieffer, A. Homs-Puron, J. Gorini, P. Van Vaerenbergh and P. Boesecke, J. Appl. Cryst., **55**, 98 (2022).

Synergizing light scattering and Machine learning for morphological quantification of small particles

Sanchita Roy [1,*], Farhana Hussain [2], Shiva Bhattacharjee[3] and Nileemoy Pathak[3]

[1]*Department of Physics, Royal School of Applied and Pure Sciences, The Assam Royal Global University, Guwahati,781035, Assam, India.*
[2]*Department of Physics, School of Applied Sciences, University of Science and Technology, Meghalaya, District- Ri Bhoi, 793101, Meghalaya, India.*
[3]*Department of Computer Science and Engineering, Royal School Engineering and Technology, The Assam Royal Global University, Guwahati,781035, Assam, India*

Abstract: Machine learning (ML) has emerged as a crucial field with applications spanning diverse domains. In this study, we present the scattering profile of microplastics in the form of polystyrene microspheres. ML has garnered significant attention in science and technology, finding applications in areas such as disease diagnosis, cybersecurity, medical imaging, chatbots, robotics, automation, and virtual assistance. However, its use in light scattering studies remains relatively unexplored, with only a few reports incorporating ML or deep learning (DL) techniques in this domain. Beyond identifying complex patterns in light scattering signatures, ML and DL can classify scattering profiles to distinguish particles of different origins, such as semiconductor materials, inorganic particles, metal oxides, and biological cells, across a size range from the nanoscale to the micrometer scale. Scientific literature indicates that ML-based integration with light scattering studies has gained attention only in recent years, approximately since 2010. The significance of ML and DL in light scattering stems from the demand for enhanced pattern recognition, data analysis, and accurate modeling. In our research, we measured the scattered light intensity from microplastic samples—specifically, the first element of the Mueller matrix—using a He-Ne laser based static light scattering device. Experimental data were collected in 50 sets. We implemented various ML and DL algorithms to improve the accuracy and efficiency of light scattering analysis. Specifically, ML and DL models were used to classify microplastic particles (Class A) and non-microplastic particles (Class B) based on their scattering signatures. To achieve this, we explored multiple ML and DL approaches. Convolutional Neural Networks (CNNs) were employed for feature extraction from scattering images, while Recurrent Neural Networks (RNNs) were utilized for analyzing time-series scattering data. Additionally, Support Vector Machines (SVMs) and Random Forests were applied for classification tasks, such as identifying particle types and sizes. We also investigated the potential of unsupervised learning techniques, including K-means clustering and Principal Component Analysis (PCA), to uncover hidden patterns in large scattering datasets. By integrating these methods, we aim to develop more robust and adaptable light scattering analysis techniques capable of handling diverse samples and experimental conditions. Our findings successfully distinguished and classified Class A (microplastics) from Class B (non-microplastics), demonstrating the potential of ML-assisted light scattering analysis for detecting microplastics in environmental samples. This work paves the way for identifying small particles such as aerosols, pathogens, and pollutants in the environment by analyzing scattering patterns and leveraging ML for classification. The details of our study will be presented at the conference.

[1] Van Trigt, C. (1997). Visual system-response functions and estimating reflectance. JOSA A, 14(4), 741-755.
[2] Hussain, F. and Roy, S. (2024). Radiative transfer of Black turmeric and its interpretation of antimicrobial property by light scattering. European Physical Journal Plus, 139, 687.
[3] He Xu et al., (2023). Rapid classification of micro-particles using multi-angle dynamic light scatting and machine learning approach. Biosensors and Biomolecular Electronics,10.
[4] Hussain, F., Mazumder, N., & Roy, S. (2023). Possibilities of simulation of coronavirus SARS-CoV-2 by using light scattering approach. Lasers in Medical Science, 38(1), 107.
[5] Yu Wan W et al. (2021). Integration of light scattering with machine learning for label free cell detection. Biomed Opt Express. May 19;12(6):3512-3529.

What can deep learning do for electromagnetic light scattering?

Giovanni Volpe[1,*]

[1]*Department of Physics, University of Gothenburg, Sweden (*giovanni.volpe@physics.gu.se)*

Electromagnetic light scattering underpins a wide range of phenomena in both fundamental and applied research, from characterizing complex materials to tracking particles and cells in microfluidic devices. Video microscopy, in particular, has become a powerful method for studying scattering processes and extracting quantitative information. Yet, conventional algorithmic approaches for analyzing scattering data often prove cumbersome, computationally expensive, and highly specialized.

Recent advances in deep learning offer a compelling alternative. By leveraging data-driven models, we can automate the extraction of scattering characteristics with unprecedented speed and accuracy—uncovering insights that classical techniques might miss or require substantial computation to achieve. Despite these advantages, deep-learning-based tools remain underutilized in light-scattering research, largely because of the steep learning curve required to design and train such models.

To address these challenges, we have developed a user-friendly software platform (DeepTrack, now in version 2.2) that simplifies the entire workflow of deep-learning applications in digital microscopy. DeepTrack enables straightforward creation of custom datasets, network architectures, and training pipelines specifically tailored for quantitative scattering analyses. In this talk, I will discuss how emerging deep-learning methods can be combined with advanced imaging technologies to push the boundaries of electromagnetic light scattering research—reducing computational overhead, improving accuracy, and ultimately broadening access to powerful, data-driven solutions.

[1] R. P. Feynman, M. Gell-Mann, and G. Zweig, Phys. Rev. Lett. **13**, 678 (1964).

[2] D. F. Edwards, "Silicon (Si)", p. 547 in *Handbook of optical constants of solids*, ed. E. D. Palik (Academic, 1997).

[3] F. Ladouceur and J. Love, *Silica-based buried channel waveguides and devices* (Chapman & Hall, 1995), Chap. 8.

[4] Author(s), "Title of paper", p. 12 in *Title of Proceeding* (Institute of Electrical and Electronics Engineers, 2023).

Simple scheme for design of 3D structured light

Alyssa Brownell,[1,2] Alexander B. Stilgoe,[1,2] Halina Rubinsztein-Dunlop,[1,2] and Timo A. Nieminen[1,2]*

[1]*School of Mathematics and Physics, The University of Queensland, Brisbane, Australia (*timo@physics.uq.edu.au)*

[2]*ARC Centre of Excellence in Quantum Biotechnology, School of Mathematics and Physics, The University of Queensland, Brisbane, Australia*

Structured light [1] has proven to be, among other applications, an excellent tool for the control of scattering. This include designing complex light fields to produce desired optical forces and torques in optical trapping, illumination and imaging through turbid media, and sensing. The simple case of producing the desired field, with a specified energy density, phase, and polarization in a two-dimensional plane is, in principle straightforward, since there is a Fourier transform relationship between the field in that plane and the far field. However, even in this ``solved'' case, many important issues remain, such as efficiency when using phase-only devices (e.g., liquid-crystal spatial light modulator (SLM)) or binary devices (e.g., digital micromirror device (DMD)), and when the illumination angle is restricted. Going beyond the simple 2D case immediately introduces many more difficulties.

In principle, a recipe for producing a desired 3D structured light field can be obtained by brute-force computational optimization methods. An immediate complication is that an electromagnetic field has infinite degrees of freedom. Computational optimization require that this infinity is truncated to a finite set, but the remaining number of degrees of freedom easily provides a great computational challenge. Possibly worse, our designed field we seek through such optimization can be fundamentally unachievable (e.g., if it doesn't satisfy the Helmholtz equation). Both of these can result in a structured light field that achieves our goals in some ways, but contains highly problematic features. For example, the energy density can vary wildly in some regions, and the optimum solution can be highly sensitive to small changes in the optical systems (e.g., if we have not characterized the aberrations in the system sufficiently precisely).

An alternative approach is to use a small set of simple beams, such as single-mode paraxial beams, Bessel beams, etc., as building blocks for our structured light field. This can reduce the number of free parameters to a small set, and sometimes to a single free parameter, making optimization a computational trivial task. For example, we can construct a "bottle beam", with a dark region surrounded by light, by combining two Gaussian beams, one more tightly focused than the other, with destructive interference between them giving the dark region in the middle of the beam (figure 1).

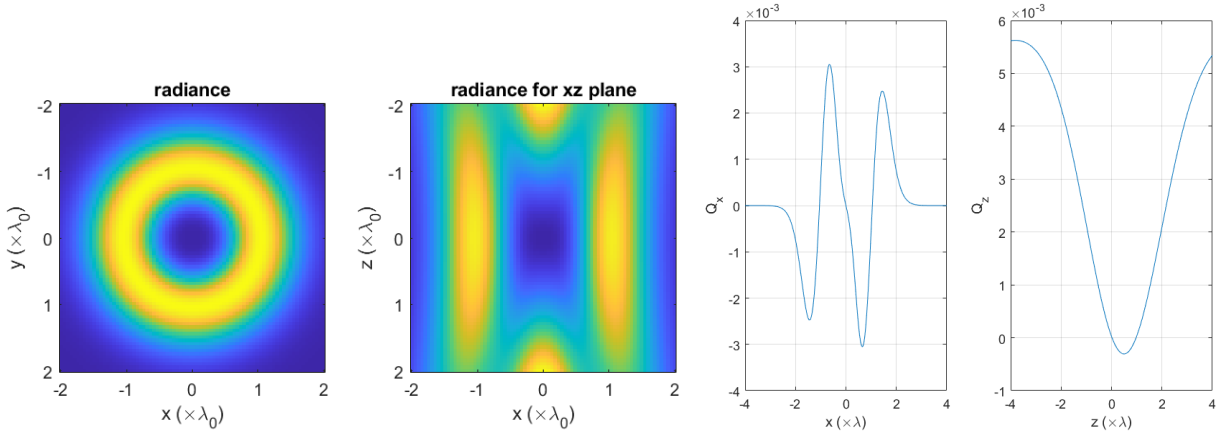

Figure 1: Left: Energy density for a bottle beam, in the focal plane (*xy*-plane) and the *xz*-plane. Right: Force on a 0.25λ air bubble in water in the bottle beam as it moves along the *x*-axis and *y*-axis. The bubble is trapped in the dark centre of the bottle beam.

In this case, the bottle beam can be used for trapping a particle with lower refractive index that the surrounding medium (e.g. an air bubble in water). We explore the usefulness of this simple design method, with a focus on applications in optical trapping.

[1] A. Forbes, M. de Oliveira, and M. R. Dennis, Nat. Photonics **15**, 253 (2021).

From the Lorenz-Mie theory in the near-field to the Fresnel Diffraction

Lilian Chabrol,[1,*] and Fabrice Onofri[1]

[1]*Aix-Marseille Université, CNRS, IUSTI, UMR 7343, 13453, Marseille, France (*lilian.chabrol@univ-amu.fr)*

The Lorenz-Mie theory (LMT) can be computationally demanding for large particles, making it impractical for optical characterization methods whether inverse or not, using machine-learning algorithms or not. In the present work, we propose approximations of the LMT that are valid both in the far- and near-field, both to improve computational efficiency and to provide new physical insights.

In van de Hulst's famous book [1], the far-field hypothesis is obtained by approximating spherical Hankel functions as $h_n(k_1 r) \simeq (-i)^n \frac{e^{ik_1 r}}{ik_1 r}$, where $k_1 = \frac{2\pi}{\lambda_1}$ is the wavenumber in the surrounding medium, r is the distance observer-particle in the spherical frame $(Or\theta\phi)$ with O the center of the particle. The scattered field is consequently a sum of spherical waves generated at the origin, and one loses information about the spatial extent of the particle. Considering the localization principle [1] which states that, for large scatterers, the index n identifies incident rays with impact parameter $\rho_n = (n+1/2)/k_1$, we propose to reintroduce the spatial extent of the scatterer by considering:

$$h_n(k_1 r) \to (-i)^n \frac{e^{ik_1 r}}{ik_1 r} e^{i\frac{(n+\frac{1}{2})^2}{2k_1 r}}. \tag{1}$$

Since the Mie series is usually capped at $n_{\max} = \alpha + 4.05\alpha^{\frac{1}{3}} + 2$ with $\alpha = k_1 a$ the size parameter [2], we introduce the new concept of Fresnel-Mie number as $F_{\text{Mie}} = \left(n_{\max} + \frac{1}{2}\right)^2 / (2\pi k_1 r)$.

Preliminary numerical investigations show very accurate estimates of the scattered field with the approximation Eq.(1) for $a \geq 10 \times \lambda_1$ and $F_{\text{Mie}} \leq 3$, independent of the refractive index (see e.g. Fig 1). The time gain over the LMT calculation is approximately one order of magnitude for $F_{\text{Mie}} \gtrsim 1$.

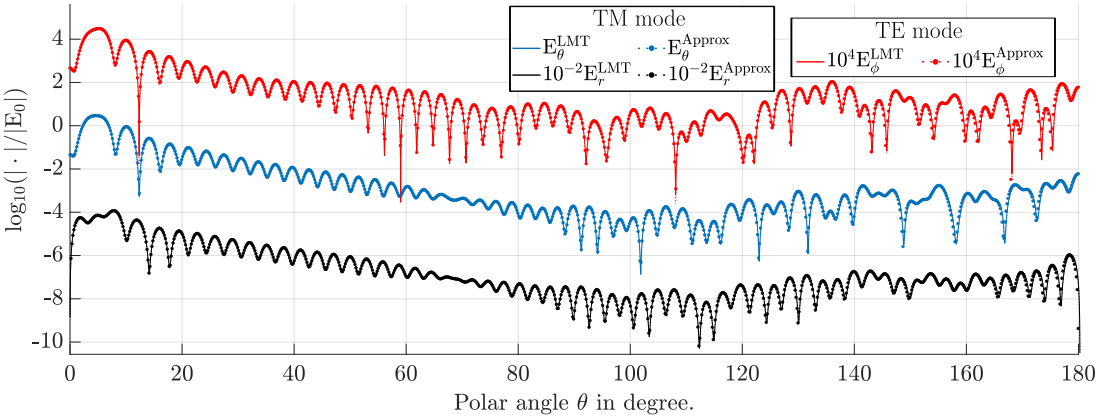

Figure 1: Comparison of the proposed approximation with the LMT. Normalized scattered electric field calculated with LMT (E^{LMT}, Eq. (4.45) of [3]) and the proposed approximation Eq. (1) (E^{Approx}). Water droplet in air: refractive index $m = 1.33$; $\lambda_1 = 0.6328\mu$m; $a = 10\lambda_1$; $\alpha \simeq 63$; $F_{\text{Mie}} = 3$; $r \simeq 35.4\mu\text{m} \simeq 6.6a$.

Considering in addition the paraxial approximation, we derive what we call the Lorenz-Mie-Fresnel (LMF) discrete scalar diffraction for a spherical scatterer illuminated by a plane wave with amplitude E_0:

$$E^{\text{LMF}} \equiv E_0 \frac{e^{ik_1 r}}{r} \sum_{n=1}^{\lfloor k_1 a \rfloor} \rho_n e^{ik_1 \frac{\rho_n^2}{2r}} J_0(k_1 \rho_n \theta) \tag{2}$$

where θ is the polar angle (the scattering angle in the far-field). This gives an accurate representation of the diffractive part of the scattered field. The parallel to the usual Fresnel scalar diffraction of a disk of radius a is clear in the limit where $\sin(\theta) \sim \theta$.

[1] van de Hulst, H. C., *Light Scattering by Small Particles* (Courier Corporation, 1981), Chap. 12.

[2] Wiscombe, W. J. , "Improved Mie Scattering Algorithms", Applied Optics, 1980.

[3] Bohren, C. F.; Huffman, D. R., *Absorption and Scattering of Light by Small Particles* (John Wiley & Sons), Chap. 4.

3D Anderson localization of light in disordered dielectric media

Yevgen Grynko[1], Dustin Siebert[2], Jan Sperling[3] and Jens Förstner[2,3]*

[1]*BASF Coatings GmbH, Münster, Germany*

[2]*Department of Theoretical Electrical Engineering, Paderborn University, Paderborn, Germany (*jens.foerstner@uni-paderborn.de)*

[3]*Institute for Photonic Quantum Systems, Paderborn University, Paderborn, Germany*

The possibility of 3D Anderson localization (AL) of light was recently demonstrated through numerical simulations for disordered layers of metallic spheres [1]. However, the existence of this phenomenon in dielectric random media remains an open question. In this work, we present the results of full-wave numerical simulations of light transmission through layers of dielectric particles, indicating that the 3D AL phenomenon can be extended to dielectric materials.

We apply the Discontinuous Galerkin Time Domain method and high-performance computing to study time-resolved light transmission, $T(t)$, through monodisperse layers containing up to 20000 irregular particles with a size parameter kr = 1.1 and refractive indices ranging from n = 2.0 to 3.0 [2]. The Bullet Physics rigid body engine is used to numerically pack these particles into layers with volume fractions up to ρ=0.5, achieving a high degree of spatial disorder and approaching the Ioffe-Regel condition for the mean free path length l^* of propagating waves, where $kl^* \lesssim 1$.

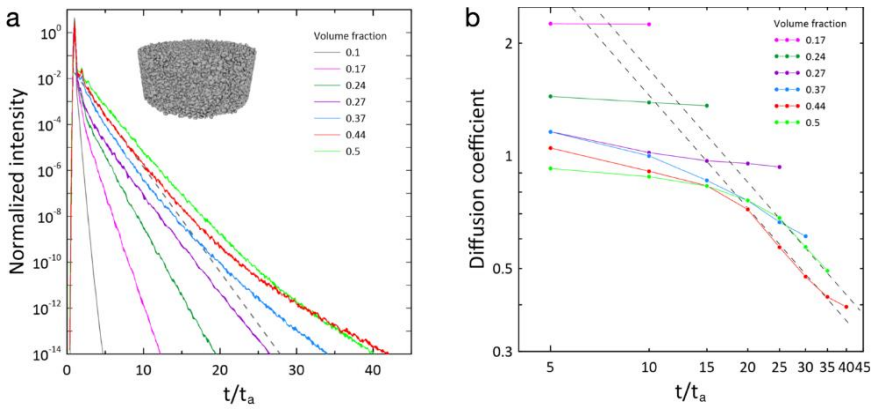

Figure 1: (a) Time-resolved short-pulse transmission $T(t)$ computed for layers of irregular particles (inset) with volume fractions ranging from ρ = 0.1 to 0.5 and refractive index n = 3.0, exhibiting a transition from the exponential decay to a non-exponential dependence. (b) Time-dependent diffusion coefficient $D(t)$ obtained by local exponential fitting of $T(t)$. Dense layers demonstrate a t^{-1} (dashed lines) dependence at longer times indicating AL regime.

Our simulations reveal a transition from exponential energy decay, indicative of diffusive transport, to localization, characterized by non-exponential $T(t)$ [1], at volume fractions ρ > 0.44 and a refractive index of n = 3.0 (Fig. 1). Under these conditions, focused beam propagation through a thick, dense layer shows an absence of transverse spreading. This observation is further supported by two additional signatures of AL. First, the time-dependent diffusion coefficient $D(t)$ follows the t^{-1} trend predicted by the analytical solution [1,3]. Second, the transmission spectrum aligns with the Thouless criterion for AL [4]. These results encourage further experimental search of AL in disordered media with realistic material refractive indices not exceeding n = 3.0.

[1] A. Yamilov, S. E. Skipetrov, T. W. Hughes, M. Minkov, Z. Yu, and H. Cao, Nat. Phys. **19**, 1308 (2023).

[2] Y. Grynko, D. Siebert, J. Sperling, and J. Förstner, arXiv:2312.14393v2 (2024).

[3] S. E. Skipetrov and B. A. van Tiggelen, Phys. Rev. Lett. **96**, 043902 (2006).

[4] A. A. Chabanov, M. Stoytchev, and A. Z. Genack, Nature **404**, 850 (2000).

Using the optical properties of plasmonic nanoalloys for the assessment and design of biodegradable nanomedicines

Vincenzo Amendola*

Department of Chemical Sciences, University of Padova - Padova, Italy

* *vincenzo.amendola@unipd.it*

Compared to traditional plasmonic materials like gold and silver, their alloys exhibit a range of unique and enhanced properties, positioning them at the intersection of nanophotonics and various other disciplines, including catalysis and magnetism.[1] Notably, and less known, some nanoalloys of Au or Ag hold significant promise for cancer theranostics, offering multiple functionalities: they can be tracked in vivo using conventional imaging techniques such as magnetic resonance imaging (MRI) or X-ray computed tomography (CT) while also exerting therapeutic effects, such as enhancing radiotherapy.[2-4]

As cancer nanomedicine advances, certain nanoalloys of Au or Ag with carefully tuned compositions have demonstrated their ability to meet also a critical requirement like biodegradability, which is essential for minimizing the risks associated with the long-term persistence of nanomaterials in the body.[5] However, despite this immense potential, the synthesis of nanoalloys with the ideal theranostic characteristics is challenging due to the natural immiscibility of Au and Ag with other functional and biocompatible elements like iron or boron. Therefore, it is crucial to rapidly and reliably monitor synthesis outcomes to optimize fabrication protocols. Additionally, identifying biodegradable nanoalloy compositions requires extensive experimentation, as it necessitates tracking their structural evolution over time and under various incubation conditions.

Fortunately, the plasmonic absorption band of these alloys is highly composition-dependent, enabling real-time monitoring of their structure. Here, we present several examples demonstrating how the optical properties of these plasmonic nanoalloys can be leveraged to design and assess an emerging class of advanced inorganic nanomedicines for cancer theranostics.[6]

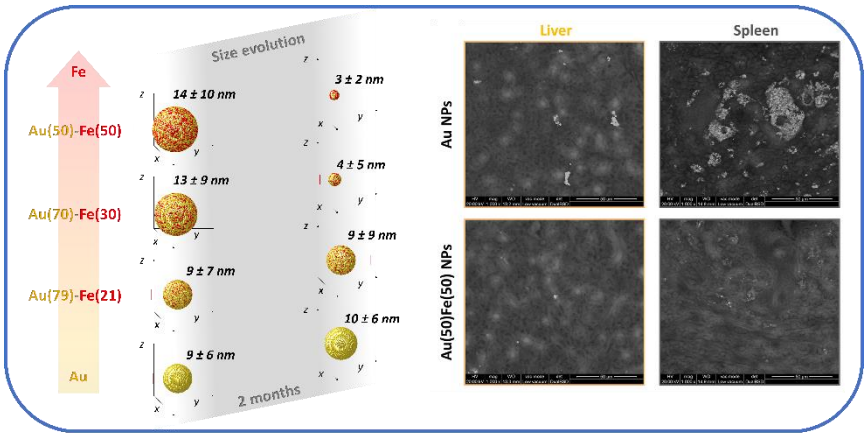

Figure 1: Left: Schematic depiction of the composition-dependent size transformation of Au-Fe nanoalloys, where an iron content above 30 at% corresponded to a size reduction below 10 nm after two months in the physiological environment. Right: The self-degradation and facilitated clearance of the Au-Fe nanoalloys was confirmed in murine models by environmental scanning electron microscopy images of their livers and spleens two months after administration. The animals treated with Au nanoparticles still show large agglomerates of gold, that are absent in the animals treated with Au-Fe nanoalloys.

[1] Coviello, V., Forrer, D. and Amendola, V., ChemPhysChem **23**, e202200136 (2022).

[2] Torresan, V., et al., ACS Nano **14**, 12840–12853 (2020).

[3] Amendola, et al.., J. Colloid Interface Sci. **596**, 332–341 (2021).

[4] Scaramuzza, S., et al., Adv. Funct. Mater. **33**, 2303366 (2023).

[5] Shi, J., Kantoff, P. W., Wooster, R. and Farokhzad, O. C., Nat. Rev. Cancer **17**, 20–37 (2017).

[6] This research was funded by AIRC under the MFAG 2021-ID. 25681 project-P.I. A.V.

Hybrid Au-Metal Oxide Nanostructures for UV-SERS Sensing Applications

Sebastiano Vasi[1,*], Fortunato Neri,[1] Rosalba Saija,[1] and Enza Fazio[1]

[1] *Department of Mathematical and Computational Sciences, Physical Science and Earth Science, University of Messina, Italy*

Traditionally, nanoplasmonics focuses on noble metals (Au, Ag, Cu) or their alloys whose Localized Surface Plasmon Resonances (LSPRs) are in visible (Vis) or near-infrared (NIR) spectral regions. In the ultraviolet (UV) region the considerable damping due to interband transitions make electromagnetic enhancements comparatively small [1]. Theoretical studies predict that metals with a large negative real part and a small imaginary part of the dielectric constant in the UV are suitable candidates for UV-SERS [2]. The most experimentally tested UV-SERS platforms are Al, Ga, In, Pb, Sn, Bi, Rh, Ru, Pt and Pd. However, these materials suffer from the formation of an oxide layer several nanometers thick that limits the UV plasmonic performance. Although encapsulating the metal core within chemically inert ultrathin silica shells is a strategy to overcome this issue, it is difficult to implement given the not-easy-to-control thickness of the SiO2 shell [3]. Among the transition metals, Rh has been discovered as a novel, nonoxidizing plasmonic contrast agent, exhibiting UV plasmonic behavior in the region between 3 eV and 7 eV, with the advantages of its oxide-free nature [4]. To date, the Rh nanostructures investigated were grown by electrochemical roughening of Rh surfaces or by chemical methods using different Rh precursors and their main limit is the photo-degradation.

In this contribution, the pulsed laser ablation technique, using a picosecond laser source coupled to a galvanometric head, was used to produce colloidal Rh- based suspensions in a suitable liquid medium. The features associated with the Surface Plasmon Resonance (SPR) of the Rh nanoparticles (NPs) have been observed below 400 nm. These LAL-synthesized Rh NPs are almost spherical, and their size and density distributions are markedly affected by the liquid (water, or ethanol) selected for LAL. Samples SERS activity was tested by considering the reference analyte Rhodamine 6G (R6G). The time-dependence of the SERS signal of R6G discloses the photo-induced degradation of the analyte adsorbed on the Rh/Rh-oxide NPs, also under the 457 nm laser irradiation. However, a prompt and well-resolved SERS response is observed after just 3 s of irradiation. To overcome the undesirable photodegradation effects and improve SERS response, the Rh-RhOx nanoparticles were nano-joined with Ag-Au NPs to tune SPR in a wide spectral range as large as possible. In this way, the reduction of electromagnetic field variations caused by external effects, as long-term storage degradation, was observed also improving the quantitative detection of analytes. Finally, a theoretical approach that makes use of the complete theory of scattering (T-matrix formalism), was used to accurately reproduce the experimental features of the extinction spectra of laser-produced samples.

[1] Knight, M.W.; et al., ACS Nano 2014, 8, 834–840
[2] McMahon, J.M. et al., Phys. Chem. Chem. Phys. 2013, 15, 5415–5423
[3] Gutierrez, Y.; et al, Opt. Express 2016, 24, 20621–20631
[4] Xie, S. et al, Nano Res. 2015, 8, 82–96

Phase engineering for steerable photonic nanojets

Mirza Karamehmedović,[1,*] Kristoffer Linder-Steinlein,[1] and Jesper Glückstad[2]

[1]*DTU Compute, Technical University of Denmark – Kgs. Lyngby, Denmark (*mika@dtu.dk)*
[2]*SDU Centre for Photonics Engineering, University of Southern Denmark – Odense, Denmark*

Photonic nanojets (PNJs) [1] are tightly focused light beams that emerge in the shadow near-field of a laser-illuminated dielectric micro-lens. These structures have potential applications in super-resolution optical microscopy, particle trapping and detection, and optical tweezers. However, their highly localized nature makes it challenging to precisely locate the area of interest. To address this, a steerable PNJ capable of rapid and accurate scanning without requiring lens adjustments or sample movement is desirable. Beyond enhancing label-free microsphere-assisted super-resolution microscopy [2], PNJ steering could advance fluorescence and Raman microscopy [3, 4] and ultimately facilitate localization, characterization (e.g., sizing), and magnified optical imaging of samples near or within a PNJ. Building further on our work in [5, 6], we propose a method for fast and precise PNJ steering using a computed spatially inhomogeneous incident wave combined with a fixed micro-lens. This approach enables rapid focal point repositioning without mechanical adjustments and is applicable beyond conventional spherical (3D) or circular (2D) micro-lenses, maintaining a consistently narrow PNJ across a broad range of positions. Figure 1 shows two numerically optimized phase modulations illuminating a 2D micro-element with a square cross-section (8 μm side length, refractive index n = 1.406) at a wavelength of 532 nm. The corresponding computed total electromagnetic field intensities are highly localized at the desired positions.

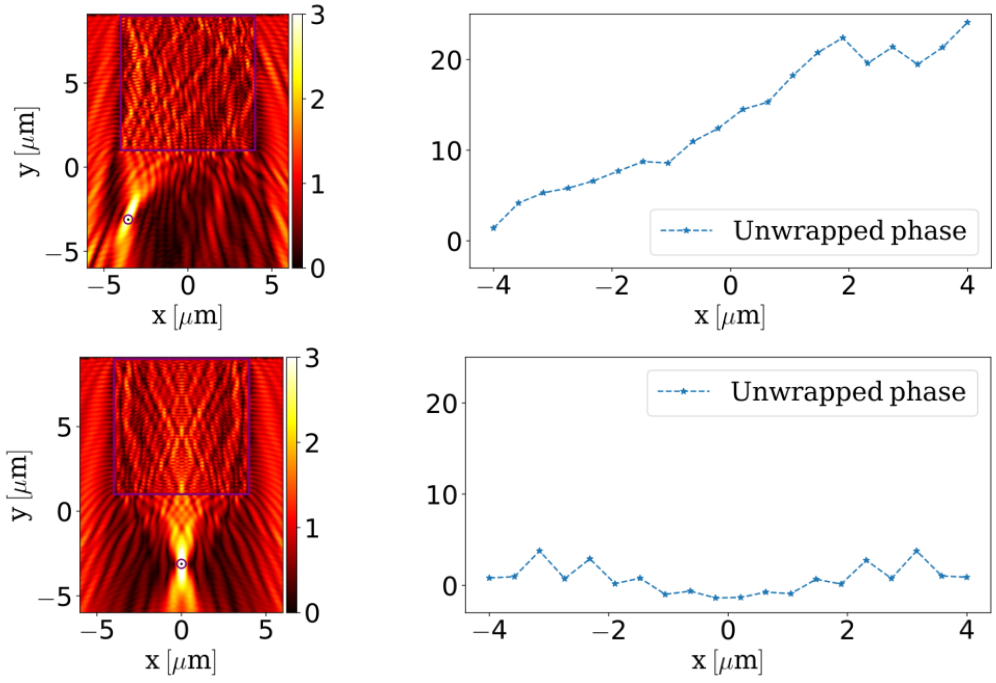

Figure 1: Highly localized fields and the corresponding optimized illumination phase profiles.

[1] A. Darafsheh, J. Phys. Photonics **3**, 2 (2021).
[2] Y. Li, C. Qiu, H. Ji, S. Duan, F. Qin, Z. Li, P. Chen, J. Huang, G. Yu, and H. Yuan, Adv. Optical Mater., 2300172 (2023).
[3] K. A. Sergeeva, M. V. Tutov, S. S. Voznesenskiy, N. I. Shamich, A. Yu. Mironenko, and A. A. Sergeeva, Sens. Actuators B Chem. **305**, 127354 (2020).
[4] I. S. Ruzankina and G. Ferrini, "Enhancement of Raman signal by the use of BaTiO3 Microspheres," p. 9285882 in *Proceedings of International Conference Laser Optics 2020*, (Institute of Electrical and Electronics Engineers, 2020).
[5] M. Karamehmedović, K. Scheel, F. L.-S. Pedersen, A. Villegas, and P.-E. Hansen, Opt. Express **30**, 23 (2022).
[6] M. Karamehmedović and J. Glückstad, Opt. Express **31**, 17 (2023).

Method and conditions to retrieve the refractive index of particles of arbitrary shapes and size distribution

Augusto García-Valenzuela,[1,*] Nadia E. Álvarez-Chávez,[1] and Anays Acevedo-Barrera[1,]

[1]*Instituto de Ciencias Aplicadas y Desarrollo Tecnológico, Universidad Nacional Autónoma de México. Apartado Postal 70-186, Ciudad de México 04510, Mexico.*

Submission abstract:

Measuring the refractive index (RI) of particles with sizes comparable to the wavelength of light presents significant challenges in practice. However, there is a pressing need to know the RI of many particles of irregular shapes and sizes comparable, or somewhat larger, than the wavelengths of light, such as aerosols or biological cells (see for instance, Refs. [1, 2]). In general, the RI of a homogeneous substance is a complex number, but here, by RI we will refer to the real part of the complex RI for simplicity.

Most frequently, particles of interest are not spherical and come with a wide size-distribution. Often their refractive index is inferred from measuring and analyzing the diffuse [2-4] or coherent reflectance [5] of light from a disordered system of many particles of different shapes and sizes. But, to obtain the particles' RI with reasonable accuracy from measurements that depend on the scattering of light by the particles, a detailed and precise knowledge of the particles' shape and size distribution is required, which in general is very difficult to know with enough accuracy. Therefore, the accuracy of this type of measurements is not well known.

As far as the authors know, the only way to measure the RI of a collection of particles, of the same chemical composition and mass density, independently of their shapes and size distribution, is by the index matching method (see for instance [6, 7]). In this method the particles are immersed in a medium of variable refractive index. When the external medium's RI is closest to that of the particles, the scattering by the particles is lowest and the transmittance through a suspension of them is maximum. The RI of the external medium is known and gives a good estimate of the particles' RI. Obtaining a precise value of the RI can be very laborious and difficult, since preparing several samples to suspend the particles with values of their RI encompassing that of the particles and differing from each other by small amounts, can be very challenging, especially for large RI values. Nevertheless, the index matching method is in principle the most robust and potentially more precise method to determine the refractive index of particles without concern about their shape or size distribution.

It should be of practical interest to ease the requirements of the index matching method to achieve a good precision in determining the RI of irregular particles, regardless of their size. This is precisely what we attempt in this work. When the RI contrast between the particles and the medium in which they are suspended is small, even if it is not too small, the measurement of the effective RI of the suspension becomes less demanding. Also, it is known that, at least for suspensions of small particles, when the RI contrast is not too large, some simple and empiric mixing formulas for the effective refractive index are accurate; such as the volume (weighted) average (VA) of the components' RI (sometimes referred to as the Arago-Biot mixing formula). We may suspect then that when the RI contrast is low, the VA mixing formula can be valid for larger particles. In this work we study the condition under which the VA can be used to infer the RI of particles in suspension with enough precision from measuring the effective RI of the suspension.

Using the so-called anomalous diffraction approximation, we have derived a formula to estimate the magnitude of the error in determining the refractive index of particles, regardless of their shape and size distribution, when using the VA mixing formula to retrieve the particles RI from the measured effective RI of particle suspension. This is,

$$\left|\delta n_p\right| \leq \frac{1}{6}\left|n_p - n_m\right|^3 k_0^2 L_{max}^2, \quad (1)$$

where n_p is the refractive index of the particles (assumed real), n_m is the RI of the medium surrounding the particles (the matrix), k_0 is the vacuum wavenumber of light and L_{max} is an average of the maximum linear dimensions of the particles.

For concreteness we set our objective to elucidate the region in the 2D space defined as (RI contrast, particle size), in which retrieving the RI of particles from the value of the effective RI of a suspension of such particles regardless of their shapes and size distribution, and using the VA mixing formula, yields the value of RI of particles with first three significant digits correct. In general, this means that the two first decimal digits of the particles' RI are inferred correctly. In a wide variety of cases, such precision in determining the RI of particles is already useful to identify the type of material the particles are made of, or at least it reduces the options to a reasonably small number of possible materials.

With Eq. (1) we find that for a RI contrast between the particles and the matrix of 0.01, 0.05 and 0.15 the maximum linear dimensions of the particles, L_{max} should be less than $27.6\ \lambda$, $2.46\ \lambda$ and $0.475\ \lambda$, respectively. In many cases, a RI contrast of 0.05 is not a very demanding condition and allows for obtaining a precision of two decimal digits in the particle's RI. The latter results say that, for wavelengths in the middle of the visible range, the particles sizes can be somewhat larger than 1 μm. Using Eq. (1), we find that, if we choose the working wavelength to be equal to the average of the maximum dimension of the particles in suspension, then the maximum RI contrast permitted when measuring the effective RI of the suspension to achieve the desired precision in determining the particle's RI, is 0.091.

In the previous analysis the relative error of the anomalous diffraction approximation, used to derive Eq. (1), is missing. We have recently estimated this error in the (RI contrast, particle's size) 2D space [8]. We will present the regions in the said 2D space where this error is negligible. Furthermore, we will present the experimental methodology and results of determining the refractive index of polymeric particles of different sizes suspended in water using the VA mixing formula that are consistent with Eq. (1). The measurements of the effective RI of the suspensions of different concentrations of the polymeric particles were obtained using a standard Abbe refractometer. One should note that the suspensions used were highly turbid. Precautions and limits of using the Abbe refractometer will also be discussed.

[1] Seohee H. Yang, Rokjin J. Park, Seungun Lee, Duseong S. Jo, Minjoong J. Kim, Impact of changes in refractive indices of secondary organic aerosols on precipitation over China during 1980–2019, Atmospheric Environment, Volume 299, 2023, 119644.

[2] Maria A. Velazco-Roa, Elitsa Dzhongova, and Suresh N. Thennadil, "Complex refractive index of nonspherical particles in the visible near infrared region--application to *Bacillus subtilis* spores," Appl. Opt. 47, 6183-6189 (2008).

[3] Gang Zhao, Fei Li, Chunsheng Zhao, Determination of the refractive index of ambient aerosols, Atmospheric Environment 240 (2020) 117800

[4] James G. Radney, ChristopherD. Zangmeister, Comparing aerosol refractive indices retrieved from full distribution and size- and mass-selected measurements, Journal of Quantitative Spectroscopy & Radiative Transfer 220 (2018) 52–66.

[5] Benjamin E. Reed, Roy G. Grainger, Daniel M. Peters, and Andrew J. A. Smith, Retrieving the real refractive index of mono- and polydisperse colloids from reflectance near the critical angle, Optics Express 24 (3), pp. 1953-1972, 2016

[6] I. Niskanen, J. Lauri, M. Yokota, R. Heikkilä, T. Hashimoto and T. Fabritius, "Determination of the Refractive Index of Particles Through the Immersion Solid Matching Method," in *IEEE Transactions on Instrumentation and Measurement*, vol. 70, pp. 1-5, 2021, Art no. 6000505.

[7] Cory Juntunen, Adam J. Rish, Carl A. Anderson, Yongjin Sung, Refractive index measurement of pharmaceutical powders in the short-wave infrared range using index matching assisted with phase imaging, Powder Technology, Volume 438, 2024, 119621.

[8] N. E. Álvarez-Chávez, A. Acevedo-Barrera, R. Márquez-Islas, and A. García-Valenzuela, Comprehensive study of the accuracy of the Anomalous Diffraction Approximation, submitted.

Modeling scattering of polarization-entangled photons

Ivan Lopushenko,[1,*] Vira Besaga,[2] Oleksii Sieryi,[1] Alexander Bykov,[1] Frank Setzpfandt[2,3] and Igor Meglinski[4]

[1]*Opto-Electronics and Measurement Techniques, University of Oulu – Oulu, Finland*
[2]*Abbe Center of Photonics, Friedrich Schiller University Jena – Jena, Germany*
[3]*Fraunhofer Institute for Applied Optics and Precision Engineering IOF – Jena, Germany*
[4]*College of Engineering and Physical Sciences, Aston University – Birmingham, UK*
*(*ivan.lopushenko@oulu.fi)*

Non-classical states of light, such as entangled photons, and states carrying orbital angular momentum, are being actively explored to boost the performance of optical metrology [1, 2] and to overcome challenges induced by high losses of the probing light in a wide range of turbid samples: from biological tissues [3] to atmospheric clouds [4]. In this work, we report on modeling the behavior of polarization-entangled photons passing through a turbid medium. We address this problem on example of Bell state $|\Psi^+\rangle = 1/\sqrt{2}\left(|H\rangle|V\rangle + |V\rangle|H\rangle\right)$ and by considering scattering-based light-matter interaction of one of its partner photons with a tissue-like medium. We describe this interaction with a technique rooted in the iterative solution to the Bethe-Salpeter (BS) equation [5]. Key mechanisms of the proposed model are the BS-based procedure for polarization state tracking of photon packets [6] and the relationship between Stokes parameters and density matrix of the quantum state [5, 7]. We show that implementation of these mechanisms in a radiative transfer Monte Carlo approach allows to follow probability amplitudes for both orthogonal polarization states of the photon interacting with the turbid sample along its statistical trajectory, which is considered the same for both polarization states due to their initial indistinguishability. We demonstrate the capabilities of the developed method by performing experimental characterization of tissue-mimicking phantoms using quantum state tomography.

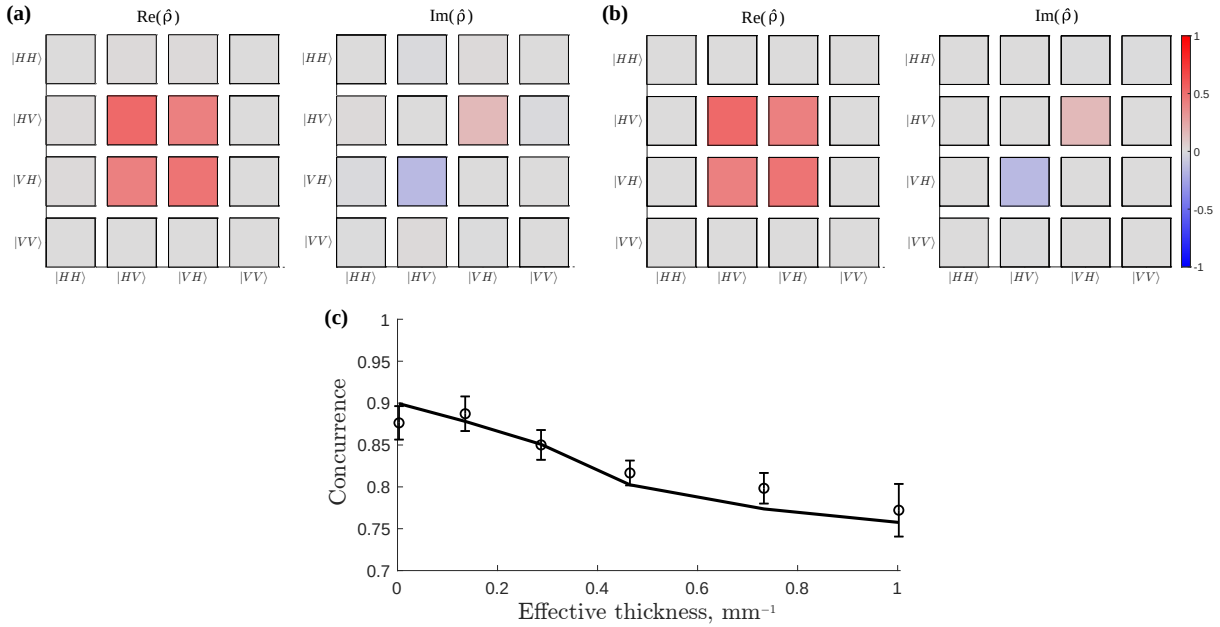

Figure 1: (a) Measured and (b) simulated density matrices $\hat{\rho}$ after interaction of one of the entangled photons with a ZnO-based tissue phantom (scattering coefficient: 2.74 mm^{-1}, thickness: 0.3 mm). (c) Simulated (line) and measured (circles) concurrence vs effective thickness of the phantom under study. Error estimation follows Ref. [7].

[1] Y. Zhang, Z. He, X. Tong, D. C. Garrett, R. Cao, and L. V. Wang, Sci. Adv. **10**, eadk1495 (2024).
[2] I. Meglinski, I. Lopushenko, A. Sdobnov, and A. Bykov, Light Sci. App. **13**, 214 (2024).
[3] L. Shi, E. J. Galvez, and R. R. Alfano, Sci. Rep. **6**, 37714 (2016).
[4] V. Nikulin et al., p. 131060A in *Photonics for Quantum* (SPIE Proceedings, 2024).
[5] V. R. Besaga, I. V. Lopushenko, O. Sieryi, A. Bykov, F. Setzpfandt and I. Meglinski, arXiv:2411.06134 (2024).
[6] I. Lopushenko, O. Sieryi, A. Bykov, and I. Meglinski, J. Biomed. Opt. **29**, 052913 (2024).
[7] D. F. V. James, P. G. Kwiat, W. J. Munro, and A. G. White, Phys. Rev. A. **64**, 052312 (2001).

Perfect Absorption and Hermitian Subspaces

Daniele Lamberto,[1,*] Claudio Bonizzoni,[2,3] Samuel Napoli,[1] Alberto Ghirri,[3] Simon Gunzler,[4] Dennis Rieger,[4] Fabio Santanni,[5] Wolfgang Wernsdorfer,[4] Marco Affronte,[2,3] Salvatore Savasta[1]

[1]*Dipartimento di Scienze Matematiche e Informatiche, Scienze Fisiche e Scienze della Terra, Università di Messina, I-98166 Messina, Italy (*daniele.lamberto@studenti.unime.it)*

[2]*Dipartimento di Scienze Fisiche, Informatiche e Matematiche Università di Modena e Reggio Emilia, via G. Campi 213/A, 41125, Modena, Italy*

[3]*CNR Istituto Nanoscienze, Centro S3, via G. Campi 213/A, 41125, Modena, Italy*

[4]*Karlsruhe Institute of Technology, Physikalisches Institut Wolfgang-Gaede-Str. 1, D-76131, Karlsruhe, Germany*

[5]*Dipartimento di Chimica Ugo Schiff, via della Lastruccia 3, 50019 Sesto Fiorentino (FI), Italy*

It has been shown that ideal effective parity-time (PT)-symmetry can be implemented using only passive materials, regarding the feeding field in an open system as an effective gain [1]. In their PT-symmetric phase these systems exhibit perfect absorption, a key concept in many photonic applications, which is related to the zeros of the scattering matrix [2]. In this work, we introduce the concept of *Hermitian subspaces* in open-cavity QED settings, which generalizes previous findings beyond PT-symmetry, and demonstrate its connection to perfect absorption. When interacting, the matter and light degrees of freedom are mixed into dressed states, leading to new eigenstates known as polaritons. It turns out that controlling the photon content of a polariton mode is the key to balance the feeding and loss rates of a cavity QED system in the absence of PT-symmetry. These findings are supported by recent experimental results in magnetic systems, based on molecular spin centers with large nuclear spin and hyperfine anisotropy. Our findings significantly enlarge the possibility to explore and apply non-Hermitian effects in open quantum systems. Moreover, Hermitian subspaces influence the overall aspect of the coherent spectra of cavity QED systems and can be exploited for the development of efficient switches and modulators with high modulation depths in a broad variety of spectral ranges.

[1] D. Zhang, X.-Q. Luo, Y.-P. Wang, T.-F. Li, and J. Q.You, Nature Communications **8**, 1368 (2017).

[2] Zanotto, S., Mezzapesa, F., Bianco, F. *et al.* Perfect energy-feeding into strongly coupled systems and interferometric control of polariton absorption. *Nature Phys* **10**, 830–834 (2014).

Abstracts – Posters

Photometric modeling of the regolith in the Reiner Gamma lunar swirl

Vesa Björn,[1,*] Karri Muinonen,[1] Antti Penttilä,[1] Deborah Domingue,[2] and John Weirich[2]

[1]*Dept. of Physics, University of Helsinki – Helsinki, Finland (*vesa.bjorn@helsinki.fi)*
[2]*Planetary Science Institute – Tucson (AZ), USA*

To deduce physical properties of the regolith of the Moon, we apply a theoretical particulate medium (PM) model [1–3] to photometric data. The model describes a regolith with a fractional Brownian motion surface, which characterizes well the surface roughness of atmosphereless bodies in the Solar System [2]. The model has three geometry parameters: the packing density v, the fractal Hurst exponent H, and the amplitude of height variation σ. Figure 1 shows the effects that the geometry parameters have on the regolith.

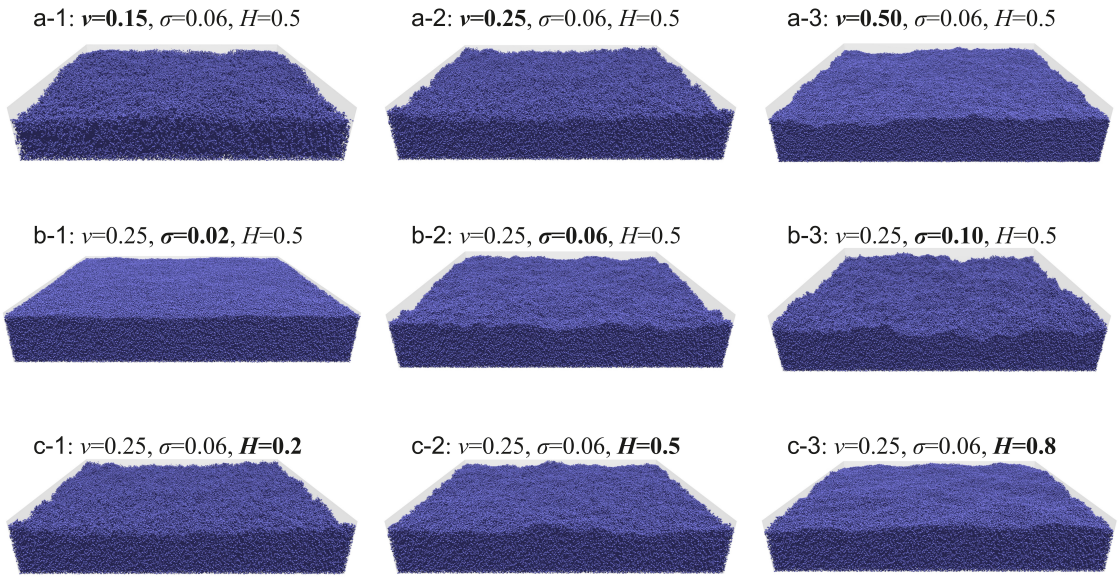

Figure 1: Regolith created by the particulate medium model, for different values of the model's parameters.

Lunar swirls are bright areas on the otherwise darker mare regions on the Moon. Our current study focuses on the Reiner Gamma swirl, centered slightly north of the equator and on the side facing Earth, at coordinates 7.5°N, 59.0°W. We are using the same data as prior research to the lunar swirl, namely the data in [4] and [5]. Our analysis of photometric data and the use of the PM model is similar to [1]. However, there is a difference in the extent of the area being examined: here, we apply the methods to a localized area on the Moon, as opposed to the average Mercury surface as in [1].

Our preliminary results suggest that the lunar regolith around the Reiner Gamma swirl is similar in surface roughness but less densely packed than Mercury's regolith: $v = 0.442 \pm 0.010$, $H = 0.601 \pm 0.005$, $\sigma = 0.0997 \pm 0.0004$. For comparison, the packing density of the regolith of Mercury was derived to be $v = 0.547 \pm 0.004$ [1]. In the future, we plan to extend the analysis to photometric data of the Mare Ingenii swirl (33.7°S, 163.5°E), and deduce the physical properties of the regolith in and around the two different lunar swirls.

[1] V. Björn, K. Muinonen, A. Penttilä, and D. L. Domingue, Planet. Sci. J. **5**, 260 (2024)
[2] K. Muinonen, H. Parviainen, J. Näränen, J. -L. Josset, S. Beauvivre, P. Pinet, S. Chevrel, D. Koschny, B. Grieger, B. Foing, and AMIE SMART-1 Team, A&A **531**, A150 (2011).
[3] O. Wilkman, K. Muinonen, and J. Peltoniemi, PS&S **118**, 255 (2015).
[4] J. Weirich, D. Domingue, F. Chuang, A. Sickafoose, M. Richardson, E. Palmer, and R. Gaskell, Planet. Sci. J. **4**, 212 (2023).
[5] D. Domingue, J. Weirich, F. Chuang, S. Courville, R. Clark, A. Sickafoose, E. Palmer, and R. Gaskell, Planet. Sci. J. **5**, 161 (2024).

Asymptotic model for the forward scattering of large refracting spheres: interference of refraction with the diffraction of a disk and a complex ring.

Lilian Chabrol,[1,*] and Fabrice Onofri[2]

[1,*] *Aix-Marseille University, CNRS, IUSTI, Marseille, France (Lilian.chabrol@univ-amu.fr)*

[2] *CNRS, Aix-Marseille University, IUSTI, Marseille, France (fabrice.onofri@univ-amu.fr)*

The computational resources required when using the Lorenz-Mie theory (LMT) to evaluate the light scattering properties of large spherical particles (drops, bubbles, beads) continue to hinder the development of optical particle characterization techniques in mechanical and chemical engineering sciences. This is obviously the case for direct and inverse real-time techniques but also for those based on databases with or without machine learning (e.g. laser diffractometry, holography, rainbow scattering, interferometric imaging, phase Doppler…) [1].

We have recently developed an asymptotic hybrid model [2] that captures most of the details of the forward scattering patterns of large spherical particles with a relative refractive index $m > 1$, while being one to two orders of magnitude faster than LMT. This model accounts for diffraction, grazing reflection and tunneling effects ($p = 0_a$) as well as pure refraction ($p = 1$) [3]. To do this, we showed that tunneling and anomalous reflection can be accounted for within the framework of scalar diffraction theory. This is achieved by considering two complex annuli for TM and TE modes, whose properties are derived from the complex angular approximation (CAM) of the zeroth order term of the Debye series that was derived by Nussenzveig and Khare [4, 5]. When combined with the usual scalar diffraction of a disk, and refraction described by a complex ray model accounting for curvature radii of the particle interface and wave fronts, this hybrid model provides accurate predictions of the total scattered field in both the near- and far-fields, see Fig. 1 for the TM-mode and a Fresnel number as high as F=5.

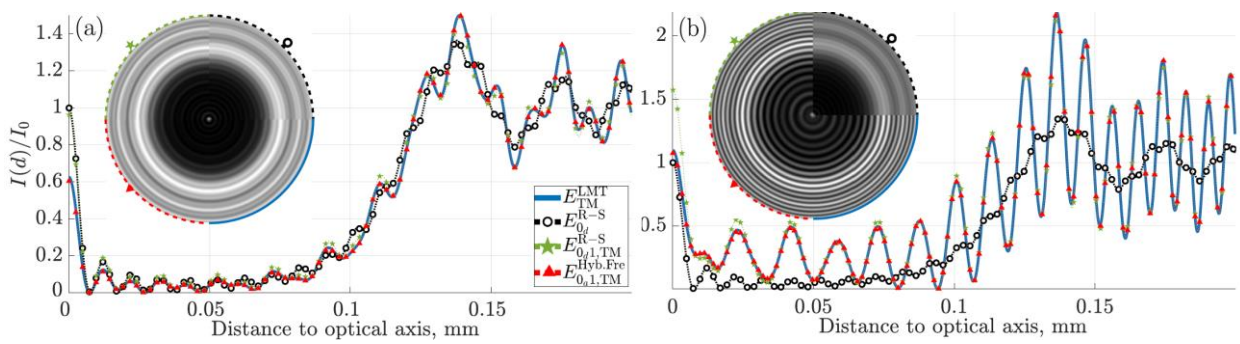

Figure 1: Comparison of the intensities of the total electrical fields and corresponding quarter holograms. (a) $m = 1.33$ and (b) $m = 1.05$. radius, $a = 0.1$mm; wavelength, $\lambda = 632.8$nm; axial distance, $z = 3.16$mm.

The mathematical background of this model will be detailed, with illustrative numerical results showing its validity over a wide range of particle parameters and distances. The examples presented will be mostly focused and commented from the point of view of in-line digital holography, and the prospects of this model to allow the simultaneous measurement of the 3D position, size and composition of droplets. Its possible extension to other types of particles in terms of shape and composition will also be discussed.

[1] F. Onofri and S. Barbosa, Laser Metrology in Fluid Mechanics (Willey, 1992), Chap. 2.

[2] L. Chabrol and F. Onofri, submitted (2025)

[3] E. A. Hovenac, and J. A. Lock. J. Opt. Soc. Am. A **9**(5): 781 (1992)

[4] H. M. Nussenzveig, Journal of Mathematical Physics **10**(1): 82 (1969)

[5] V. Khare, *Short-Wavelength Scattering of Electromagnetic Waves by a Homogeneous Dielectric Sphere*, Ph.D. Thesis, University of Rochester (1976)

Transmission of millimeter electromagnetic waves through pigmented automotive coatings

Yevgen Grynko,* Jari Rodewald, Ralf Nickolaus and Thomas Kantimm

*BASF Coatings GmbH, Münster, Germany (*yevgen.grynko@basf.com)*

Radar is a key technology in the automotive industry, essential for Advanced Driver Assistance Systems (ADAS) and autonomous driving. High-frequency radio-wave sensors provide ADAS with critical information to guide a car through the traffic. For design reasons, these sensors are concealed behind coated plastic parts. Therefore, metal-pigmented high-permittivity coatings [1] need to be highly transmissive in the required frequency range. Additionally, methods for robust calculation of their dielectric permittivities are needed for practical applications. To address this electromagnetic problem, we do laboratory studies of transmissive properties of basecoats filled with different types of metallic pigments and simulate numerically electromagnetic transmission through model layers.

In our numerical model, we consider layers of disk-shaped and irregular aluminum flakes randomly distributed in a dielectric matrix (Fig. 1). With a source frequency of 85 GHz and a pigment layer thickness of 20 µm, we enter an extremely sub-wavelength regime. Despite the small scale of spatial disorder, wave phenomena can be non-trivial in such structures, e.g., [2]. We apply the Discontinuous Galerkin Time Domain method for a full-wave solution as the problem is multi-scale. The Drude model, with parameters extrapolated from the data for aluminum [3], is used to represent the metallic material. We vary particle size, shape, concentration and orientation distribution to identify the physical factors that most significantly influence electromagnetic transmission.

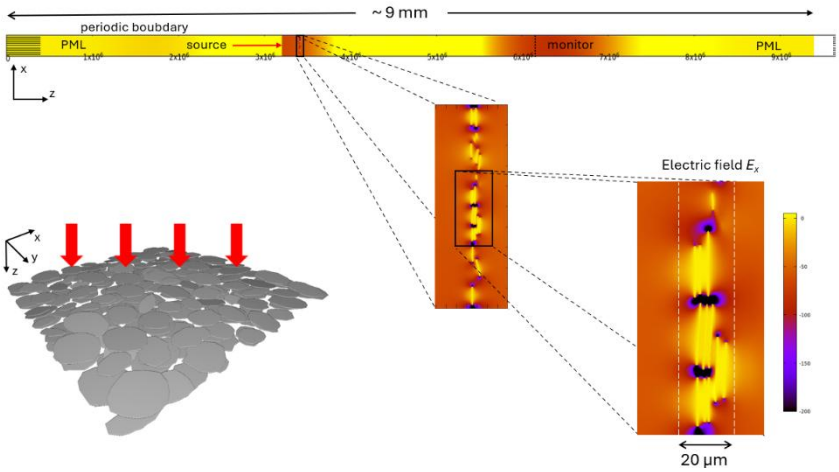

Figure 1: An example of a model layer of irregular metal plates and a cross-section of the multi-scale computational domain, showing a pulse propagating in z-direction, with excited near-fields formed between the particles.

Simulations show that the number density of flakes is the primary factor controlling transmission with the volume filling fraction playing only an indirect role. At higher concentrations, near-field interactions become significant. Specifically, at number densities corresponding to volume fractions $f \gtrsim 3$ %, the reduced separations between flakes lead to interactions between the excited near fields and field damping. This phenomenon is akin to the collective near-field damping observed in arrays of subwavelength plasmonic resonators [4]. Consequently, thin metal-pigmented layers cannot be treated as a classic effective medium, and estimating their dielectric permittivities requires more complex approaches.

[1] G. Pfaff, M. R. Bartelt and F. J. Maile, Phys. Sci. Rev. **6**, 179 (2021).

[2] H. H. Sheinfux, I. Kaminer, A. Z. Genack and M. Segev, Nat. Commun. **7**, 12927 (2016).

[3] A. D. Rakić, A. B. Djurišić, J. M. Elazar, and M L. Majewski, Appl. Opt. **37**, 5271-5283 (1998).

[4] S. Linden, F. B. Niesler, J. Förstner, Y. Grynko, T. Meier and M. Wegener, Phys. Rev. Lett. **109**, 015502 (2012).

RELAX : REtrieve complex fieLds from Amplitude via X-words (on some recent recent advances in 2D Phase Retrieval Problems)

Tommaso Isernia,[1,*] Roberta Palmeri[1], Andrea Morabito[1], Lorenzo Crocco[2], and Giada Battaglia[1]

[1]*DIIES, Università Mediterranea di Reggio Calabria – Reggio Calabria, Italy (tommaso.isernia@unirc.it)*

In Phase Retrieval Problems one aims to recover the phase of a complex field (or even the corresponding field) from the intensity of the radiated or scattered light. The problem is of interest for electron microscopy, Optics, X-ray crystallography, mm-waves antennas, inverse scattering, and more.

The ill-posedness and non linearity of the problem have challenged researchers for many years researchers, so that many efforts have been performed to develop measurement set-ups and procedures allowing a robust and accurate phase retrieval with the minimal number of measurements, in particular for the case where such a retrieval has to be performed on a 2D domain (for example, a plane). In fact, effective solution procedures do exist for the PR in the 1D case (where the solution is not unique) allowing to retrieve all the different solution to the problem.

Leveraging this circumstance, we have recently proposed to solve the corresponding 2D problem by emulating the process of solving cross-words puzzles. In fact, one can solve along column and rows [1], or diameters and concentric circles [2], or on nested rings [3], and then finding the solution (which in the 2D case is known to be unique but for special instances) by enforcing congruence amongst the solutions on the different 1D curves.

A detailed discussion of the (very positive) outcomes, and possible improvements by means of hybridizations with more classical methods, will be given at the Conference.

[1] G. M. Battaglia, R. Palmeri, A. F. Morabito, P. G. Nicolaci, and T. Isernia, "A non-iterative crosswords-inspired approach to the recovery of 2-D discrete signals from phaseless Fourier transform data," IEEE Open J. Antennas Propag., vol. 2, pp. 269–280, 2021.

[2] R. Palmeri, G.M. Battaglia, A.F. Morabito, T. Isernia Reflector Antennas Characterization and Diagnostics Using a Single Set of Far-Field Phaseless Data and Crosswords-Like Processing, IEEE Trans. On Antennas and Propagation, vol. 70, n.9, 2022

[3] G.M. Battaglia, A.F. Morabito, R. Palmeri, T. Isernia Effective Non-Iterative Phase Retrieval of 2-D Bandlimited Signals With Applications to Antenna Characterization and Diagnostics, IEEE Trans. On Antennas and Propagation, vol. 71, n. 8, 2023

[1] R. P. Feynman, M. Gell-Mann, and G. Zweig, Phys. Rev. Lett. **13**, 678 (1964).

[2] D. F. Edwards, "Silicon (Si)", p. 547 in *Handbook of optical constants of solids*, ed. E. D. Palik (Academic, 1997).

[3] F. Ladouceur and J. Love, *Silica-based buried channel waveguides and devices* (Chapman & Hall, 1995), Chap. 8.

[4] Author(s), "Title of paper", p. 12 in *Title of Proceeding* (Institute of Electrical and Electronics Engineers, 2023).

Aerosol Retrievals using GRASP from LES and 1D/3D RT Simulations for HARP like instruments in Twilight Regions

Nirandi Jayasinghe,[1,2]* Reed Espinosa,[3] Daniel Miller,[1,3] Anin Puthukkudy,[1,2] and Vanderlei Martins[1,2]

[1]*University of Maryland Baltimore County– Baltimore, USA (*nirandj1@umbc.edu)*
[2]*Goddard Earth Science Technology and Research (GESTAR) II– Baltimore, USA*
[3]*NASA Goddard Space Flight Center-Greenbelt, USA*

Aerosol-cloud transition zones, also known as twilight zones, exhibit characteristics between clouds and aerosols. In these zones, aerosols undergo rapid changes in their microphysical and optical properties, particularly in humid near-cloud regions. Studying these areas has been challenging over the past decade due to their complex dynamics and the inadequacy of globally distributed datasets with sufficient information content. Understanding the underlying mechanisms of twilight zone aerosols is essential for advancing our knowledge of global aerosol-cloud interactions (ACI) and reducing the associated uncertainties in global climate feedbacks.

New-generation satellite-based Earth observing systems, equipped with multi-angular, multi-spectral polarimeters, will collect global measurements with high information content, allowing for a deeper understanding of twilight zone aerosols. The deployment of the Hyper Angular Rainbow Polarimeter (HARP-2) aboard NASA's Plankton, Aerosol, Cloud, and Ocean Ecosystem (PACE) Satellite in early February 2024, for instance, facilitates global measurements that can enhance aerosol retrievals in twilight regions.

In this study, we utilize Large Eddy Simulations (LES) and corresponding 1D/3D radiative transfer simulations from Spherical Harmonic Discrete Ordinate Method (SHDOM) for multi-angular, multi-spectral polarimeters along with the Generalized Retrieval of Aerosols and Surface Properties (GRASP) algorithm. By analyzing Stokes measurements across multiple viewing geometries and retrieved aerorol properties, we aim to identify and characterize twilight zone aerosol variations. Integrating these simulations with PACE and PACE Postlaunch Airborne eXperiment(PAX) polarimetric observations will refine aerosol characterization, enhance ACI understanding, and improve retrieval accuracy in these complex regions.

Scattering Properties and Lidar Characteristics of Asian Dust Particles Based on Realistic Shape Models

Anthony La Luna[1], Zhibo Zhang[1]*, Diana Ortiz-Montalvo[2], Jianyu Zheng[1], Qianqian Song[1], Hongbin Yu[3], Jiachen Ding[4], Ping Yang[4], Masanori Saito[5]

[1]*University of Maryland Baltimore County, Baltimore (MD), USA (*zzbatmos@umbc.edu)*

[2]*National Institute of Standards and Technology, Gaithersburg (MD), USA*

[3]*NASA Goddard Space Flight Center Greenbelt (MD), USA*

[4]*Texas A&M University, College Station (TX), USA*

[5]*University of Wyoming, Laramie (WY), USA*

Atmospheric dust particles affect the climate system in a multitude of ways, for example, through the global radiative energy balance, air quality impacting public health, and inducing phytoplankton bloom in ocean deposits contributing to biogeochemical cycles. To better track and quantify dust plumes, we use lidar instruments to measure the particles on a large scale. Thus, it is important to have accurate quantifications of how these particles interact with electromagnetic radiation from these sensors. Often it is assumed that dust particles have simple theoretical geometries to compute the single-scattering properties (extinction efficiency, single-scattering albedo, asymmetry factor, and scattering phase matrix) necessary for lidar measurements, which may lead to inaccurate optical properties. In this study, we use realistic particle morphology from a library of highly detailed 3D scans previously produced through focused-ion beam tomography of collected dust samples from the Mauna Loa Observatory, linking lidar properties to physical measurements. We use discrete dipole approximation software to calculate important optical properties for lidar instruments and develop a convergence index for a sufficiently random number of orientations, creating a meaningful test for future calculations using the discrete dipole approximation technique. We calculate lidar ratios and depolarization ratios for the realistic dust particles at 355 nm, 532 nm, and 1064 nm wavelengths and analyze the properties as a function of mineralogy, size, and effective sphericity. A parameterization scheme for dust depolarization ratio (DPR) based on size to quantify volumetric DPR from the median volume equivalent sphere radius of multiple lognormal functions was developed, creating a simplistic method of approximating depolarization ratio of commonly used particle size distributions.

Optical signature modeling of proton-irradiated space white paint

Agnès Lecadre-Scotto[1,*], Christophe Inguimbert[1], Simon Lewandowski[1], Romain Ceolato[2]

[1] *DPHY, ONERA, Université de Toulouse, 31000, Toulouse, France (*agnes.lecadre-scotto@onera.fr)*
[2] *DOTA, ONERA, Université de Toulouse, 31000, Toulouse, France*

In space environment, space white paint used as a coating for radiators in space systems undergoes aging which significantly impacts the thermal balance of these systems. This aging process leads to changes in the optical signature of the white paint, particularly in its solar absorptance, which gives an indication of its degradation level.

Global prediction models provide an efficient and fast way to complement the monitoring of thermo-optical characterizations of materials degraded by simulated space aging in ground-based facilities. To develop such a model, we use the Monte Carlo method. The simulations are performed using the GEANT4 particle transport toolkit [1]. The radiative transfer code, developed using the optical module of GEANT4 [2], is supplied with the physical parameters of the white paint that govern the transport of optical photons. The space white paint studied consists of a PDMS silicone binder encapsulating zinc oxide (ZnO) pigments. As a first approximation, we use the Bohren and Huffman Mie scattering code (BHMIE) [3] based on Mie theory to calculate the physical scattering parameters of the paint, with absorption by the silicone matrix considered.

The degradation of the paint is studied under proton irradiation at 45 keV and 240 keV with applied fluences varying from 1×10^{15} to 1×10^{16} p+/cm², simulating conditions encountered in space environment. Paint samples and their constituent materials are irradiated using a Van de Graaff accelerator, and in-situ reflectance measurements are performed during the irradiation. To model the evolution of reflectance and transmittance—and consequently solar absorptance—we assume that there is a modification of the optical properties responsible for absorption, specifically the imaginary parts of the refractive indices of the pigment and the binder. The evolution of these absorption parameters as a function of the radiation dose is modeled empirically, based on in-situ experimental results. These new physical parameters are integrated into the Monte Carlo radiative transfer code to simulate the optical signatures of the studied materials as a function of the radiation dose received.

Figure 1: PDMS/ZnO white paint proton-induced aging

[1] S. Agostinelli, J. Allison, K. Amako, J. Apostolakis, H. Araujo, P. Arce, *et al.*, "Geant4—a simulation toolkit," *Nucl. Instrum. Methods Phys. Res. A.*, vol. 506, no. 3, pp. 250–303, 2003.

[2] Geant4 Collaboration, "Electromagnetic - Optical Photons," in *Physics Reference Manual - GEANT4 A simulation toolkit*, 11.2., 2023, pp. 211–215.

[3] C. F. Bohren and D. R. Huffman, *Absorption and scattering of light by small particles*. John Wiley & Sons, 2008.

Carbon Dots from Laser Ablation of Graphene Oxide in Biocompatible Solutions

L. Torrisi[1], D. Lombardo[1], A. Torrisi[2], and M. Cutroneo[1]

[1]*MIFT Department, University of Messina, Messina, Italy*
[2]*Medicine and Surgery Department, University of ENA Kore, Enna, Italy*

A biocompatible carbon dots (CDs) dispersion has been obtained by laser irradiation of graphene oxide (GO) placed in liquids. The CDs synthesis uses an IR repetition pulsed laser operating at 970 nm, 100 ms pulse duration, and 350 J/cm2 fluence.

The carbon target is constituted by micrometric GO foils immersed in a common phosphate-buffered saline (PBS) solution used in biology.

CDs are functionalized by the solution salts and, under UV excitation, produce a high-intensity dispersion luminescence in the visible region.

The optical properties and other physical characteristics of the dispersion are presented. The CDs fluorescent emission occurs in the blue region, around 478 nm, upon excitation at 365 nm.

The synthesized CDs showed high biocompatibility, stability, and nontoxicity.

This study provides an inexpensive and simple synthesizing CDs for useful applications in bioimaging, diagnostics and therapy.

Modeling the Spectral Slope of the Lidar and Depolarization Ratio of Mineral Dust

Thomas Oppermann,[1,*] Moritz Haarig,[1] Masanori Saito,[2] Adrian Walser,[3] Bernadett Weinzierl,[3] Ulla Wandinger,[1] and Andreas Macke[1]

[1] *Leibniz Institute for Tropospheric Research – Leipzig, Germany (*oppermann@tropos.de)*
[2] *Department of Atmospheric Science, University of Wyoming – Laramie, USA*
[3] *Faculty of Physics, University of Vienna – Vienna, Austria*

As the most abundant aerosol in the atmosphere, mineral dust constitutes an important part of radiative calculations in atmospheric physics. In order to understand its role, proper knowledge of its microphysical properties is required. One possible way to obtain these properties is to infer them from optical lidar measurements. However, in this approach, a proper optical model for relating the observed optical properties at 180° scattering angle (exact backscatter), such as the extinction-to-backscatter ratio (lidar ratio) and depolarization ratio, with the desired microphysical properties is required. Since mineral dust particles exhibit a diverse morphology, simplifying assumptions about the shape of these particles are required.

We investigate the performance of three simplified shape models for mineral dust, namely spheroids [1], the irregularly shaped particles proposed by Gasteiger et al. [2], and irregular hexahedra [3]. We compare the model results against polarization Raman lidar measurements during the Saharan Aerosol Long-range Transport and Aerosol-Cloud-Interaction Experiment (SALTRACE) in 2013 [4]. The dataset consists of triple-wavelength (355 nm, 532 nm, and 1064 nm) observations of the lidar and depolarization ratio of long-range transported Saharan dust plumes. We are using collocated airborne observations of the particle size distribution as input for the optical models. For the complex refractive index, different literature values are used.

As a result, we find that the studied models could reproduce, albeit with different inputs for the refractive index, the observed spectral slope of the lidar ratio. However, none of the models was able to accurately model the spectral slope of the depolarization ratio from 355 nm to 1064 nm so far. Hence, further investigations on the influence of both the real and imaginary part of the refractive index, and potentially new particle shape models are required. Out of the three studied models, the irregular hexahedra model seems to be the most promising. It is planned to incorporate surface inhomogeneities into this particle shape model for potentially better accuracy of modeling the observed spectral slope of the depolarization ratio of mineral dust, especially in the UV range.

[1] O. Dubovik *et al.*, *Application of spheroid models to account for aerosol particle nonsphericity in remote sensing of desert dust* (*Journal of Geophysical Research: Atmospheres*, vol. 111, no. D11, 2006)
[2] J. Gasteiger et al., *Modelling lidar-relevant optical properties of complex mineral dust aerosols* (Tellus B, 2011)
[3] M. Saito et al., *A Comprehensive Database of the Optical Properties of Irregular Aerosol Particles for Radiative Transfer Simulations* (Journal of the Atmospheric Sciences, 2021)
[4] M. Haarig et al., *Triple-wavelength depolarization-ratio profiling of Saharan dust over Barbados during SALTRACE in 2013 and 2014* (Atmospheric Chemistry and Physics, 2017)

Satellite retrievals over snow-covered surfaces: a Global Sensitivity Analysis of polarimetric measurements

Matteo Ottaviani,[1,2,*] Gabriel Harris Myers,[3,1] and Nan Chen[4]

[1]*NASA Goddard institute for Space Studies – New York, NY 10025, USA (*matteo.ottaviani@nasa.gov)*
[2]*Terra Research Inc – Hoboken, NJ 07030, USA*
[3]*Courant Institute of Mathematical Sciences, New York University – New York, NY 10012, USA*
[4]*Stevens Institute of Technology – Hoboken, NJ 07030, USA*

We present a detailed theoretical assessment of the information content of passive polarimetric observations over snow scenes, using a global sensitivity analysis (GSA) method. Conventional sensitivity studies focus on varying a single parameter while keeping all other parameters fixed. In contrast, the GSA correctly addresses the covariance of state parameters across their entire parameter space, hence favoring a more correct interpretation of inversion algorithms and the optimal design of their state vectors. The Stokes vector at visible, near-infrared and shortwave infrared wavelengths is simulated at the top of the atmosphere when the surface is modeled as a vertically resolved snowpack consisting of non-spherical grains. The presence of light-absorbing particulates (LAPs), either embedded in the snow or aloft in the atmosphere above in the form of aerosols, is also considered. The Sobol indices, which are the main metric for the GSA, were used to select the state parameters in retrievals performed on data simulated for multiple instrument configurations. The results show that multi-angle polarimetric observations can (i) effectively partition LAPs between the atmosphere and the surface, which represents a notorious challenge for snow remote sensing based on measurements of total reflectance only and (ii) lead to better estimates of grain shape and roughness and, in turn, the asymmetry parameter, which is critical for the determination of albedo. The results encourage the development of new remote sensing algorithms that fully leverage multi-angle and polarimetric capabilities of modern remote sensors. The better characterization of surface and atmospheric parameters in snow-covered regions advances research opportunities for scientists of the cryosphere and ultimately benefits albedo estimates in climate models.

[1] M. Ottaviani, G. H. Myers, and N. Chen, Atmos. Meas. Tech. **17(15)**, 4737-4756 (2024).

Aerosol Products from PACE Polarimeter HARP2 Observations using GRASP

Anin Puthukkudy[a,b,*], J. Vanderlei Martins[a,b,c], Xiaoguang Xu[a,b,c], Chong Li[d], Pavel Litvinov[d], David Fuertes[d], Alejandro García Gómez[d], Anton Lopatin[d], Christian Matar[d], Juan Carlos Antuña-Sánchez[d], and Oleg Dubovik[e]

[a]*Earth and Space Institute, UMBC, MD, USA*
[b]*GESTARII, UMBC, MD, USA*
[c]*Physics Department, UMBC, MD, USA*
[d]*GRASP SAS, Lezennes, France*
[e]*Université de Lille, CNRS, UMR 8518 - LOA - Laboratoire d'Optique Atmosphérique, Lille, France*

The Hyper-angular Rainbow Polarimeter-2 (HARP2), a state-of-the-art multi-angular polarimeter (MAP) deployed on NASA's PACE (Plankton, Aerosol, Cloud, ocean Ecosystem) platform, commenced data acquisition in March 2024. This research focuses on the comprehensive validation and in-depth analysis of Level 2 aerosol and surface reflectance products generated from HARP2's unique top-of-atmosphere (TOA) observations. HARP2's capabilities are significant, providing observations across a wide range of viewing angles (from -54.5° to +54.5°) and four spectral bands (440, 550, 670, and 870 nm), enabling detailed characterization of atmospheric aerosols and surface properties.

A crucial aspect of this study is the rigorous validation of Aerosol Optical Depth (AOD), a key parameter for quantifying atmospheric aerosol loading. This validation will leverage data from the globally distributed Aerosol Robotic Network (AERONET) of ground-based sun photometers. The validation will employ advanced methodologies integrated within the Generalized Retrieval of Aerosol and Surface Properties (GRASP) algorithm. Specifically, we will utilize GRASP's multi-pixel retrieval approach, exploiting both spatial and temporal correlations in HARP2's data to enhance retrieval accuracy and robustness. This allows for improved constraints on aerosol properties, even in challenging conditions. Beyond standard AOD validation, we will present preliminary findings from component-based retrievals. These retrievals decompose the aerosol signal into contributions from different aerosol types (e.g., dust, smoke, sea salt), providing more physically meaningful outputs that are directly suitable for assimilation into Earth-System Models (ESMs). This represents a significant step towards improving the representation of aerosols in climate and weather forecasting.

Furthermore, to illustrate the capabilities and potential impact of HARP2 data, we will analyze several compelling case studies. These include: (1) long-range smoke transport events originating from wildfires in North America, Africa, and Amazonia, demonstrating HARP2's ability to track aerosol plumes and characterize their properties; and (2) severe air pollution events over the Indian subcontinent, highlighting HARP2's contribution to monitoring and understanding anthropogenic aerosol emissions. In summary, this poster will provide a comprehensive overview of the initial performance and validation of HARP2 aerosol products, derived using the advanced GRASP retrieval framework. It highlights the expected advancements in aerosol characterization enabled by this next-generation multi-angular polarimeter and emphasizes the significant contribution HARP2 will make to the overarching scientific goals of the PACE mission, particularly in improving our understanding of aerosol-cloud interactions and their role in the Earth's climate system

[1] R. P. Feynman, M. Gell-Mann, and G. Zweig, Phys. Rev. Lett. **13**, 678 (1964).
[2] D. F. Edwards, "Silicon (Si)", p. 547 in *Handbook of optical constants of solids*, ed. E. D. Palik (Academic, 1997).
[3] F. Ladouceur and J. Love, *Silica-based buried channel waveguides and devices* (Chapman & Hall, 1995), Chap. 8.
[4] Author(s), "Title of paper", p. 12 in *Title of Proceeding* (Institute of Electrical and Electronics Engineers, 2023).

Combined Lidar and MAP dust retrieval using Spheroid and Hexahedral aerosol shape models in GRASP

Greema Regmi[1,2*], W. Reed Espinosa[3], J. Vanderlei Martins[1,2], Anin Puthukkudy[1,2], Masanori Saito[4], Oleg Dubovik[5]

[1] *Department of Physics, University of Maryland, Baltimore County, Baltimore, MD, USA (*gregmi1@umbc.edu)*
[2] *Goddard Earth Sciences Technology and Research (GESTAR)II, Baltimore, MD, USA*
[3] *NASA Goddard Space Flight Center, Greenbelt, MD, USA*
[4] *Department of Atmospheric Science, University of Wyoming, WY, Laramie, USA*
[5] *Univ. Lille, CNRS, UMR 8518 LOA - Laboratoire d'Optique Atmosphérique, Lille, France*

Accurate retrieval of aerosol geophysical properties is essential for informing policies aimed at a sustainable future. New generation sensors designed to measure polarization are highly sensitive to the shape of scattering particles. Since different non-spherical particles scatter light uniquely—especially at side and backscattering angles—oversimplifying aerosol shape in retrieval algorithms, particularly for non-spherical aerosols like dust, can introduce biases in the retrieved properties.

We examined two shape models—spheroid and hexahedral from the TAMUdust2020 database—to represent dust in the Generalized Retrieval of Aerosol and Surface Properties (GRASP) model. The performance of retrievals in dust-dominated scenes observed by the Research Scanning Polarimeter (RSP) and the Second Generation High Spectral Resolution Lidar (HSRL-2) during the ObseRvations of Aerosols above CLouds and their intEractionS (ORACLES) field campaigns were compared across different sensor configurations—HSRL-only, RSP-only, and combined HSRL-2+RSP retrievals—for both shape models. Our results indicate that incorrect assumptions about aerosol morphology significantly impact the retrieval of single scattering albedo and size distribution, whereas aerosol optical depth (AOD) remains relatively unaffected.

By identifying the properties most sensitive to shape assumptions, we aim to recommend optimal shape models for accurately characterizing dust aerosols. This research is particularly relevant for developing retrieval algorithms for future missions such as NASA's Atmosphere Observing System (AOS), which will integrate advanced polarimeter and lidar measurements to enhance aerosol characterization.

Enhanced optical behavior of micro and nano-plastics coupled with metal nano particles

Shadi Rezaei,[1,2,*] Pietro G. Gucciardi,[2] Onofrio M. Maragò[2], Rosalba Saija[1,2], Maria Antonia Iatì[2]

[1] *Dipartimento di Scienze Matematiche e Informatiche, Scienze Fisiche e Scienze della Terra, Università di Messina, Messina, Italy (*shadi.rezaei@unime.it)*

[2] *CNR-IPCF, Istituto per i Processi Chimico-Fisici, Messina, Italy*

Abstract: Metal nanoparticles have attracted ever-increasing interest in recent decades, becoming a prominent focus of extensive and rapidly expanding research. These particles exhibit unique properties that make them suitable for a broad range of applications, including nanotechnology, material science, and biomedicine. On the other side, micro and nanoplastics have garnered increasing attention from the scientific community due to their pervasive presence in the environment and their potential toxicity to human health and ecosystem.

Identifying micro and nanoplastics is particularly challenging, especially for smaller sizes, making the development of accurate detection and characterization methods crucial. Recently, optical and Raman tweezers have proved to be an efficient tool to trap, manipulate and characterize micro and nano plastics, allowing a contamination-free investigation [1,2]. Great scientific interest has also been directed towards the development of sensitive SERS (Surface-Enhanced Raman Scattering) structures with the aim to enable a better detection and particle characterization thanks to hot spots formation and electromagnetic field enhancement.

Computational methods capable of efficiently simulating the enhanced optical response of micro and nano-plastics in presence of metal nanoparticles could be very helpful in the design of SERS substrates and in the development of SERS detection methods. To this end, we study the near and far-field optical properties of nano clusters composed by nano-plastics particles coupled with metal nanoparticles, using a combined approach based on the Transition matrix (T-matrix) method and on neural networks [4]. The T-matrix approach allows an accurate description of the optical forces acting on model metal-plastic nano-clusters and appears as a useful tool to address the experimental effort in the detection ad characterization of trapped plastics nanoparticles. Furthermore, this combined approach significantly optimizes the efficiency of computations.

This work has been funded by European Union (NextGeneration EU), through the MUR-PNRR project SAMOTHRACE (ECS00000022) PRIN2022 "EnantioSelex" (grant number 2022P9F79R) and National Centre for HPC, Big Data and Quantum Computing (HPC)" Codice progetto CN00000013 - SPOKE 10 CUP D43C22001240001.

[1] R. Gillibert, G. Balakrishnan, Q. Deshoules, M. Tardivel, A. Magazzù, M. G. Donato, O. M Maragò, M. Lamy de La Chapelle, F. Colas, F. Lagarde, et al. "Raman tweezers for small microplastics and nanoplastics identification in seawater". Environmental Science & Technology, 53(15): 9003–9013, 2019

[2] R. Gillibert, A. Magazzù, A. Callegari, D. Bronte-Ciriza, A. Foti, M. G. Donato, On. M Maragò, G. Volpe, M. Lamy de La Chapelle, F. Lagarde, et al. "Raman tweezers for tire and road wear micro-and nanoparticles analysis." Environmental Science: Nano, 9(1):145–161, 2022

[3] L. Xie, K. Gong, Y. Liu, L. Zhang. "Strategies and challenges of identifying nanoplastics in environment by Surface-Enhanced Raman spectroscopy." Environmental Science & Technology, 57: 25-43, 2023

[4] S. Rezaei, D. Bronte Ciriza, A. Hassanzadeh, F. Kheirandish, P.G. Gucciardi, O.M. Maragò, R. Saija, M.A. Iatì. "Faster Calculations of Optical Trapping Using Neural Networks Trained by T-Matrix Data: An Application to Micro-and Nanoplastics". ACS Photonics. 11(8):3424-32, 2024

Hygroscopic behavior of inorganic salt from inelastic scattering and extinction cross-section measurements

Gema Sánchez-Jiménez,[1,2,] * Alberto Martín-Molina,[2] Lucas Alados-Arboledas, [1,2] Francisco J. Olmo-Reyes[1,2] and Antonio Valenzuela[1,2]

[1]*Andalusian Institute for Earth System Research (IISTA-CEAMA) – Granada, Spain (*gemasj@ugr.es)*
[2]*Dept. of Applied Physics, University of Granada – Granada, Spain*

Inorganic ions play a fundamental role in several physicochemical processes. In particular, specific ion effects (SIEs), commonly known as the Hofmeister series, are observed across the medical, biological, chemical and industrial sciences. The Hofmeister series describes the influence of ions on intermolecular interactions, and it has been recently proved that it plays an important role in the hygroscopic behavior of mixed aerosols made of Hofmeister ions and glycine [1]. However, the Hofmeister effect on the hygroscopicity of aerosols has been scarcely studied. Therefore, we study the hygroscopic growth of single particles of inorganic salts using a Paul Electrodynamic Trap (PET) coupled with Double Cavity Ring-Down Spectroscopy (D-CRDS) under controlled humidity [2]. This configuration allows us to obtain directly and simultaneously from the same particle the elastic scattering and the ring down times to determinate the radius and the extinction cross-sections. These independently obtained databases during humidity evolution enable the robust calculation of the hygroscopicity parameter (κ) and to observe the deliquescence (DRH) and efflorescence (ERH) points.

The measurements of NaH_2PO_4, NaCl and $NaNO_3$ (Figure 1) shows notable differences in their hygroscopic growth. NaH_2PO_4 exhibited minimal hysteresis, with less than 1.5% difference between ERH and DRH (24% ERH and 25% DRH). In contrast, NaCl showed a pronounced discrepancy exceeding 23% (47% ERH and 73% DRH), characterized by abrupt phase transitions. Meanwhile, $NaNO_3$ displayed a smooth and continuous dehydration-hydration cycle (9%-12% ERH and DRH). These observations correspond to their respective κ values: NaCl (0.99) demonstrates the highest water uptake, NaH_2PO_4 (0.60) features enhanced cycling consistency, and $NaNO_3$ (0.83) represents an intermediate behavior.

These preliminary results emphasize the influence of inorganic anions in modulating water uptake, phase stability and hysteresis. The pronounced hysteresis of NaCl contrasts with the reversible behavior of NaH_2PO_4, suggesting SIEs in deliquescence and efflorescence. Understanding these ion-specific effects in hygroscopic growth provides valuable insights into the atmospheric and environmental behavior of inorganic salts.

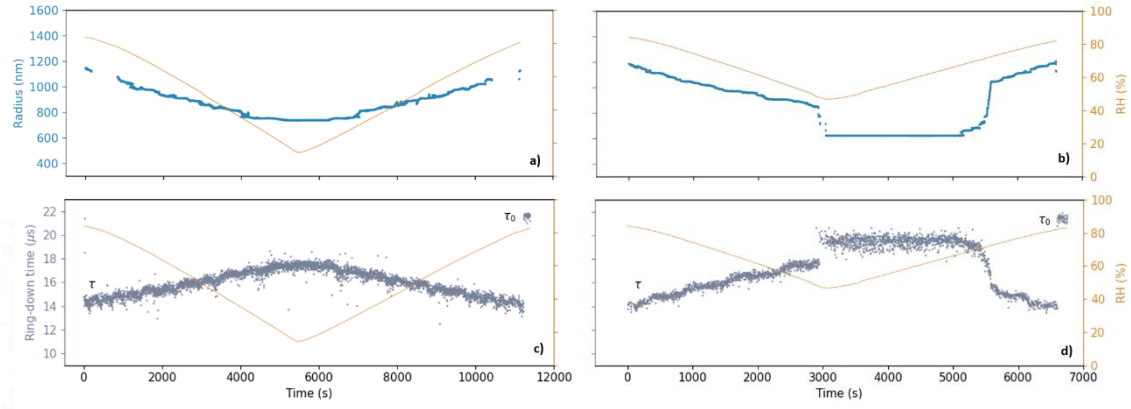

Figure 1: Example of the dehydration-hydration cycle (orange line) for two single inorganic salt particles: the top graphs show the radius (nm) (blue line) of (a) NaH_2PO_4 and (b) NaCl; the bottom graphs show the ring down-time (μs) (grey dots) for (c) NaH_2PO_4 and (d) NaCl.

[1] H. Ashraf, Y. Guo, N. Wang, S. Pang and YH. Zhang. J Phys Chem A. **125**(7), 1589-1597 (2021).
[2] A. Valenzuela, et al. Journal of Aerosol Science. **175**, 106292 (2024)

Partial Mueller polarimetry for some natural scattering scenes

Sergey N. Savenkov,[1],* Yevgen A. Oberemok,[1] and Ivan S. Kolomiets[1]

[1]*Taras Shevchenko National University of Kyiv, Kyiv, Ukraine (* sns@univ.kiev.ua)*

It is known that the Mueller polarimetry completely characterizes the anisotropy and depolarization properties of any natural scattering scenes. This assumes, on the one hand, the measurement of the Mueller matrix in the given geometry of the experiment and the wavelength of the EM radiation. On the other hand, the measured Mueller matrices of the scattering scenes under study are further analyzed using a fairly wide range of methods that exist today to get anisotropy and depolarization characterization of studied scenes.

At the same time, it is well known that the Mueller matrix formalism of for a wide range of inverse problems is redundant. This problem has recently attracted close attention. Only a brief list of references in this subject to note is Refs.1-6. The latter is evidently due to the fact that this makes it possible to reduce considerably the time and errors of polarimetric measurements and simplify the design of the polarimeters, in particular, to get rid of the need to use movable polarization elements.

In this paper, we explore the mathematical framework necessary to obtain common anisotropy and depolarization parameters of interest for some groups of soil and vegetation scenes [7-9] with partial Mueller polarimetry.

[1] S. N. Savenkov, Opt. Eng. **41**, 965 (2002).

[2] E. A. Oberemok and S. N. Savenkov, J. Appl. Spectr. **70** (2003).

[3] E. A. Oberemok and S. N. Savenkov, J. Appl. Spectr. **71** (2004).

[4] S. N. Savenkov, R. S. Muttiah, E. A. Oberemok, and A. S. Klimov, JQSRT **112**, 1796 (2011).

[5] J. J. Gil and R. Ossikovski, *Polarized Light and the Mueller Matrix Approach* (CRC Press, 2022), Chap. 11.

[6] T. Novikova and J. C. Ramella-Roman, Opt. Lett. **47**, 5549 (2022).

[7] S. N. Savenkov, A. A. Kokhanovsky, E. A. Oberemok, and I. S. Kolomiets, IEEE Geoscience and Remote Sensing Letters **17**, 1383 (2020)

[8] S. N. Savenkov, E. A. Oberemok, I. S. Kolomiets, R. S. Muttiah, Photonics **10**, 1361 (2023).

[9] S. N. Savenkov, E. A. Oberemok, I. S. Kolomiets, R. S. Muttiah, R. Kurylenko, Photonics **11**, (2024).

Light Scattering from Single Atmospheric Ice Particles

F. Martin Schnaiter,[1,2]* Harry Ballington[1], and Emma Järvinen[1]

[1]*University of Wuppertal – Wuppertal, Germany*
[2]*schnaiTEC GmbH – Wuppertal, Germany (martin.schnaiter@schnaitec.com)*

The interaction of solar radiation with ice particles in clouds plays a critical role in redistributing solar light before it reaches the ground. Understanding this process is essential for accurately modeling shortwave radiative transfer in climate models and retrieving cloud bulk properties from satellite observations. However, current optical models often rely on simplified ice particle morphologies, limiting our understanding of the light scattering behavior of atmospheric ice particles.

To address this gap, the Particle Habit Imaging and Polar Scattering (PHIPS) airborne probe was developed to perform in-situ measurements of single atmospheric ice particles. PHIPS combines a stereo microscopic bright-field imager with a polar nephelometer to analyze individual atmospheric cloud particles. Through several aircraft campaigns, PHIPS has provided a unique and comprehensive dataset of the microphysical properties and correlated angular light scattering functions of real atmospheric ice particles.

This dataset is valuable for scientists developing and applying single-particle light scattering models. In this study, we evaluate three surface roughness models used in ray-tracing optical simulations: (1) the widely used tilted-facet angle distribution method, a less physical approach; (2) the bi-directional scattering distribution function (BSDF) method, a physically based implementation of surface roughness; and (3) the parent beam tracer (PBT) method, which represents surface roughness using physical optics. Using example ice crystals, we assess their performance and highlight the critical role of in-situ measurements in improving our understanding of atmospheric ice particle light scattering.

Non-Spherical and Inhomogeneous Effects on Deriving Mineral Dust Refractive Indices from Laboratory Measurements

Senyi Kong,[1] Zheng Wang,[1] and Lei Bi[1,*]

[1]*School of Earth Sciences, Zhejiang University – Hangzhou, China (*bilei@zju.edu.cn)*

Mineral dust aerosols exhibit inherent nonspherical morphologies and internal inhomogeneity. Accurate representation of their optical properties is critical. This study develops an inhomogeneous super-spheroid dust model to systematically evaluate the implications of internal inhomogeneity on dust aerosol optical characteristics, while addressing potential biases introduced by the prevalent homogeneous assumption in existing remote sensing studies. Through comparative numerical simulations across diverse particle sizes and wavelengths, we quantify discrepancies in refractive index determination and optical property simulations between conventional spherical models and super-spheroid representation. The analysis particularly focuses on resolving uncertainties in laboratory-measured shortwave refractive indices through comprehensive process modeling that replicates actual experimental characterization procedure. Key findings reveal that spherical approximations induce systematic underestimation of refractive index imaginary components, consequently leading to overestimated single-scattering albedo values. This artifact primarily originates from erroneous geometric diameter conversions in optical particle counters when assuming spherical morphology. Conversely, the super-spheroid model demonstrates superior alignment with inhomogeneous model predictions through better morphological representation. Our results emphasize the necessity of incorporating both particle non-sphericity and internal inhomogeneity in laboratory measurements, while recommending the adoption of non-spherical models for enhanced accuracy in optical simulations and remote sensing applications.

Polarimetric properties of cometary dust based on DBCP V3.0

Olena Shubina[1,2]*

[1]*Astronomical Institute of Slovak Academy of Sciences – Tatranská Lomnica, Slovak Republic (*oshubina@ta3.sk)*
[2]*Main Astronomical Observatory of NAS of Ukraine – Kyiv, Ukraine*

Understanding the light-scattering properties of cometary dust is crucial for constraining its physical characteristics. However, the inverse problem of light scattering by arbitrary dust particles remains unsolved, making the interpretation of polarimetric data inherently uncertain. Despite these challenges, polarimetry provides a powerful tool for diagnosing the dust and gas components of comets, offering insights into their composition, structure, and evolutionary processes.

In this study, we use an updated version of the Database of Cometary Polarimetry (DBCP V3.0), which has been extended by the author to include new observational data and improved parameterization. The database now contains polarimetric measurements for 147 comets, covering a wide range of phase angles, heliocentric distances, and observational filters. Given the difficulty of obtaining phase-angle polarization curves for individual comets across a broad phase-angle range, we employ an approach that derives average phase-angle dependencies from a diverse comet sample. This method allows us to distinguish common polarization patterns among different dynamical classes of comets and identify unique characteristics of individual objects.

Our analysis focuses on the phase-angle dependence of linear polarization as a function of wavelength, heliocentric distance, and dynamical properties. By correlating these parameters, we aim to refine our understanding of the physical properties of cometary dust and explore possible links between their formation regions in the Solar System and their subsequent evolutionary pathways. Our findings contribute to the broader effort of characterizing the diversity of cometary dust populations and their implications for planetary system formation and evolution.

Brown carbon formed by a microreactor of levitated aqueous Fe (III) droplet with fumaric acid

Antonio Valenzuela,[1,2,] * Gema Sánchez Jiménez,[1,2] Hind A. Al-Abadleh, [3] Lucas Alados-Arboledas[1,2] and Francisco .José Olmo Reyes [1,2]

[1] *Andalusian Institute for Earth System Research (IISTA-CEAMA), Granada, 18006, Spain (*avalenzuela@ugr.es)*

[2]*Dept. of Applied Physics, University of Granada, Granada, 18071, Spain*

[3]*Dept. of Earth, Environmental and Resource Sciences, University of Texas at El Paso, 500 West University Avenue, El Paso, Texas 79902, United States.*

The characterization of light-absorbing organic compounds and their complex atmospheric reactions poses a significant challenge in uncovering the molecular mechanisms that govern the optical properties of brown carbon (BrC). The uncertainty regarding the atmospheric absorption potential of BrC remains a critical limitation in accurately interpreting aerosol optical depth—a key parameter quantifying light extinction in the atmospheric column due to scattering and absorption. In this study, we introduce a novel experimental approach using a microreactor with single levitated aqueous Fe (III) droplets containing fumaric acid to investigate BrC formation as a function of reaction time. This pathway emerges as a potentially significant secondary mechanism for the formation of dicarboxylic acid complexes with transition metals. By systematically monitoring the evaporation and hydration dynamics of the droplet (Figure 1), we assessed the resulting transformations in particle morphology, size, and complex refractive index, elucidating their substantial impact on the optical properties of the particle. A detailed analysis of the experimental results revealed that particle radius increased following the acceleration of the reaction during the dehydration and hydration cycle, even when relative humidity returned to levels comparable to its initial state. Furthermore, the real refractive index (*n*) increased to values between 1.55 and 1.65, characteristic of brown carbon [1], while the imaginary refractive index (*k*) showed an increase of 0.001 to 0.005 compared to the control experiment, indicating enhanced radiation absorption by the particle. This study provides critical insights into the secondary formation mechanisms of BrC and their implications for atmospheric optical properties, advancing the understanding of aerosol behavior and its impact on radiative forcing.

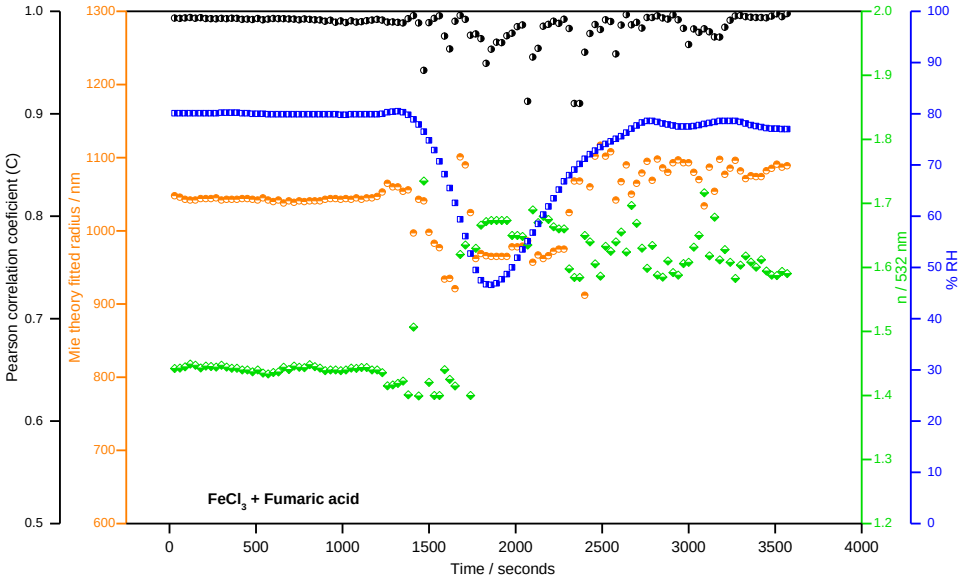

Figure 1: Reaction of $FeCl_3$ with fumaric acid in a levitated aqueous microdroplet. Multi-axes plots showing the values in measured %RH (outer right axis), microdroplet radius from Mie theory (inner left axis), *n* at 532 nm (inner right axis) and Pearson correlation coefficient (C) (outer left axis) with increasing reaction time.

[1] J.M. Flores et al., Phys. Chem. Chem. Phys. **16 (22)**, 10629–10642, (2014).

Highly Focused Laser Beams for Driving Janus Microengines and detecting sea microplastics

Alessandro Magazzù,[1,*] David Bronte Ciriza,[1] Agnese Callegari,[2] Maria Grazia Donato,[1] Antonino Foti,[1] Giovanni Volpe,[2] Luca Biancofiore, [3] Onofrio M. Maragò,[1] and Pietro G. Gucciardi [1]

[1]*CNR-IPCF, Istituto per i ProcessiChimico-Fisici, I-98158 Messina, Italy (*alessandro.magazzu@cnr.it)*
[2]*Department of Physics, University of Gothenburg, SE-41296 Gothenburg, Sweden*
[3]*Department of Industrial and Information Engineering and Economics, University of L'Aquila, L'Aquila, Italy*

Optical tweezers (OT) are a powerful tool capable of exerting optical forces on microparticles for their manipulation and confinement [1]. Over time, OT have gained increasing importance as a contactless technique for isolating single micro- and nanoparticles in environments such as liquids, air, or vacuum. They enable the transfer of energy, linear and angular momentum to particles, facilitating the study of their response to optical forces [3,4]. When combined with Raman spectroscopy, optical tweezers form Raman tweezers (RT), allowing single-particle characterization and overcoming the bulk-averaging limitations of conventional spectroscopic methods [4,5].

We present a microengine that exploits both optical and thermal effects for enhanced controllability. A gold-silica Janus particle, when illuminated by a highly focused laser beam, becomes confined at a stationary point where optical and thermal forces balance. Circularly polarized light breaks the symmetry between these forces by transferring angular momentum to the particle, inducing a tangential force that drives orbital motion [3]. By adjusting the ellipticity of the light beam and laser power, we achieve simultaneous control over the particle's velocity, rotation direction, and orbital radius. Our results are validated using a geometrical optics model that incorporates optical forces, optical absorption, and the resulting particle heating.

Additionally, we introduce the development and first applications of a portable Raman tweezers system integrated with a microfluidic platform for investigating microplastics in water. This system enables real-time counting and characterization of microplastics in their natural collection areas, such as seas, rivers, and lakes, directly after sampling [5]. By performing analyses immediately after collection, we mitigate issues related to sample aging, such as sedimentation or bacterial growth, ensuring more accurate and reliable measurements.

A. Magazzù and O. M. Maragò acknowledge financial support by the European Union (NextGeneration EU), through the MUR-PNRR project SAMOTHRACE(ECS00000022).

[1] A. Ashkin, et al., Observation of a single-beam gradient force optical trap for dielectric particles, Optics letters 11.5: 288-290 (1986).

[2] A. Ashkin, M. D. James, T. Yamane, Optical trapping and manipulation of single cells using infrared laser beams, Nature 330.6150: 769-771 (1987).

[3] D. Bronte Ciriza et al. Optically driven Janus microengine with full orbital motion control. *ACS photonics* 10.9, 3223-3232 (2023)

[4] A. Magazzù, et al. Investigation of dust grains by optical tweezers for space applications. The Astrophysical Journal 942.1 (2022).

[5] R. Gillibert, et al. Raman tweezers for small microplastics and nanoplastics identification in seawater. Environmental science & technology 53.15 (2019).

Electric field induced effect on dipole moment and vibrational properties of the biosynthetic dye Violacein

S. Trusso[1*], D. Spadaro[1], R.C. Ponterio[1], D. Giuffrida[1], M. Tommasini[2],F. Saija[1], G. Cassone[1]
[1]*IPCF-CNR, Istituto per i Processi Chimico-Fisici,V.le F.S. d'Alcontres 37, I-98158 Messina, Italy;*
[2]*Dipartimento di Chimica, Materiali Ing. Chimica "G. Natta", Politecnico di Milano, 20133 Milano, Italy;*
**sebastiano.trusso@cnr.it*;

Abstract: Violacein is a biological produced dye found in Chromobacterium violaceum and Janthinobacterium lividum bacteria [1]. Recently there is an increased interest regarding this compound due to its peculiar antibacterial or antiviral activities among the others. In this work we report a the structural, optical and vibrational property of violacein and deoxyviolacein, as they are both produced the bacterial activity by means of Density Functional Theory calculations. Geometrical optimization and vibrational analyses of the normal modes of the isolated molecule were performed under zero-field conditions. Additionally, these analyses were conducted under the influence of static and oriented external electric fields (OEEF). In different numerical experiments, the OEEF was applied along three mutually orthogonal molecular axes relative to the direction of the dipole moment (**μ**) of the molecule. The behavior of molecules under OEEF are of great interest, in fact, EF as large as 1 V/Å can be observed because of fluctuations of molecular dipoles or in presence of ions in water solutions, but also in experiments like scanning tunnelling Microscopy (STM), atomic force microscopy (AFM), tip enhanced Raman scattering (TERS), or even at nanogaps in SERS measurements. The presence of an OEEF can be exploited spectroscopically through the observation of the vibrational Stark effect, where frequency shifts or even the activation of forbidden modes are induced by the OEEF [2]. In the case of Violacein the presence of OEEF has a strong influence on both the intensity and orientation of the dipole moment (Fig.1) and on the position of the strongest Raman mode (C=C stretching), that shows a peculiar behavior depending on the relative orientation of the OEEF and of **μ** (Fig.2). The most intense Raman mode appears at 1556 cm^{-1}, corresponding to the stretching of the two C=C bonds linking the 2-pyrrolidone ring to the oxindole and 5-hydroxyindole units. This mode exhibits an upshift under the influence of an OEEF aligned in the opposite direction of the molecule direction (white areas in Fig.2), reaching its peak not at the maximum OEEF value but when the dipole moment component along the OEEF direction is at its minimum. When the OEEF is aligned along the direction of the dipole moment a monotonic downshift of the C=C stretching mode is observed. The variations in the structure and vibrational properties of violacein observed through DFT can be leveraged to understand the behavior of the molecule in complex systems where strong electric fields may be present.

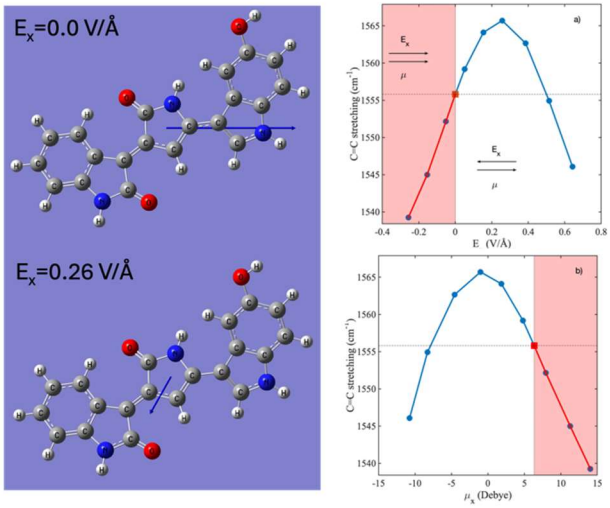

Figure 1) Left panel : Structure and μ orientation (blue arrow) of Violacein at E=0.0 and 0.26 V/Å. Figure 2) Right panel: a) behavior of the C=C stretching position as a function of the OEEF and b) as a function of the μ_x component. The red shaded areas correspond to OEEF oriented along the **μ** direction.

[1] J.J. Fuller, R. Ropke, J. Krausze, K.E. Rennhack, N. P. Daniel, W. Blankenfeldt, S. Schultz, D. Jahn, J. Moser, J. Biological Chemistry, **291**,20068 (2016).
[2] V.M. Nardo, G. Cassone, R.C. Ponterio, F. Saija, J. Sponer, M. Tommasini, S. Trusso, J. Phys. Chem A, **124**, 10856 (2020).

Zr-MOFs as an efficient adsorbent of biomolecules and environmental analytes

Govar M. Abdullah,[1,3,4,*] Emily. Worobiej[4], Timothy L Easun[4], G. Neri[2], R. Saija[1]

[1]Dipartimento di Scienze Matematiche e Informatiche, Scienze Fisiche e Scienze della Terra (MIFT) Università di Messina – Viale Ferdinando Stagno d'Alcontres, 31 – 98166 Messina, Italy (govar.abdullah@studenti.unime.it)

[2]Department of Engineering, University of Messina, Contrada di Dio, 1, I-98166 Messina, Italy

[3]Department of Physics, College of Education, Salahaddin University – Erbil, Erbil, Kurdistan Region, Iraq

[4]School of Chemistry, University of Birmingham, Birmingham, United Kingdom, B15 2TT

Abstract: MOFs are porous structures formed by combining metal ions with organic linkers, featuring adjustable pore sizes, high surface areas, and active sites. These properties make them useful for applications like catalysis, energy storage, and sensing. Zirconium-based MOFs (Zr-MOFs) are particularly promising for sensing due to their versatility, stability, and extensive internal surface areas. Zirconium-based MOFs typically comprise zirconium clusters connected by carboxylate linkers. They are chemically stable and resistant to a wide range of pH and solvents. They are often synthesised under solvothermal conditions; however, due to the durability of zirconium chemistry, they can be synthesised at higher temperatures. We attempted the synthesis of these frameworks from ZrO_2 as the metal precursor. This is a new approach and has shown limited signs of success when analyzing the resulting materials by powder X-ray diffraction. Therefore, we synthesised three zirconium-based metal-organic frameworks: UiO-66, UiO-67, and MOF-808. These are all water-stable frameworks synthesised using standard methods [1], in which the nodes are based on Zr_6 clusters, and their necessary characterization has been done, including TGA, XRD, FTIR, BET, SEM, and UV-Vis spectroscopy. A protocol was developed for measuring the uptake of five analytes from water by the three MOFs. The analytes are uric acid, dopamine HCL, tyrosine, catechol and hydroquinone. Then, used UV/vis absorption spectroscopy on solutions of the analytes to i) see how they change in the absence of the MOFs (there are signs of aggregation in solution that change the spectra over hours – days), and ii) see how much and how rapid the uptake is in the presence of each of the three MOFs[2,3]. This preliminary data results in 15 experiments/datasets at each time point, and we have looked at ~30 minutes, 2 hours, 4 hours, 6 hours, 24 hours, 48 hours and 72 hours. When uptake into the MOFs occurs, it is all quite rapid under the conditions used; MOF-808 has the best analyte sorption across the analytes, and there are distinct differences in the uptake of each analyte that can largely be justified by the differences in chemical structure and interactions with the host MOFs, the uptake absorbance peaks as a function of time for all three MOFs with analytes has been analyzed as shown in Fig 1. So, we obtained that UiO-66, UiO-67, and MOF-808 have excellent potential to be used for adsorption of the analytes of interest, which we are currently investigating.

[1] Zhou, H. C., Long, J. R., & Yaghi, O. M. (2012). Introduction to metal–organic frameworks. Chemical reviews, 112(2), 673-674.

[2] Olmo, F., Garoz-Ruiz, J., Colina, A. and Heras, A., 2020. Derivative UV/Vis Spectro electro chemistry in a thin-layer regime: deconvolution and simultaneous quantification of ascorbic acid, dopamine, and uric acid. Analytical and Bioanalytical Chemistry, 412, pp.6329-6339.

[3] Øien, S., 2012. Synthesis and characterization of modified Uio-67 metal-organic frameworks (master's thesis).

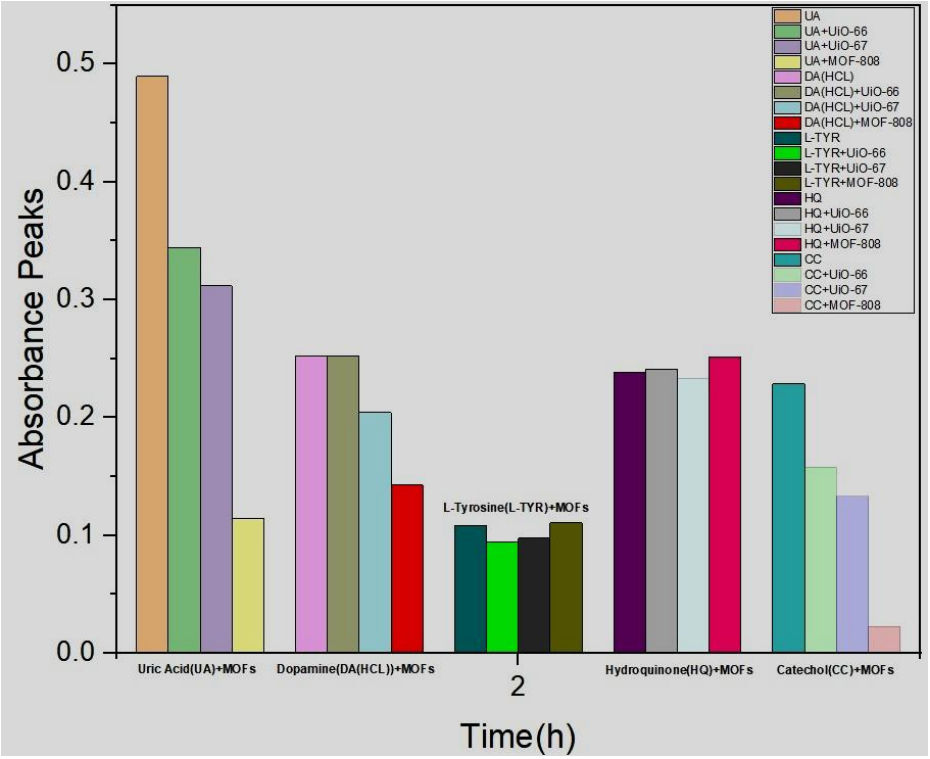

Figure 1: UV-vis absorbance peaks of the MOFs uptake of five different analytes as a function of time

Finanziato dall'Unione europea NextGenerationEU

This work has been partially funded by European Union (NextGeneration EU), through the MUR-PNRR project SAMOTHRACE (ECS00000022).

samothrace www.samothrace.eu

[1] Zhou, H. C., Long, J. R., & Yaghi, O. M. (2012). Introduction to metal–organic frameworks. Chemical reviews, 112(2), 673-674.

[2] Olmo, F., Garoz-Ruiz, J., Colina, A. and Heras, A., 2020. Derivative UV/Vis Spectro electro chemistry in a thin-layer regime: deconvolution and simultaneous quantification of ascorbic acid, dopamine, and uric acid. Analytical and Bioanalytical Chemistry, 412, pp.6329-6339.

[3] Øien, S., 2012. Synthesis and characterization of modified Uio-67 metal-organic frameworks (master's thesis).